Analysis of the Combined Effect of Major Influencing Parameters for Designing High Performance Single (sBHE) and Double (dBHE) U-Tube Borehole Heat Exchangers

Esa Dube Kerme , Alan S Fung * , Wey H Leong

Posted Date: 7 March 2024

doi: 10.20944/preprints202403.0448.v1

Keywords: borehole heat exchanger; heat transfer per unit borehole depth; shank spacing; borehole size; combined impact of parameters; convective heat transfer coefficient

 doi:10.20944/preprints202403.0448.v1

Article

Analysis of the Combined Effect of Major Influencing Parameters for Designing High Performance Single (sBHE) and Double (dBHE) U-Tube Borehole Heat Exchangers

Esa Dube Kerme, Alan S. Fung * and Wey H. Leong

Department of Mechanical, Industrial and Mechatronics Engineering, Toronto Metropolitan University, Toronto M5B 2K3, Canada

* Correspondence: alanfung@torontomu.ca

Abstract: In this paper, comprehensive analysis of combined effect of major influencing parameters on heat transfer in the single U-tube BHE (sBHE) and double U-tube BHE (dBHE) with two independent circuits was performed by using validated numerical heat transfer model. Geometrical parameters, such as shank spacing (with maximum, average and minimum values) and borehole diameter (large, medium and small borehole sizes) and borehole depth (shallow, average and deep borehole depths) as well as thermal conductivity of soil and grout which ranges from minimum to high value were considered. The combined impact of these parameters was included under four major cases: 1) combined effect of borehole depth, borehole size and shank spacing; 2) combined effect of borehole depth, and soil and grout thermal conductivity; 3) combined effect of soil and grout thermal conductivity and borehole size; and 4) combined effect of soil thermal conductivity, borehole size and shank spacing. Each of these major cases has nine different design options of both sBHE and dBHE. Series of results of heat transfer per unit borehole depth were generated for all the considered various cases. With the given parameters, the BHE case that provides highest heat transfer among the various cases of sBHE and dBHE were obtained.

Keywords: borehole heat exchanger; heat transfer per unit borehole depth; shank spacing; borehole size; combined impact of parameters; convective heat transfer coefficient

1. Introduction

Ground source heat pump (GSHP) technologies integrated with ground heat exchanger play a significant role in reducing the global energy consumption for space heating and cooling, and hence crucial in mitigating building's energy contribution to greenhouse gas emission. Because of this, GSHP system has recently received more attention globally. Particularly in North America and Europe, the demand for GSHP technology for space heating and cooling application in the reduction of energy consumption (Pasquier and Marcotte, 2012) is growing due to its higher energy efficiency and environmentally friendly (Hu et al., 2013; Sarbu and Sebarchievici, 2014) as compared to the common heat pump system that utilizes ambient air as heat source. This could be attributed to the fact that the GSHP system utilizes the ground with balanced temperature which in turn results in improving its performance. GSHP system can be integrated with ground heat exchangers of different pipe installations: horizontal (where continuous pipe loops are placed horizontally) and vertical (pipe loops are placed vertically). Most commonly, GSHP system is integrated with vertical ground heat exchanger, called borehole heat exchanger (BHE), where the working fluid that flows in the U-tube pipe exchanges heat with both the refrigerant of the heat pump and the ground around the borehole. As the basic component, BHE is commonly coupled to GSHP because of its flexibility, high efficiency, high heat transfer capacity in a limited area (Florides and Kalogirou, 2007) and less land area requirement than horizontal ground heat exchanger (Javadi et al., 2019; Fang et al., 2017). However, the cost of installation of vertical ground heat exchanger is much higher (Rosen and Koohi-Fayegh,

 doi:10.20944/preprints202403.0448.v1

2017). On the other hand, horizontal ground heat exchangers are more economical in the place where more land area is available, and trenches are easy to excavate (Florides et al., 2013). Among the various geometry of U-tube (single, double, triple and multiple U-tube), BHEs with single and double U-tube configurations are commonly integrated with GSHP system to provide space heating and cooling.

Ground source heat pump (GSHP) systems integrated with ground heat exchangers have a variety of applications in both residential and commercial settings. The main applications of GSHP systems include space heating and cooling, providing domestic hot water for residential and commercial buildings, industrial process heating and cooling and agricultural applications. Aside from direct heating and cooling of buildings, various reports have shown that GSHP can also be utilized in industrial processes, such as in food and textile production (Erbay et al., 2017a; Erbay et al., 2017b). GSHPs can also be utilized to effectively and sustainably heat and cool greenhouses, increasing agricultural output and reducing waste (Xu et al., 2022; Yang et al., 2022). GSHPs provide energy-efficient refrigeration and temperature control, reducing food spoilage and waste. GSHPs can also be used for heating and cooling food storage facilities, warehouses, and other infrastructure, allowing items to be kept in good conditions for extended periods of time. Moreover, the application of GSHPs (for heating and cooling) is growing wider by integrated it with different heating and cooling storage technologies (such as solar collectors, phase change material and ice storage tank) (Zhu et al., 2014).

Various research studies have been done on these two common BHE configurations with respect to heat transfer analysis, modelling and performance comparison between the two. Specifically, these investigations mainly emphasized on heat transfer performance assessment of various BHE configurations, effect of geometric parameters and thermo-physical properties of fluid and material and ground water movement on overall heat transfer in the BHE, whereas other studies focused on comparative assessment of performance between different BHE configurations.

Over the last decade, the heat transfer performance of ground heat exchangers has become the core subject of several research investigations on BHE with different configurations. In this regard, several researchers have studied the performance of BHE through the development of different model for the prediction of heat transfer in the borehole heat exchanger. The heat transfer performance of the BHE was studied by Molina-Giraldo et al. (2011) through the development of a new analytical method (moving finite line source model) that considers the impact of ground water flow and axial heat transfer. In their approach, the authors compared the new method with previous standard finite line source model and moving infinite line source model. Moreover, the new approach was validated with 3D numerical model, the temperature response predicted by the new method agreed well with the corresponding numerical solution. However, the model was restricted to a constant heat transfer per unit borehole length while it is not capable of analyzing variable heat load and multiple boreholes. To evaluate the impact of unsaturated and inhomogeneous ground conditions on performance of vertical ground heat exchanger (BHE) with single U-tube, Jung et al. (2011) established a three-dimensional numerical transient heat transfer model and compared with analytical infinite line source model. With the developed model, the authors evaluated the performance of the BHE in the intermittent and continuous operation in both heating and cooling mode of operation. Their simulation result revealed that the performance of the ground heat exchanger in unsaturated soil is reduced by 40% compared to that in saturated soil condition. It was also reported that the ground temperature in unsaturated condition revealed larger variation than that below ground water table. Finally, the authors obtained that intermittent operation of the ground heat exchanger provided better thermal performance than that of continuous operation.

Using experimental method, Luo et al. (2013) evaluated the thermal performance of the double U-tube BHE integrated with GSHP system that supply heating and cooling effect for office building. The impact of borehole diameter on thermal performance, and the effect of ambient temperature on operation mode of BHE was investigated. Their result indicated that the thermal performance of the BHE is slightly improved with increasing borehole diameter; and it was also obtained that the ambient temperature strongly affected system operation. In order to study the thermal performance

 doi:10.20944/preprints202403.0448.v1

of the BHE, Yang et al. (2014) developed an analytical heat transfer model that takes the variation of fluid temperature along the borehole length and thermal interference between two adjacent legs of the BHE. Using the developed model, the impact of various parameters on thermal effectiveness of the BHE was conducted. It was concluded that enhancement of the thermal effectiveness of the BHE is primarily achieved by improving the thermal properties of the grout material and layout style of the U-tube, and by increasing the spacing between two legs of the BHE; while the thermal effectiveness was found to be independent of fluid inlet temperature, borehole wall temperature and fluid flow direction. Based on multipole theory, Hu et al. (2013) developed an experimentally validated analytical heat transfer model to evaluate the heat transfer performance of the single U-tube BHE. The model improved the boundary shape restriction of traditional analytic model; however, the heat transfer outside the BHE was not taken into consideration, and hence, the ground thermal response cannot be studied by this model. The authors performed dynamic simulation to investigate the impact of key borehole geometrical parameters and thermal properties on thermal effectiveness of the BHE. The result of their study indicated that increasing the thermal conductivity of grout and soil, widening the shank spacing, increasing the borehole depth and flow velocity improve the thermal effectiveness of the BHE. Using quasi-three-dimensional approach along with effectiveness-NTU (number of transfer units) theory, Conti et al. (2016) developed analytical heat transfer model that can effectively predict the thermal performance of the double U-tube BHE. Specifically, the authors proposed comprehensive expressions that can be used to determine the heat transfer rate per unit borehole length and the return temperature of the working fluid in a BHE with different geometric features, flow arrangement (series or parallel) and operating conditions. However, the proposed model cannot be applied for the application of short-time thermal responses. For example, time evolution of the supply conditions from heat pump unit cannot be predicted, and hence the model cannot be applied to evaluate the thermal responses of the BHE that varies within short period of time. Biglarian et al. (2017) developed a 2D numerical heat transfer model along with thermal capacity model that can be applied to perform dynamic simulation of heat transfer in single U-tube BHE. The developed model can be applied to predict short- and long-term thermal responses of the single U-tube BHE while it cannot be implemented for the prediction of the thermal performance of the BHE with double U-tube configuration. Cao et al. (2017), applied both experimental and CFD simulation methods to study the thermal performance of BHE in terms of heat transfer per unit borehole depth and temperature difference (between inlet and outlet fluid temperature). The authors compared the thermal performance BHEs made of steel and polyethylene (PE) materials in both continuous and intermittent operating conditions. It was concluded that BHE with steel pipe exhibited better thermal performance and lower thermal resistance (with up to 7% difference) than that of BHE made PE material. For the overall understanding of the heat transfer characteristics in the borehole thermal energy storage, Zhu et al. (2019) presented an experimentally validated three-dimensional numerical model that can predict unsteady heat transfer in the double U-tube BHE. Using the model, the authors analyzed transient thermal performance of the BHE and ground temperature distribution. They also studied the impact of borehole operating parameters on axial and radial ground temperature distribution while investigation of the impact of other factors (borehole geometrical parameters, thermal properties, permeability, ground water movement etc.) on thermal performance and various temperature distribution were not covered in their study. To analyze transient heat transfer inside and outside the single U-tube BHE, Kerme and Fung (2020a) presented numerical heat transfer model. Various temperature distributions were investigated, and sensitivity analysis were also made to investigate the impact of various borehole parameters on thermal performance and temperature distribution. In another investigation, Kerme and Fung (2020b) developed a numerical model that can predict transient heat transfer and temperature distributions for different cases of operating conditions of the double U-tube BHE.

Several investigations, which were mostly done by developing heat transfer model and some through experimental set up, have been made on thermal performance comparison among different BHEs with different design configurations (Zeng et al., 2003a; Li et al., 2006; Gao et al., 2008; Florides et al., 2013; Pu et al., 2015; Zhang et al., 2015; Conti et al., 2016; Adamovskýa et al., 2017; Fang et al.,

 doi:10.20944/preprints202403.0448.v1

2017; Sivasakthivel et al., 2017; Qi et al., 2019). For the better understanding of the heat transfer process in the borehole heat exchanger (BHE), Zeng et al. (2003) developed quasi-three-dimensional analytical heat transfer model that considers vertical convective heat transfer and thermal interference between the legs of the BHE. Analytical expressions that can predict fluid temperature profiles along the borehole length as well as the total borehole thermal resistance were generated for single and double U-tube BHE with various possible borehole configurations and fluid flow circuit arrangements. The result of their analysis revealed that double U-tube BHE with parallel circuit arrangement exhibited better heat transfer thermal performance and less borehole thermal resistance than single and double BHE with series configurations. Even though the model developed by Zeng et al. (2003) can be utilized for cases of steady state performance analysis of BHE, it cannot be used to evaluate the dynamic thermal performance of the BHE since steady state heat transfer within the BHE was assumed; moreover, vertical borehole wall temperature variation and ground temperature distribution cannot be predicted by their model. In order to examine the thermal performance of BHE, Li et al. (2006) prepared an experimental set up for BHE with single and double U-tube borehole configuration. The authors investigated the impact of various conditions (such as soil and grout thermal properties, borehole operating conditions/modes and number of U-tube pipes) on thermal performance of the BHE. The result of their investigation showed that the heat transfer rate per unit borehole depth of the double U-tube BHE is 50% and 45% more than that of the single U-tube BHE in the heat injection and extraction mode respectively. Among the studied parameters, the heat transfer is highly influenced by the change in fluid inlet temperature; for instance, in the heat injection mode, it was found that when inlet temperature is increased by 5 °C (30 to 35 °C), the heat transfer rate per unit borehole depth is improved by 20% and 100% for single and double U-tube BHE, respectively.

Heat transfer performance of the single, double U-tube and BHE with multi-tube in the cooling mode of operation was experimentally studied by Jalaluddin et al. (2011). The BHEs were compared in terms of heat transfer per unit borehole length for the same working condition. It was concluded that double U-tube BHE exchanged highest heat transfer while the BHE with single U-tube resulted in lowest heat transfer rate. It was also obtained that the heat transfer rate of double U-tube and multitube increases with highest flow rate while it stays constant for single U-tube. In most of the BHE models, the ground around the BHE has been assumed homogeneous (i.e., availability of different ground layers has been neglected). In order to overcome this short coming, Florides et al. (2013) developed 3D conduction and convective heat transfer model that can be applied to a BHE with single and double U-tube surrounded by multiple layers of ground regime by dividing the vertical depth of the borehole into equal parts. Using the model, the authors investigated the performance comparison between single and double U-tube BHE; they also studied the impact of multiple ground layer on the outlet temperature of the working fluid. Their results showed that double U-tube with parallel configuration is 26-29% more efficient than BHE with single U-tube. Furthermore, their result revealed that the thermal energy is stored (distributed) more on the top layer. Adamovskya et al. (2017) experimentally investigated the performance of the commonly utilized BHE configurations (single and double U-tube) in terms of specific thermal power and specific thermal energy in the heating period. Their result revealed that BHE with double U-tube is more effective with more total specific energy and heat transfer rate per unit length than that of single U-tube. Experimental set up was developed by Sivasakthivel et al. (2017) in order to investigate dynamic thermal performance of the single and double U-tube BHE (in both heating and cooling mode of operation). Their experimental result showed that the thermal potential for heat transfer and effectiveness is more for double U-tube BHE than that of single U-tube BHE. The performance and ground temperature distribution of GSHP system is substantially affected by the connection configuration (series and parallel) of ground heat exchangers. In order to investigate this impact, Pu et al. (2019) investigated the heating performance of the GSHP system both numerically and experimentally. It was concluded that ground heat exchangers with parallel configuration resulted in more thermal performance and less pressure drop (between inlet and outlet) than that of series configuration. Nevertheless, the authors did not study the profile of the thermal performance and

 doi:10.20944/preprints202403.0448.v1

pressure loss in turbulent flow condition. Similar investigation was made by Qi et al. (2019) where the thermal performance comparison between BHEs linked in parallel and series configurations was done based on experimentally validated dynamic model. Here too, their simulation result indicated that BHE with parallel configuration showed higher thermal performance than that of BHE with series configuration.

A number of studies have been conducted to investigate the variations in thermal performance of BHE due to changes in BHE geometry such as pipe separation. According to Makasis et al. (2018), the commonly held assumption that vertical pipes (loops) of the BHE remain equally spaced over the length of the borehole can result in thermal interference and degrade system performance. Using model with a sinusoidal-based pipe geometry, these researchers evaluated the influence of this interference comparing different geometries and modelling both constant and variable pipe separations. They identified some significant design parameters and found that the back fill material can reduce the negative effects of thermal interference by up to 60%. More recently, Choi et al. (2022) used probabilistic uncertainty quantification to investigate the thermal resistance of BHEs. They used Monte Carlo simulations to probabilistically quantify the uncertainty of thermal resistance caused by uncertain characteristics, considering four scenarios. They found that the use of spacers greatly improved thermal resistance and reduced its uncertainty range, and their results suggested that thermal response tests cannot sufficiently represent the entire borefield. Sadler et al. (2017) evaluated the impact of thermal shunt effect (TSE) on overall performance of BHE. They found that TSE increases with larger borehole depth, pipe diameter and pipe-to-pipe spacing; and they obtained that pipes arrangement has great impact on elimination of TSE in deep U-pipes. However, these studies have not included the comparison between single and double U-tube BHE.

A number of research investigations have also been made on sensitivity analyses of parameters or factors that significantly impacts the rate of heat transfer in the borehole heat exchanger (BHE) as stated in various literatures (Zeng et al., 2003; Hu et al., 2013; Casasso and Sethi, 2014; Minaei and Maerafat, 2017a; Tang and Nowamooz, 2019; Kerme and Fung, 2020a; Zhang et al., 2020). These investigations mainly focused on the effect of borehole geometrical parameters such as borehole depth (Jun et al., 2009; Sandler et al., 2017; Chen et al., 2016; Li et al., 2014; Casasso and Sethi, 2014; Zhai et al., 2017), borehole diameter (Luo et al., 2013, Minaei and Maerafat, 2017a) and shank spacing (Jun et al., 2009; Casasso and Sethi, 2014; Zhang et al., 2015; Minaei and Maerafat, 2017a). The result of these studies revealed that the thermal performance of the BHE improves with increasing borehole diameter, borehole depth and shanks spacing. The effect of pipe material of the BHE (Hantsch and Gross, 2013; Cao et al., 2017; Kim et al., 2016) and pipe diameter (Zhang et al., 2015; Zhou et al., 2016) was also investigated; and it was concluded that the thermal performance slightly improves with pipe outer diameter and pipe material. Various researchers have also examined the effect of thermal conductivity of grout and ground/soil on thermal performance and design of BHE (Jun et al., 2009; Casasso and Sethi, 2014; Zhang et al., 2015; Han and Yu, 2016; Minaei and Maerafat, 2017a; Kerme and Fung, 2020a). A number of studies which put emphasis on the impact of BHE operating parameters such as fluid inlet temperature (Jun et al., 2009; Zhang et al., 2015; Han and Yu, 2016) and flow velocity (Jun et al., 2009; Zhou et al., 2016; Jalaluddin et al., 2011; Han and Yu, 2016) have also been made.

However, the aforementioned research works are not comprehensive as they deal with the impact of only a single or some few parameters. Detailed combined impact of increasing grout and/or soil thermal conductivity along with borehole geometrical parameters (borehole size or diameter, shank spacing) on total heat transfer per unit borehole depth was not investigated. For example, if a BHE with deep or shallow borehole depth with low or high grout thermal conductivity is required to be designed to deliver the highest heat transfer rate per unit borehole depth, then which cases of design option of BHE is the best to consider? Is that sBHE or dBHE with large or small borehole size, high or low shank spacing and low or high soil thermal conductivity? The response to such important BHE design questions have not yet been covered in the previous studies of BHE. In fact, these questions cannot be easily answered as simple as they seem since the heat transfer in the BHE

 doi:10.20944/preprints202403.0448.v1

is complex and need thorough analysis. Hence, investigation of combined effect of BHE parameters in a systematic approach is important.

Due to the complex nature of heat transfer in the BHE, presentation of this heat transfer in tabular/graphical form that enables BHE designers to conveniently and easily select the case that suits/fulfills the respective thermal design requirement (i.e., high heat transfer) is highly demanded. Such detailed investigation of the overall impact of various parameters on heat transfer in the BHE is used as quick reference for the design and optimization of the BHE integrated with GSHP system. Such investigation was not done before. Hence, comprehensive sensitivity analysis that involves combined impact of parameters becomes necessary.

Therefore, in this paper, combined effect of major influencing parameters that affect the heat transfer in the single U-tube BHE (sBHE) and double U-tube BHE (dBHE) was performed. The combined impact of different parameters was included and studied under four major cases: combined effect of borehole depth, borehole size and shank spacing; combined effect of borehole depth, and soil and grout thermal conductivity; combined effect of soil and grout thermal conductivity and borehole size; combined effect of soil thermal conductivity, borehole size and shank spacing. Each of these major cases has various design options of sBHE and dBHE. Using validated numerical heat transfer model, series of heat transfer data in graphical form that helps to investigate the combined impact various parameters on heat transfer per unit borehole depth will be generated for all the considered cases. Among the various cases of sBHE and dBHE., the case that provides highest heat transfer per unit borehole depth will also be specified.

Furthermore, the impact of convection heat transfer coefficient and flow regime on heat transfer per unit borehole depth of sBHE and dBHE was studied. Evaluation of total pressure loss in the BHE as well as pumping power required to circulate the fluid in the BHE was made; and the two BHEs were also compared in terms of total pressure loss/head loss as well as pumping power.

Proper design and optimization of BHEs is crucial for improving the overall thermal performance and total cost of the GSHP system, making it more attractive for widespread adoption. As a result, design of BHE is crucial for design and performance analysis of GSHP system. On the other hand, the heat transfer in the BHE is complex as it involves different modes of heat transfer processes that depends on multiple factors: borehole geometrical parameters, thermal properties, flow types and geological conditions (underground water flow) etc. The heat transfer process in the BHE includes conduction (which occurs in the ground, the back-fill material and the pipe walls and partially in the fluid) and convection that occurs primarily in the heat transfer fluid. Because of this heat transfer complexity, there is a challenge on thermal design of BHE that considers the overall dynamics of the BHE, and hence used for proper design of the GSHP system integrated with BHE.

Overall, the four major cases considered in the analysis are significant because they help to identify the combined effects of various parameters on the heat transfer performance of single and double U-tube borehole heat exchangers (BHEs). The result of this study is important as a quick reference in the design and optimization of single and double U-tube BHEs that can be integrated with ground source heat pump system.

2. Description of the Model Adopted

The heat transfer mechanism in the BHE consists of convection between working fluid and tube wall, conduction between tube wall and back fill material as well as conduction between back-fill material and the soil/ground. Evaluation of the total heat transfer in the BHE is performed by considering the borehole region as inside and outside, and analysis of the two regions are related by the surface (wall) temperature of the borehole. For the simulation and analysis of heat transfer in the single and double U-tube BHEs, our previously developed model (Kerme and Fung, 2020b) was adopted. Firstly, the numerical model is developed for the double U-tube BHE and then this model is modified to allow the simulation and analysis of BHE with single U-tube configuration. This applied numerical model, which was developed from energy balance made on nodes inside and outside the BHE, is presented in detail in our previous work (Kerme and Fung, 2020b). The differential heat transfer equations that govern the heat transfer between fluid in the BHE and the

 doi:10.20944/preprints202403.0448.v1

soil/ground are obtained by making energy balance on fluid, grout and ground elements. These heat transfer equations are then discretized in order to be solved by numerical method. Due to its high accuracy and stability, implicit numerical method proposed by Crank-Nicolson (Nellis, 2009), is implemented to iteratively solve the equations at each time step. MATLAB is used as the numerical solving tool.

The sectional view of the double U-tube pipe configuration and geometrical borehole parameters are shown in Figure 1. The pipes are considered symmetrically placed in the borehole with two independent circuits: 1-3 and 2-4. In the considered parallel arrangement 1-3, 2-4: 1 and 2 are the inlets while 3 and 4 are outlets of the working fluid. Arrangement 1-3 was considered for the single U-tube BHE configuration.

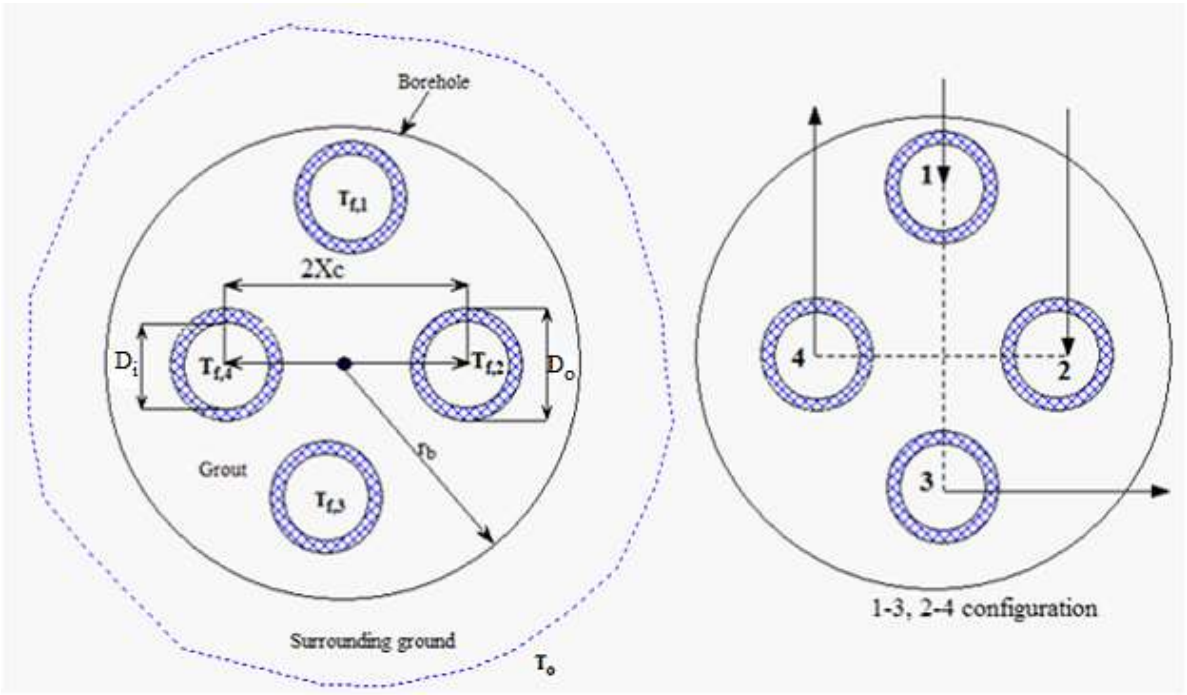

Figure 1. Borehole parameters and the cross-section of the borehole configuration.

Different thermal resistances of fluid and grout inside the considered vertical double U-tube BHE and the surrounding soil thermal resistances is shown in Figure 2a. The corresponding single U-tube configuration is obtained by removing one U-tube from the double U-tube configuration shown in Figure 1, without altering the other geometrical parameters. The corresponding thermal circuit of BHE with single U-tube is presented in Figure 2b.

Preprints.org (www.preprints.org) | NOT PEER-REVIEWED | Posted: 7 March 2024 doi:10.20944/preprints202403.0448.v1

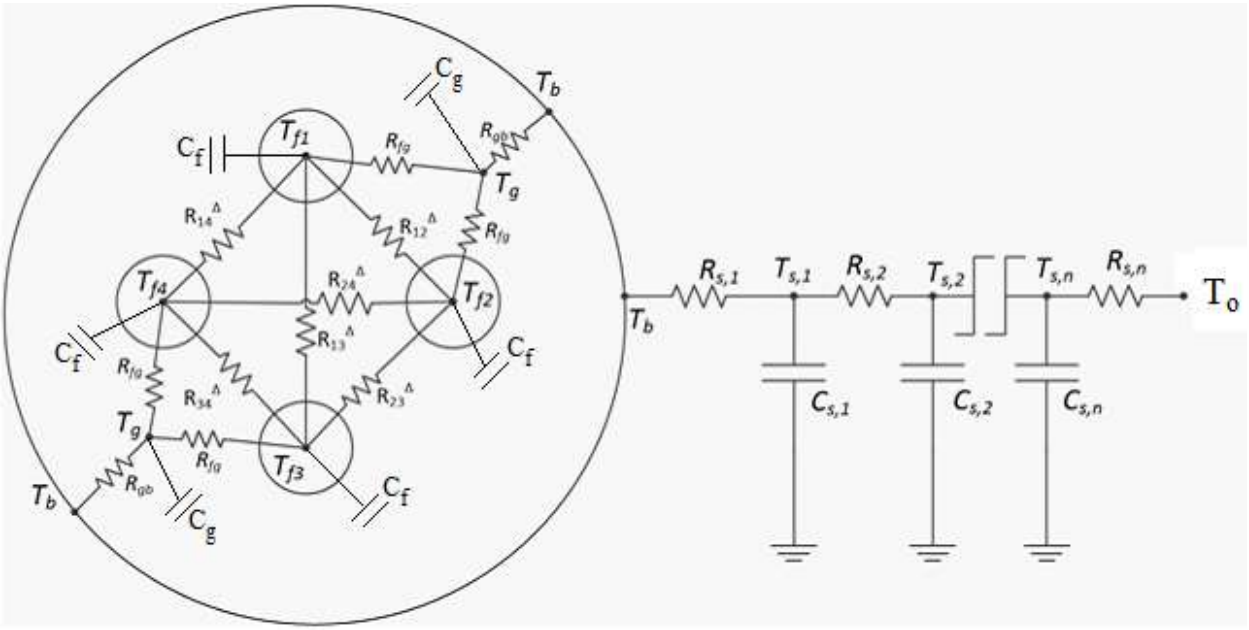

Figure 2. a. Thermal circuit of the BHE with double U-tube configuration.

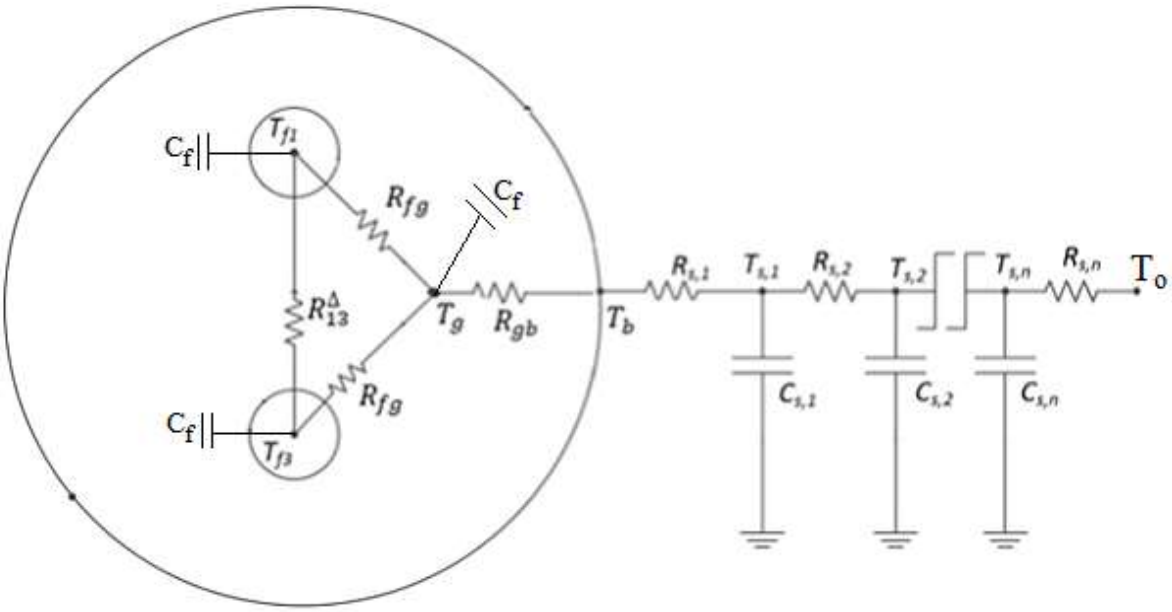

Figure 2. b. Thermal circuit for the BHE with single U-tube configuration.

The governing heat transfer Equations (1) to (6) are obtained by making energy balance on fluid grout and ground nodes outside the borehole (Kerme and Fung, 2020b).

Heat transfer equation for the i^{th} fluid node in *pipe-1* is given by Equation:

$$M_{f1}C_{f1}\frac{dT_{f1}}{dt} = \dot{m}_{f1}C_{f1}\,T_{f1,i-1} - \dot{m}_{f1}C_{f1}T_{f1,i} + \frac{T_{f2,i}-T_{f1,i}}{R_{12}^{\Delta}/\Delta z} + \frac{T_{f3,i}-T_{f1,i}}{R_{13}^{\Delta}/\Delta z} + \frac{T_{f4,i}-T_{f1,i}}{R_{14}^{\Delta}/\Delta z} + \frac{T_{g,i}-T_{f1,i}}{R_{fg}/\Delta z} \quad (1)$$

In Equation (1) and other equations, *i* designates the location of the node in the vertical direction; and *i-1* and *i+1* in all Equations represents upper and lower nodes with respect to node i, the fluid element on which the energy balance was made.

 doi:10.20944/preprints202403.0448.v1

Similarly, the heat transfer equation for the i[th] fluid node in *pipe-2* is given as:

$$M_{f2}C_{f2}\frac{dT_{f2}}{dt} = \dot{m}_{f2}C_{f2}\,T_{f2,i-1} - \dot{m}_{f2}C_{f2}T_{f2,i} + \frac{T_{f1,i}-T_{f2,i}}{R_{21}^{\Delta}/\Delta z} + \frac{T_{f3,i}-T_{f2,i}}{R_{23}^{\Delta}/\Delta z} + \frac{T_{f4,i}-T_{f2,i}}{R_{24}^{\Delta}/\Delta z} + \frac{T_{g,i}-T_{f2,i}}{R_{fg}/\Delta z} \quad (2)$$

The governing equation for the i[th] fluid node in *pipe-3* is obtained by:

$$M_{f3}C_{f3}\frac{dT_{f3}}{dt} = \dot{m}_{f3}C_{f3}\,T_{f3,i+1} - \dot{m}_{f3}C_{f3}T_{f3,i} + \frac{T_{f1,i}-T_{f3,i}}{R_{31}^{\Delta}/\Delta z} + \frac{T_{f2,i}-T_{f3,i}}{R_{32}^{\Delta}/\Delta z} + \frac{T_{f4,i}-T_{f3,i}}{R_{34}^{\Delta}/\Delta z} + \frac{T_{gi}-T_{f3,i}}{R_{fg}/\Delta z} \quad (3)$$

Likewise, energy balance made on i[th] fluid element inside *pipe-4* provides the following equation:

$$M_{f4}C_{f4}\frac{dT_{f4}}{dt} = \dot{m}_{f4}C_{f4}\,T_{f4,i+1} - \dot{m}_{f4}C_{f4}T_{f4,i} + \frac{T_{f1,i}-T_{f4,i}}{R_{41}^{\Delta}/\Delta z} + \frac{T_{f2,i}-T_{f4,i}}{R_{42}^{\Delta}/\Delta z} + \frac{T_{f3,i}-T_{f4,i}}{R_{43}^{\Delta}/\Delta z} + \frac{T_{gi}-T_{f4,i}}{R_{fg}/\Delta z} \quad (4)$$

The governing heat transfer equation for the grout node is given by the following equation:

$$M_gC_g\frac{dT_{g,i}}{dt} = \frac{T_{f1,i}-T_{g,i}}{R_{fg}/\Delta z} + \frac{T_{f2,i}-T_{g,i}}{R_{fg}/\Delta z} + \frac{T_{f3,i}-T_{g,i}}{R_{fg}/\Delta z} + \frac{T_{f4,i}-T_{g,i}}{R_{fg}/\Delta z} + \frac{T_{b,i}-T_{g,i}}{R_{gb}/\Delta z} \quad (5)$$

The governing heat transfer equation for the soil node outside the BHE is given by:

$$\left.\begin{aligned}\frac{dT_{s,(i,k)}}{dt} &= \frac{T_{s,(i,k-1)}-T_{s,(i,k)}}{M_{s,k}C_s\,R_{s,k}/\Delta z} - \frac{T_{s,(i,k)}-T_{s,(i,k+1)}}{M_{s,k}C_sR_{s,k+1}/\Delta z}\\ &where \quad k = 1,2,3\ldots,m\end{aligned}\right\} \quad (6)$$

for k = 1, $T_{s,0} = T_b$ and for $k = m$, $T_{s,m+1} = T_o$

In Equation (6), *i* and *k* represents the location of the node in the vertical and radial direction respectively. To solve the above equations, an implicit numerical method was adopted due to its ensured stability. In this regard, an implicit Crank-Nicolson numerical approach which has high accuracy and unconditional stability, was utilized to solve the developed differential heat transfer equations (Nellis and Klein, 2009).

According to the Crank-Nicolson approach, the temperature at the time step *j+1* is given by:

$$T_{j+1} = T_j + \left\{\left[\frac{dT}{dt}\right]_{T=T_j,t=t_j} + \left[\frac{dT}{dt}\right]_{T=T_{j+1},t=t_{j+1}}\right\}\frac{\Delta t}{2} \quad (7)$$

Equation (7) is then applied on each of the Equations (1) to (6).

The heat transfer outside the borehole (or the ground temperature around the borehole) varies in axial and radial direction. Thus, the corresponding Crank-Nicolson equation for the soil node (where i and k represent the location of the node in the vertical and radial direction respectively) outside the borehole is given by:

$$T_{s(i,k)}^{j+1} = T_{s,(i,k)}^{j} + \left\{\left[\frac{dT_{s,(i,k)}}{dt}\right]^{j} + \left[\frac{dT_{s,(i,k)}}{dt}\right]^{j+1}\right\}\frac{\Delta t}{2} \quad (8)$$

Finally, all Equations (1) to (7), except Equation (2) and (4), are also the heat transfer modelling equations for the corresponding BHE with single U-tube configuration. Hence, various temperature and heat transfer profiles for the corresponding single U-tube BHE can be obtained by using these equations.

 doi:10.20944/preprints202403.0448.v1

To solve the above modeling equations, boundary conditions of the following were applied (Kerme and Fung, 2020b):

- For the upper fluid node in tube-1 and tube-2, the temperature will become $T_{f1,0}$ and $T_{f2,0}$ respectively, and it will be the same as inlet temperature of the working fluid in the corresponding U-tubes. That is, $T_{f1,0} = T_{f,in}$ and $T_{f2,0} = T_{f,in}$. The fluid inlet temperature in tube 1 and 2 can be made the same or different.
- For both U-tubes, the fluid temperature of the last nth node of downward flow pipe is the same as the temperature of the fluid entering the upward flow pipe: $T_{f1,n} = T_{f3,n+1}$ and $T_{f2,n} = T_{f4,n+1}$.

For the ground nodes outside the borehole:

- The temperature of far-field boundary is assumed to be the same as undisturbed ground temperature (T_o = 10 °C).

2.1. Modelling of Heat Transfer and Other Parameters

In this sub-section, analytical expressions that are used to calculate various thermal resistances appeared in modeling equations are given. In addition, equations that describe the total heat transfer between fluid and ground, borehole thermal resistance and thermal effectiveness of the BHE are provided.

The total heat transfer rate per unit depth between fluid and the ground around the single and double U-tube BHE is evaluated by Equation (9a) and (9b) respectively (Biglarian et al., 2017; Kerme and Fung, 2020b):

$$\left.\begin{aligned} q_b &= \frac{T_{f,1} - T_b}{R_1^{\nabla}} + \frac{T_{f,3} - T_b}{R_1^{\nabla}}, && (a) \\ q_b &= \frac{T_{f,1} - T_b}{R_1^{\nabla}} + \frac{T_{f,3} - T_b}{R_1^{\nabla}} + \frac{T_{f,2} - T_b}{R_1^{\nabla}} + \frac{T_{f,4} - T_b}{R_1^{\nabla}}, && (b) \end{aligned}\right\} \quad (9)$$

Where R_1^{∇} for single and double U-tube BHE are given by Equation (10a) and (10b) respectively (Zeng et al., 2003a; Zeng et al., 2003b).

$$\left.\begin{aligned} R_1^{\nabla} &= R_{11}^{\Delta} + R_{13}^{\Delta} && (a) \\ R_1^{\nabla} &= R_{11}^{\Delta} + R_{13}^{\Delta} + 2R_{12}^{\Delta} && (b) \end{aligned}\right\} \quad (10)$$

where R_{11}^{Δ}, R_{12}^{Δ} and R_{13}^{Δ} are evaluated by the following expressions (Zeng et al., 2003b):

$$\left.\begin{aligned} R_{11}^{\Delta} &= \frac{1}{2\pi k_g}\left[ln\left(\frac{r_b}{r_{po}}\right) - \frac{k_g - k_s}{k_g + k_s} ln\left(\frac{{r_b}^2 - D^2}{{r_b}^2}\right)\right] + R_p \\ R_p &= \frac{1}{2\pi k_p} ln\left(\frac{r_{o,p}}{r_{i,p}}\right) + \frac{1}{2\pi r_i h} \\ R_{12}^{\Delta} &= \frac{1}{2\pi k_g}\left[ln\frac{r_b}{\sqrt{2}D} - \frac{k_g - k_s}{2(k_g + k_s)} ln\left(\frac{{r_b}^4 + D^4}{{r_b}^4}\right)\right] \\ R_{13}^{\Delta} &= \frac{1}{2\pi k_g}\left[ln\left(\frac{r_b}{2D}\right) - \frac{k_g - k_s}{k_g + k_s} ln\left(\frac{{r_b}^2 + D^2}{{r_b}^2}\right)\right] \end{aligned}\right\} \quad (11)$$

 doi:10.20944/preprints202403.0448.v1

where k_g and k_s are the thermal conductivities of the grout and soil (ground) respectively. R_p is the sum of the thermal resistance of fluid and pipe wall, and it is evaluated by:

$$R_p = \frac{1}{2\pi k_p} ln\left(\frac{r_{po}}{r_{pi}}\right) + \frac{1}{2\pi\, r_{pi} h} \quad (12)$$

Where, h is the convection heat transfer coefficient. Since the flow in the U-tube may not be fully turbulent, the Gnielinski (1976) correlation which is valid for turbulent flow down to transitional flow is applied to evaluate the convection heat transfer coefficient (h) as given by Equation (13a); while for laminar flow, the corresponding h is evaluated by Equation (13b) (Shah and Sekulic, 2003; Beier et al., 2014).

$$\left.\begin{aligned} h = \frac{k_f}{D} Nu_D = \frac{k_f}{D} \frac{(f/8)(Re_D - 1000)Pr}{1 + 12.7(f/8)^{\frac{1}{2}}\left(Pr^{\frac{2}{3}} - 1\right)} \quad (a) \\ h = \frac{k_f}{D} Nu_D = 4.36\ \frac{k_f}{D} \quad (b) \\ where, D = 2r_{pi} \end{aligned}\right\} \quad (13)$$

In Equation (13a) , D is the inside diameter of the U-tube pipe; Pr is the Prandtl number and Re_D is the Reynolds number. The Darcy friction factor (f) for turbulent flow can be estimated by the correlation (Colebrook, 1939) given by Equation (14a); while for laminar flow ($Re_D < 2300$), f can be calculated by Equation (14b) (Fox et al., 2011):

$$\left.\begin{aligned} \frac{1}{\sqrt{f}} = -2\log_{10}\left[\frac{\frac{e}{D}}{3.7} + \frac{2.51}{Re_D\sqrt{f}}\right], \quad Re_D \geq 2300 \quad (a) \\ f = \frac{64}{Re_D}, \quad Re_D < 2300 \quad (b) \end{aligned}\right\} \quad (14)$$

In Equation (14a) , D is the inside diameter of the U-tube pipe; e is the roughness and its value for PVC and drawn tubing is 0.0015mm (Fox et al., 2011).

The other important parameter that needs to be evaluated for a BHE is the total borehole thermal resistance (R_b) which is the sum of the conductive resistance of the back-fill material, conductive resistance of the pipe wall and the convective resistance between fluid and pipe wall. Borehole thermal resistance for the single and double U-tube BHE can be obtained as in Equation (15a) and (15b) respectively (Minaei and Maerafat, 2017b).

$$\left.\begin{aligned} R_b = R_g + {R_p}/{2} \quad (a) \\ R_b = R_g + {R_p}/{4} \quad (b) \end{aligned}\right\} \quad (15)$$

Where R_p is the sum of the thermal resistance of fluid and pipe wall; R_g is the grout thermal resistance. The Bauer et al. (2011) expression for grout thermal resistance which was improved for four legs of the double U-tube, as reported by Javed and Spitler (2016), is given by:

$$\left.\begin{aligned} R_g = \frac{1}{8\pi k_g}\left[(3.098 - 4.432\theta_1 + 2.364\theta_1^2)cosh^{-1}\left(\frac{\theta_2}{2} + \frac{1}{2\theta_2} - \frac{\theta_1}{4\theta_3}\right)\right] \\ where \quad \theta_1 = \frac{D}{2r_b};\ \theta_2 = \frac{r_b}{r_{po}};\ \theta_3 = \frac{r_{po}}{D} = \frac{1}{2\theta_1\theta_2} \end{aligned}\right\} \quad (16)$$

The grout thermal resistance for the single U-tube BHE is evaluated by the best fit-correlation suggested by Liao et al. (2012) is given by the following expression:

$$\left.\begin{aligned} R_g = \frac{1}{2\pi k_g}\left[(-0.50125\ \ln\theta_1 + 0.51248\ln\theta_2) + 0.51057\frac{k_g - k_s}{k_g + k_s} ln\left(\frac{1}{1-\theta_1^4}\right) - 0.36925\right] \\ where \quad \theta_1 = \frac{D}{2r_b};\ \theta_2 = \frac{r_b}{r_{po}} \end{aligned}\right\} \quad (17)$$

Thermal resistance between working fluid and grout for double U-tube and single U-tube BHE is obtained by the following Equations (18a) and (18b), respectively (Minaei and Maerafat, 2017b):

 doi:10.20944/preprints202403.0448.v1

$$\left.\begin{aligned} R_{fg} &= 4\left(R_b - R_{gb}\right) \quad (a) \\ R_{fg} &= 2\left(R_b - R_{gb}\right) \quad (b) \end{aligned}\right\} \tag{18}$$

The grout to borehole-wall thermal resistance (R_{gb}) is evaluated by (Minaei and Maerafat, 2017b):

$$\left.\begin{aligned} R_{gb} &= \frac{1}{2\pi k_g}\ln\left(\frac{r_b}{r_g}\right) \\ &where: \\ r_g &= \sqrt{\frac{{r_e}^2 + {r_b}^2}{2}} \\ r_e &= \sqrt{2}\, r_{po} \end{aligned}\right\} \tag{19}$$

Where r_g and r_e are the location of the grout node and equivalent radius respectively.

The pumping power reaching the fluid (which is required to maintain circulation of the fluid in the closed loop of the BHE) and the total pressure drop in the total pipe length of the BHE are other important factors (parameters) that must be considered in the performance study of the BHE. The useful pumping power that is required to keep the circulation of working fluid in the closed loop of the borehole heat exchanger (BHE), the total pressure drop between inlet and outlet of the U-tube pipe and the corresponding total head loss are given by the following equation:

$$\left.\begin{aligned} W_{pump} &= \dot{m}\frac{\Delta P_L}{\rho} \\ \Delta P_L &= \rho g h_L \\ h_L &= \frac{V^2}{2g}\left(K_L + f\left(\frac{L}{D}\right)\right) \end{aligned}\right\} \tag{20}$$

Where m is the total mass flow rate; V is fluid velocity; f is the friction factor evaluated by Equation (14); and D is internal U-tube pipe diameter; ΔP_L is the total pressure loss between inlet and outlet of the U-tube pipe; h_L is the total head loss and K_L is the loss factor where a value of 0.2 was used taking the U-tube as a return bend. The total length (L) in Equation (21) is twice and four times of the borehole depth (H) for single and double U-tube BHE, respectively.

3. Results and Discussion

3.1. Analysis of Major Influencing Parameters on Performance of Borehole Heat Exchanger

Borehole heat exchanger (BHE) is the key component of the ground source heat pump system (GSHP) that delivers space heating and cooling of buildings. It determines the overall thermal performance of the GSHP system. In addition, the total cost of the GSHP system depends on the installation and drilling cost of the BHE.

Due to the complex nature of heat transfer in the BHE, proper modelling and thermal design of BHE that meets the required demand is still challenging. In the design of BHE, thermal performance is an important parameter that determines the effective heat transfer between the soil and GSHP system. Moreover, thermal performance of BHE also determines effectiveness of the operational and running cost of the GSHP system. As a result, comprehensive investigation of BHE from the perspectives of the combined impact of different factors (borehole geometrical parameters and thermal properties) that affect its thermal performance is indispensable.

Heat transfer in the BHE is affected by various factors: geometrical, thermal, geological, and operational parameters. In this regard, investigation of combined effect of parameters in a systematic approach is important. Due to the complex nature of heat transfer in the BHE, presentation of this heat transfer in tabular/graphical form that enables one to conveniently and easily select the case that suits/fulfills the respective thermal design requirement (i.e., high heat transfer) is highly demanded. Such detailed investigation of the overall impact of various factors on heat transfer in the BHE is used as quick reference for the design and optimization of the BHE integrated with GSHP system. In this paper, combined effect of major influencing parameters that affect the performance of both single U-

 doi:10.20944/preprints202403.0448.v1

tube BHE (sBHE) and double U-tube BHE (dBHE) will be performed. For the sake of convenience, the combined impact of different parameters is included under the following four major cases (where each of them has nine different sub-cases shown in Table 2):

A) Combined effect of borehole depth (H), borehole size (D_b or r_b) and shank spacing (X_c)

B) Combined effect of borehole depth (H), and soil (k_s) and grout (k_g) thermal conductivities

C) Combined effect of soil (k_s) and grout (k_g) thermal conductivities and borehole size (D_b or r_b)

D) Combined effect of soil thermal conductivity (k_s), borehole size (D_b or r_b) and shank spacing (X_c)

The values of fixed borehole geometrical parameters and thermal properties considered under each case studies are listed in Table 1.

Table 1. Fixed input values of parameters and thermal properties used in the analysis.

PARAMETERS	VALUES	REMARKS
Inner radius of the pipe	0.014m	Pipe thickness of 2mm
Outer radius of the pipe	0.016m	Pipe outer diameter 32mm
Thermal conductivity of the HDPE pipe	0.4 W/m-K	
Working Fluid Properties:		
Fluid type	Water	
Specific heat capacity of fluid	4183 J/kg-K	
Density of circulating fluid	997 kg/m^3	
Thermal conductivity fluid	0.5947 W/m-K	
Dynamic viscosity of fluid	0.8905x10^{-3} kg/m-s	
Inlet fluid temperature	40 °C	
Grout thermal properties:		
Specific heat capacity of the grout	1850 J/kg-K	
Density of grout	2650 kg/m^3	
Soil thermal properties		
Specific heat capacity of the soil	2016 J/kg-K	
Density of the soil	2650 kg/m^3	
Undisturbed ground temperature	10 °C	

Table 2. The four major cases considered to investigate the combined effect of different parameters on performance of the sBHE and dBHE.

A. Combined effect of borehole depth, borehole size and shank spacing	**B. Combined effect of borehole depth and thermal conductivity of grout and soil**	**C. Combined effect of soil and grout thermal conductivity and borehole size**	**D. Combined effect of soil thermal conductivity, borehole size and shank spacing**
1: Small borehole size	***1: Minimum soil thermal conductivity***	***1: Minimum grout thermal conductivity***	***1: Small (minimum) borehole size***
D_b = 100mm	k_s= 0.3 W/m.K	k_g = 0.5 W/m.K	D_b = 100mm
X_c = 0.034m (maximum)	k_g = 2.2 W/m.K (maximum)	r_b = 0.1m (maximum)	X_c = 0.034m (maximum)
X_c = 0.025m (medium)	k_g = 1.5 W/m.K (medium)	r_b = 0.073m (medium)	X_c = 0.025m (medium)
X_c = 0.016m (minimum)	k_g = 0.5 W/m.K (minimum)	r_b = 0.05m (minimum)	X_c = 0.016m (minimum)

 doi:10.20944/preprints202403.0448.v1

2: Medium borehole size	*2: Average soil thermal conductivity*	*2: Average grout thermal conductivity*	*2: Medium borehole size*
D_b =146mm	k_s = 2.2 W/m.K	k_g = 1.5 W/m.K	D_b = 146mm
X_c = 0.057m (maximum)	k_g = 2.2 W/m.K (maximum)	r_b = 0.1m (maximum),	X_c = 0.057m (maximum)
X_c = 0.037m (medium)	k_g = 1.5 W/m.K (medium)	r_b = 0.073m (medium),	X_c = 0.037m (medium)
X_c = 0.016m (minimum)	k_g = 0.5 W/m.K (minimum)	r_b = 0.05m (minimum), X_c= 0.025m	X_c = 0.016m (minimum)
3: Large borehole size	***3: Maximum soil thermal conductivity***	***3: Maximum grout thermal conductivity***	***3: Large (maximum) borehole size***
D_b = 200mm	k_s = 4 W/m.K	k_g = 2.2 W/m.K	D_b = 200mm
X_c = 0.084m (maximum)	k_g = 2.2 W/m.K (maximum)	r_b = 0.1m (maximum)	X_c = 0.084m (maximum)
X_c = 0.05m (medium)	k_g = 1.5 W/m.K (medium)	r_b = 0.073m (medium)	X_c = 0.05m (medium)
X_c = 0.016m (minimum)	k_g = 0.5 W/m.K (minimum)	r_b = 0.05m (minimum)	X_c = 0.016m (minimum)
• H varied from 50 to 275m • With 9 different cases of k_g and k_s	H varied from 50 to 275m (With 9 different Cases of r_b and X_c)	k_s varied from 0.3 to 4 (With 9 different cases of borehole depth (H) and Xc)	k_s varied from 0.3 to 4 (With 9 different cases of borehole depth (H) and k_g)

Table 3. The nine sub-cases considered under each major cases of A to D.

Cases	A. **Combined effect of borehole depth, borehole size and shank spacing** (with 9 different cases of k_g and k_s)	B. **Combined effect of borehole depth and thermal conductivity of soil and grout** (with 9 different Cases of r_b and Xc)	C. **Combined effect of borehole size and thermal conductivity of soil and grout** (with 9 different cases of borehole depth (H))	D. **Combined effect of soil thermal conductivity, borehole size and shank spacing** (with 9 different cases of k_g and H)
1	k_g = 0.5 and k_s = 0.3 W/m.K (minimum-minimum)	r_b = 0.05m, Xc = 0.016m (small BH, minimum Xc)	H = 50m and all Xc (minimum)	k_g = 0.5W/m.K and H = 50m (min. k_g & low H)
2	k_g = 0.5 and k_s = 2.0 (W/m.K) (minimum-average)	r_b = 0.05m, Xc = 0.025m (small BH, average. X_c)	H = 50m and all Xc (average)	k_g = 0.5W/m.K and H = 100m (min. k_g, avg. H)
3	k_g = 0.5 and k_s = 4 (W/m.K) (minimum-maximum)	r_b = 0.05m, Xc = 0.034m (small BH, maximum X_c)	H = 50m and all Xc (maximum)	k_g = 0.5W/m.K and H = 300m (min. k_g, high H)
4	k_g = 1.5 and k_s =0.3 (W/m.K) (average-minimum)	r_b = 0.073m, Xc = 0.016m (medium BH, minimum Xc)	H=100m and all Xc (minimum)	k_g =1.5W/m.K and H = 50m (Avg.k_g & low H)

 doi:10.20944/preprints202403.0448.v1

5	k_g = 1.5 and k_s = 2 (W/m.K) (average-average)	r_b = 0.073m, Xc = 0.037m (medium BH, average X_c)	H = 100m and all Xc (average)	k_g = 1.5W/m.K and H = 100m (avg. k_g, avg. H)
6	k_g = 1.5 and k_s = 4.0 (W/m.K) (average-maximum)	r_b = 0.073m, Xc = 0.057m (medium BH, maximum X_c)	H = 100m and all Xc (maximum)	k_g = 1.5W/m.K and H = 300m (avg. k_g, high H)
7	k_g = 2.2 and k_s = 0.3 (W/m.K) (maximum-minimum)	r_b = 0.1m, Xc = 0.016m (large BH, minimum Xc)	H = 300m and all Xc (minimum)	k_g = 2.2 W/m.K and H = 50m (max. k_g & low H)
8	k_g = 2.2 and k_s = 2.0 (W/m.K) (maximum-average)	r_b = 0.1m, Xc = 0.05m (large BH, average X_c)	H = 300m and all Xc (average)	k_g = 2.2W/m.K and H = 100m (max. k_g, avg. H)
9	k_g = 2.2 and k_s = 4 (W/m.K) (maximum-maximum)	r_b = 0.1m, Xc = 0.084m (large BH, maximum X_c)	H = 300m and all Xc (maximum)	k_g = 2.2 W/m.K and H = 300m (max. k_g, high H)

*Note: X_c is half of the center-to-center distance (half shank spacing).

A. Combined Effect of Borehole Depth, Borehole Size and Shank Spacing

The optimal design of a borehole heat exchanger (BHE) for a ground source heat pump (GSHP) system depends on various factors such as geometrical parameters (borehole depth, borehole size (diameter), and shank spacing), soil thermal conductivity and others. Borehole depth is particularly important because it affects both the performance and cost of the BHE. Although deeper borehole depth may seem to increase the performance of BHE, it can also lead to thermal interaction between the legs of the BHE, which can reduce heat transfer between the working fluid and the ground. Furthermore, deeper boreholes are more expensive to drill. Various questions arise on BHEs. One question is whether a single or double U-tube BHE has lower thermal interaction between legs (thermal short-circuit) at deep borehole depths. Another question is whether it's better to use a deep BHE with small or large shank spacing and with medium or high soil thermal conductivity; and it is important to determine which borehole configuration, sBHE or dBHE, is preferable in each scenario.

Borehole size (diameter) is another crucial geometrical parameter impacting heat transfer in the BHEs. While larger boreholes are generally preferred to enhance heat transfer between the working fluid and the surrounding ground, it is unclear whether small, medium or large boreholes are most effective for shallow or deep boreholes, as other parameters also play a significant role. Furthermore, increasing borehole size raises the cost of the BHE. Another geometrical parameter that affects the heat transfer in the BHE is the shank spacing, which is the center-to-center distance between U-tube legs of the BHE.

Overall, the heat transfer in the BHE is complex and depends on multiple factors, and hence, comprehensive sensitivity analysis that considers combined impact of all parameters should be done. Investigating a single impact of parameter on heat transfer in the BHE is inadequate to determine the variation of the total heat transfer in the BHE. Comprehensive investigation that involves combined effect of various parameters on heat transfer is highly needed for the design and optimization of the BHE. Therefore, presenting the variation of total heat transfer rate per unit borehole depth with different borehole parameters and thermal properties in a convenient way such as in tabular or graphical form becomes essential. Such series of heat transfer data in tables/graphs can be conveniently implemented during the thermal design of the BHE. In other words, when the results of such case studies of BHE with different options of various parameter is available, then BHE designers can utilize such result as a quick reference for the thermal design and optimization of BHE that can be integrated with GSHP system.

 doi:10.20944/preprints202403.0448.v1

To fully assess such combined effect of parameters on total heat transfer per unit borehole depth, analysis involving the combined impact of borehole depth, borehole radius and shank spacing with different cases of soil and grout thermal conductivities will be performed in this section. The analysis of this subsection was done for both sBHE and dBHE with: small borehole size (D_b = 100 mm, and half shank spacing of X_c = 0.034 m (maximum), X_c = 0.025 m (medium) and X_c = 0.016 m (minimum)); medium borehole size with (D_b =146 mm, and half shank spacing of X_c = 0.057 m (maximum), X_c = 0.037 m (medium), X_c = 0.016 m (minimum)); and large borehole size with (D_b = 200 mm and half shank spacing of X_c = 0.084 m (maximum), X_c = 0.05 m (medium) and X_c = 0.016 m (minimum)). This case of combined effect of borehole depth, borehole size and shank spacing was done for nine different cases of combined values of grout and soil thermal conductivities (with minimum, medium, and maximum values) as shown in Table 3. This case is important as a quick reference for the design of BHE with the given nine cases of thermal conductivities of grout and soil. Then one can select the case that provides the highest heat transfer among the various cases of sBHE and dBHE presented under column A of Table 2. The results of these cases are presented in Figs. 3 to 8. Various important information can be obtained from such results.

Figs. 3, 4 and 5 illustrate combined impact of borehole depth, borehole size and shank spacing on heat transfer rate per unit borehole depth for minimum grout and soil thermal conductivity (k_g = 0.5, k_s = 0.3 W/m·K), minimum grout and medium soil thermal conductivities (k_g = 0.5, k_s = 2.2 W/m·K), minimum grout and maximum soil thermal conductivities (k_g = 0.5, k_s = 4 W/m·K) respectively. Comparison of the results depicted in Figs. 3,4 and 5 shows that the case with minimum grout and maximum soil thermal conductivity (shown in Figure 5) provides the highest heat transfer rate per unit borehole depth than all other cases while the case with minimum grout and soil thermal conductivities (shown in Figure 3) provides the lowest heat transfer rate. It is also interesting to note from Figure 3 that when both grout and soil thermal conductivity values are minimum, the dBHE (due to its more surface area) transfers more heat than the sBHE. This is also seen in the other remaining cases. On the other hand, for the other cases of thermal conductivities, the sBHE becomes better to transfer more heat than dBHE particularly at deep borehole depth; for example, sBHE with large borehole size and maximum shank spacing (r_b = 0.1 m and X_c = 0.084 m) seem to provide more heat transfer than dBHE with large borehole size and minimum shank spacing (r_b = 0.1 m, X_c = 0.016 m). As you can see on the trends of Figs. 4 and 5, it seems that for the deep borehole depth, the sBHE transfers more heat than dBHE. The reason for this is that as the borehole depth increases, the short-thermal circuit (thermal interaction between the U-tube legs) increases, and its impact becomes more in dBHE than in sBHE. A close look at Figs. 4 and 5 also shows that (when grout conductivity is low and soil thermal conductivity is at average or high value), using BHE with maximum shank spacing is effective in the largest borehole size while using minimum shank spacing is more effective in BHE with the smallest borehole size. This could also be attributed to the phenomenon of thermal short-circuit.

Overall, the results depicted in Figs. 3, 4 and 5 reveal that the dBHE is preferable to transfer more heat when used in shallow borehole depth, while for the BHE with deep borehole depth, sBHE is better to exchange more heat between the working fluid and the ground that of dBHE. Figs. 3, 4, and 5 also show that in both sBHE and dBHE, BHE with large borehole size (r_b = 0.1 m) and maximum shank spacing (X_c = 0.084 m) provides the highest heat transfer. This could be due to the available more surface area for the heat transfer when borehole size is enlarged and U-tubes are widely spaced.

 doi:10.20944/preprints202403.0448.v1

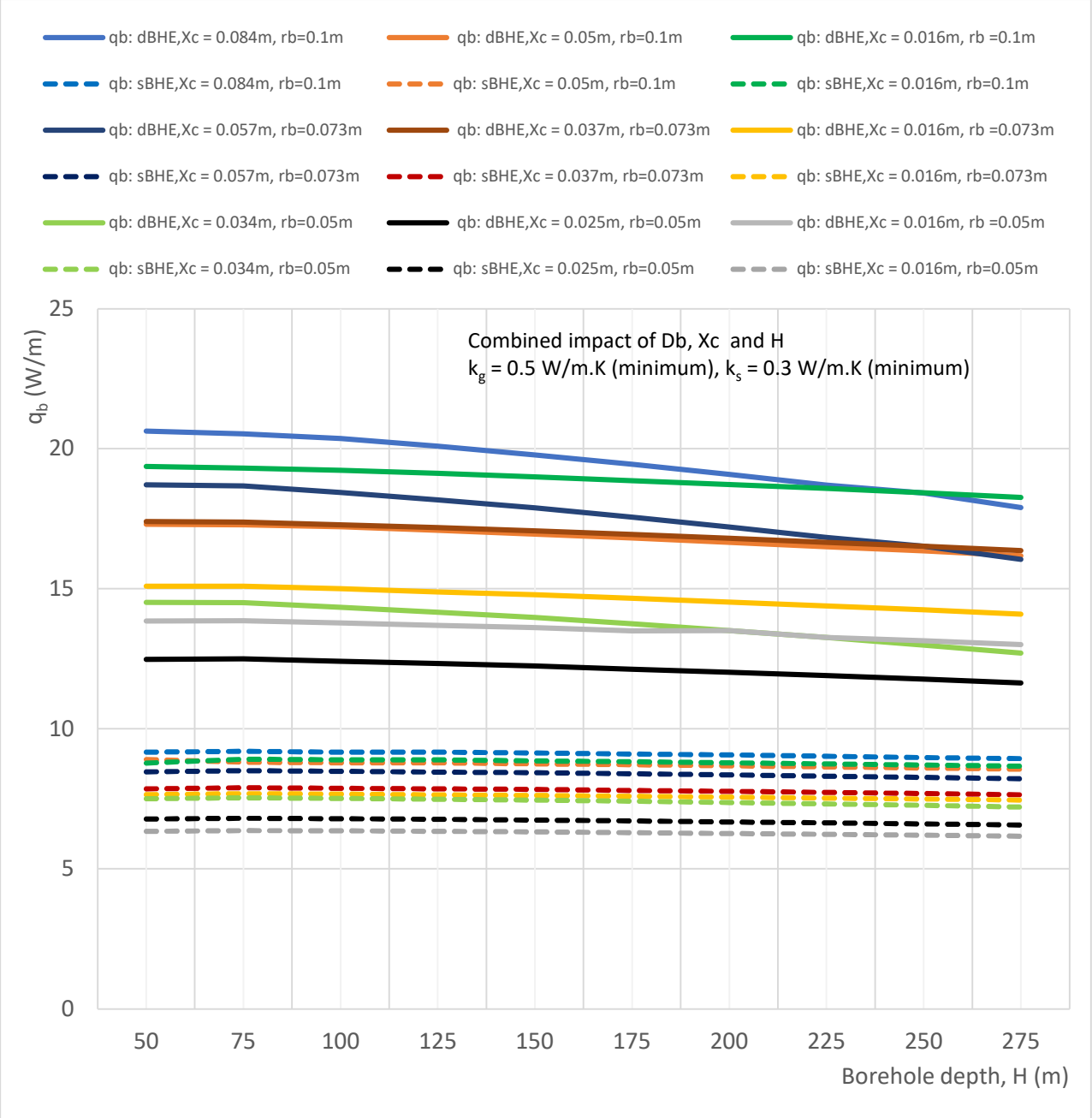

Figure 3. Combined effect of borehole depth, borehole size and shank spacing on heat transfer rate per unit borehole depth in sBHE and dBHE for the case of minimum grout and soil thermal conductivities (k_g = 0.5 W/m·K, k_s = 0.3 W/m·K).

 doi:10.20944/preprints202403.0448.v1

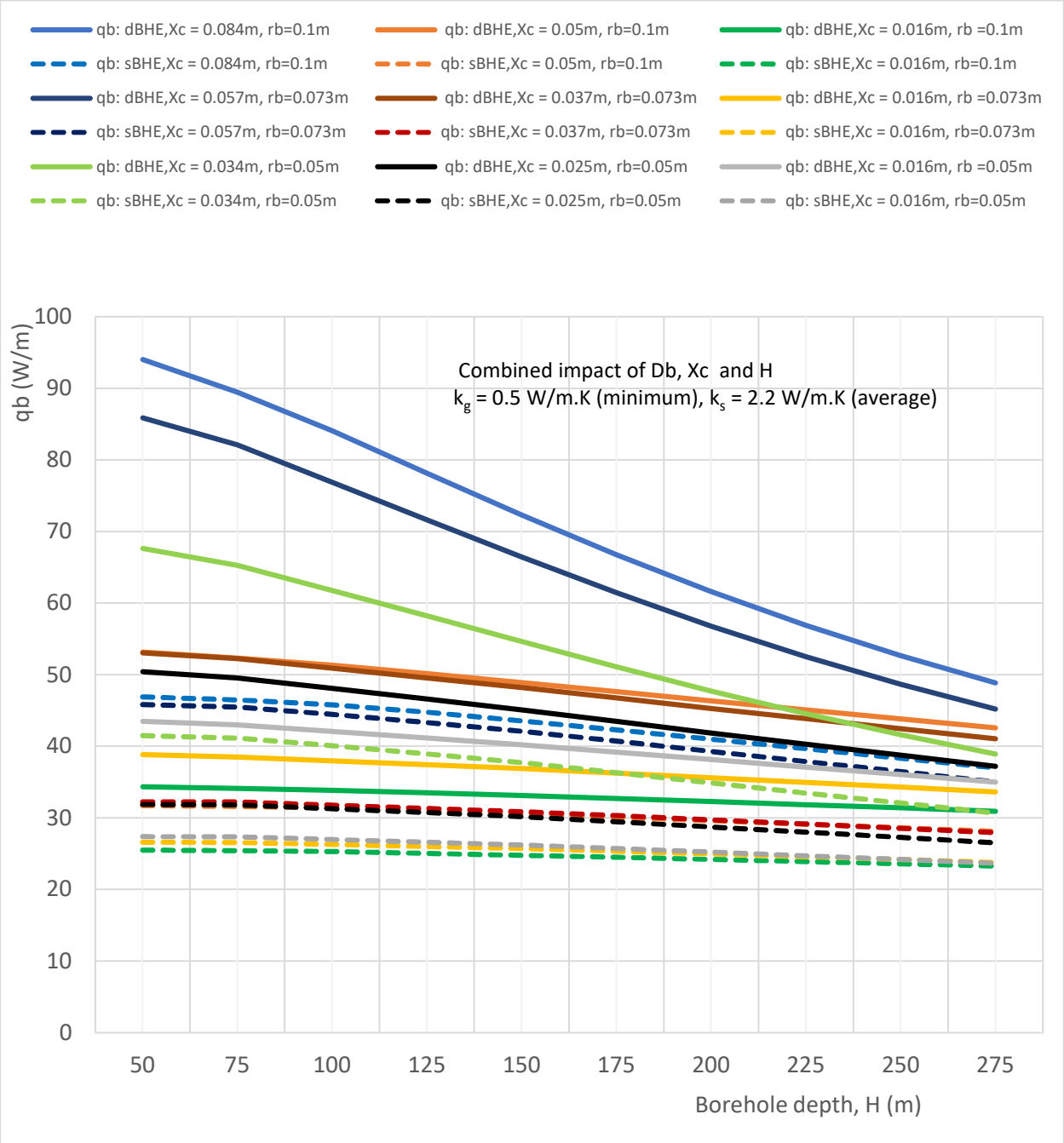

Figure 4. Combined effect of borehole depth, borehole size and shank spacing on heat transfer rate per unit borehole depth in sBHE and dBHE for the case of minimum grout conductivity and average soil thermal conductivities (k_g = 0.5 W/m.K, k_s = 2.2 W/m.K).

 doi:10.20944/preprints202403.0448.v1

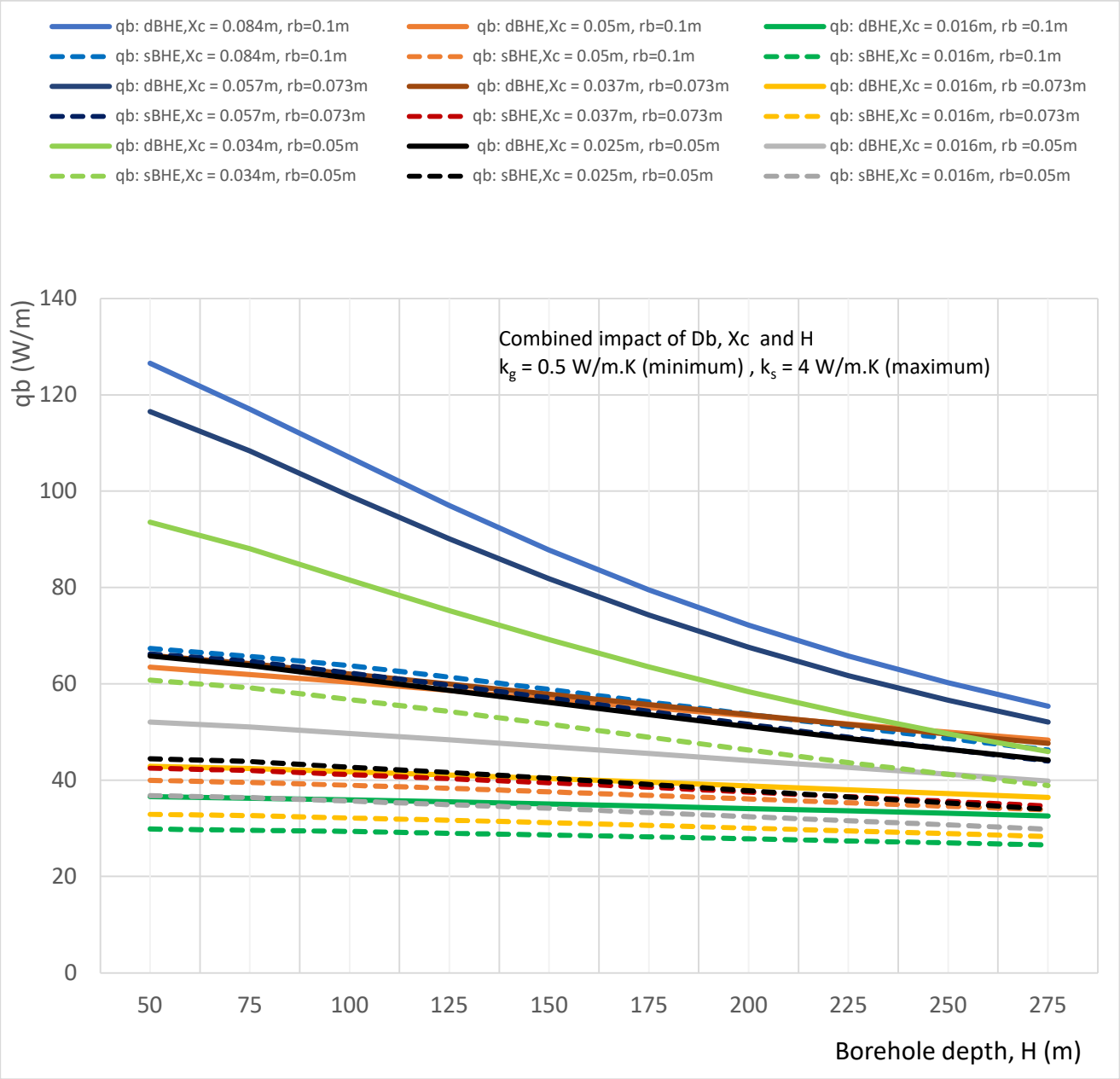

Figure 5. Combined effect of borehole depth, borehole size and shank spacing on heat transfer rate per unit borehole depth in sBHE and dBHE for the case of minimum grout conductivity and maximum soil thermal conductivities (k_g = 0.5W/m.K, k_s = 4W/m.K).

The results generated for the case of the average grout thermal conductivity is almost similar to the to the other results and hence not discussed here. The simulation result generated for the combined impact of borehole depth, borehole size and shank spacing on heat transfer rate per unit borehole depth in sBHE and dBHE for the cases of maximum grout thermal conductivity (k_g = 2.2 W/m.K) combined with minimum, average and maximum soil thermal conductivity is illustrated in Figs. 6, 7 and 8. Now, in these cases though the grout thermal conductivity is maximum, the heat transfer per unit borehole depth is lower than all other corresponding previously discussed cases (cases 1 to 6 in Table 3) depicted in Figs. 3 to 8. This is because employing excessive thermal conductivity of back-fill-material in the BHE may produce thermal interference (thermal short-circuit) between U-tube pipe legs leading to the reduced heat transfer, and hence, reduced BHE performance; and the phenomenon of short-thermal-circuit for the cases in Figs. 6 to 8 could be more

 doi:10.20944/preprints202403.0448.v1

for dBHE with deep borehole depth than sBHE, and it is also relatively higher than the other previously discussed cases of this subsection.

For case of low soil thermal conductivity (k_s = 0.3 W/m.K) shown in Figure 6, all the considered dBHE cases transfer more heat than the corresponding sBHE. However, at deep borehole depth, sBHE (with large borehole size and high shank spacing) seems to transfer more heat than dBHE with small borehole size. This impact is more augmented for the other cases, shown in Figs.10 and 11. That is at the deep borehole depth, the heat transferred by the dBHE with large borehole size (r_b = 0.1m) and maximum shank spacing (X_c = 0.084 m) is significantly reduced and becomes lower than that of the corresponding sBHE. In addition, as shown in Figs. 6 to 8, dBHE with maximum shank spacing provides more heat transfer than all other cases when used in shorter borehole depth; while dBHE with minimum shank spacing is preferable to transfer more heat into the ground when applied in deeper borehole depth. Similarly, in sBHE, BHE with largest borehole size and maximum (highest) shank spacing is preferred to deliver more heat transfer into the ground when employed with shallow borehole depth (see Figs. 7 and 8).

Overall, among the 9 cases listed under the combined effect of borehole depth, borehole size and shank spacing depicted in Figs. 3 to 8, increasing the borehole size and shank spacing is more effective to transfer more heat irrespective of borehole depth for case 3, and dBHE with large BH size and maximum shank spacing employed with low grout thermal conductivity and maximum soil thermal conductivity provides the highest heat transfer per unit borehole depth. On the other hand, the lowest heat transfer is obtained for case 7 where back-fill material with maximum thermal conductivity (k_g = 2.2 W/m.K) is used in the BHE installed at the ground with low soil thermal conductivity (0.3 W/m.K). The reason for this could be the thermal-short-circuit (thermal interference) associated with excessive thermal conductivity of the gout utilized in the BHE.

 doi:10.20944/preprints202403.0448.v1

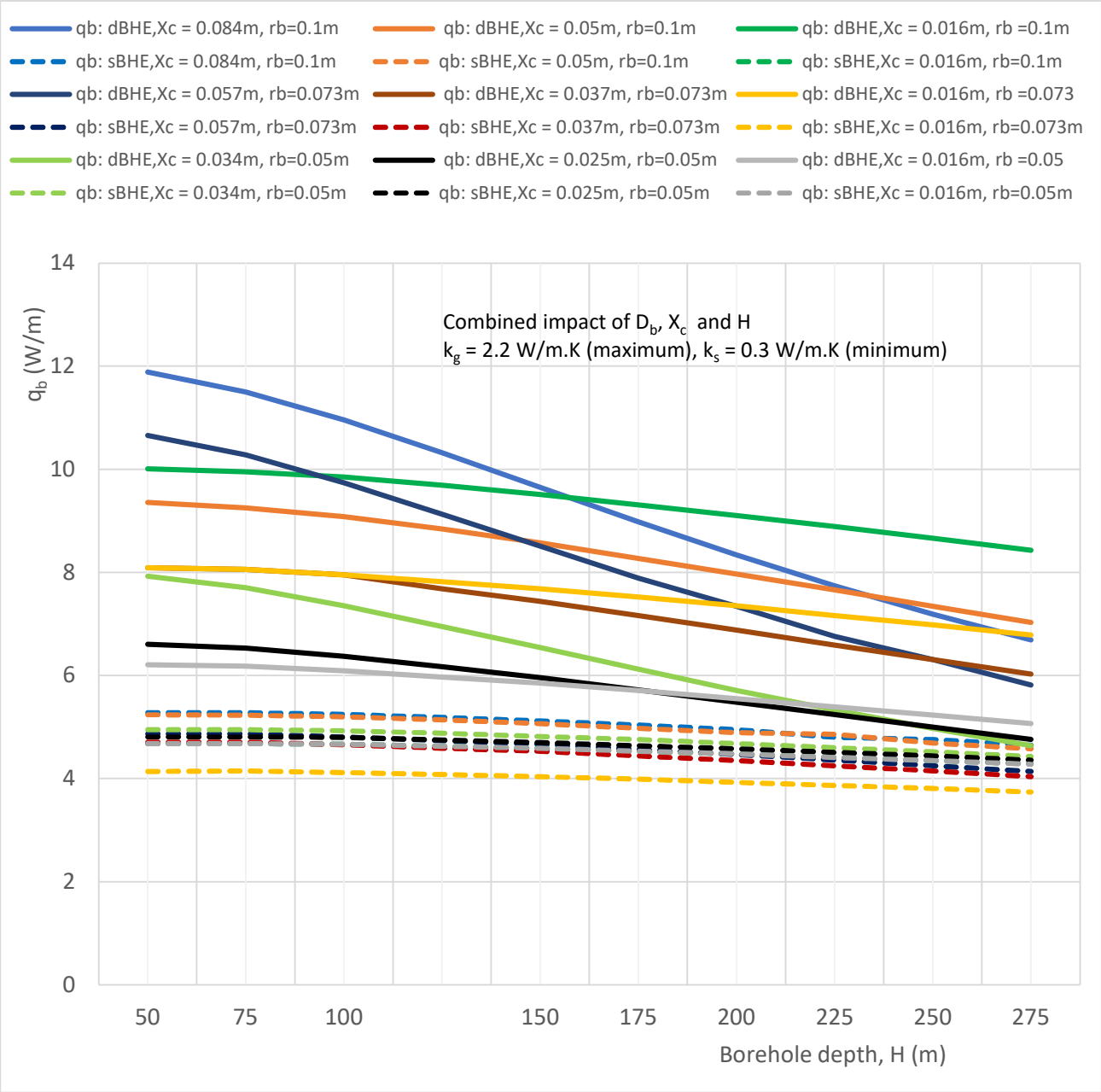

Figure 6. Combined effect of borehole depth, borehole size and shank spacing on heat transfer rate per unit borehole depth in sBHE and dBHE for the case of maximum grout thermal conductivity and minimum soil thermal conductivities (k_g = 2.2 W/m.K, k_s = 0.3 W/m.K).

 doi:10.20944/preprints202403.0448.v1

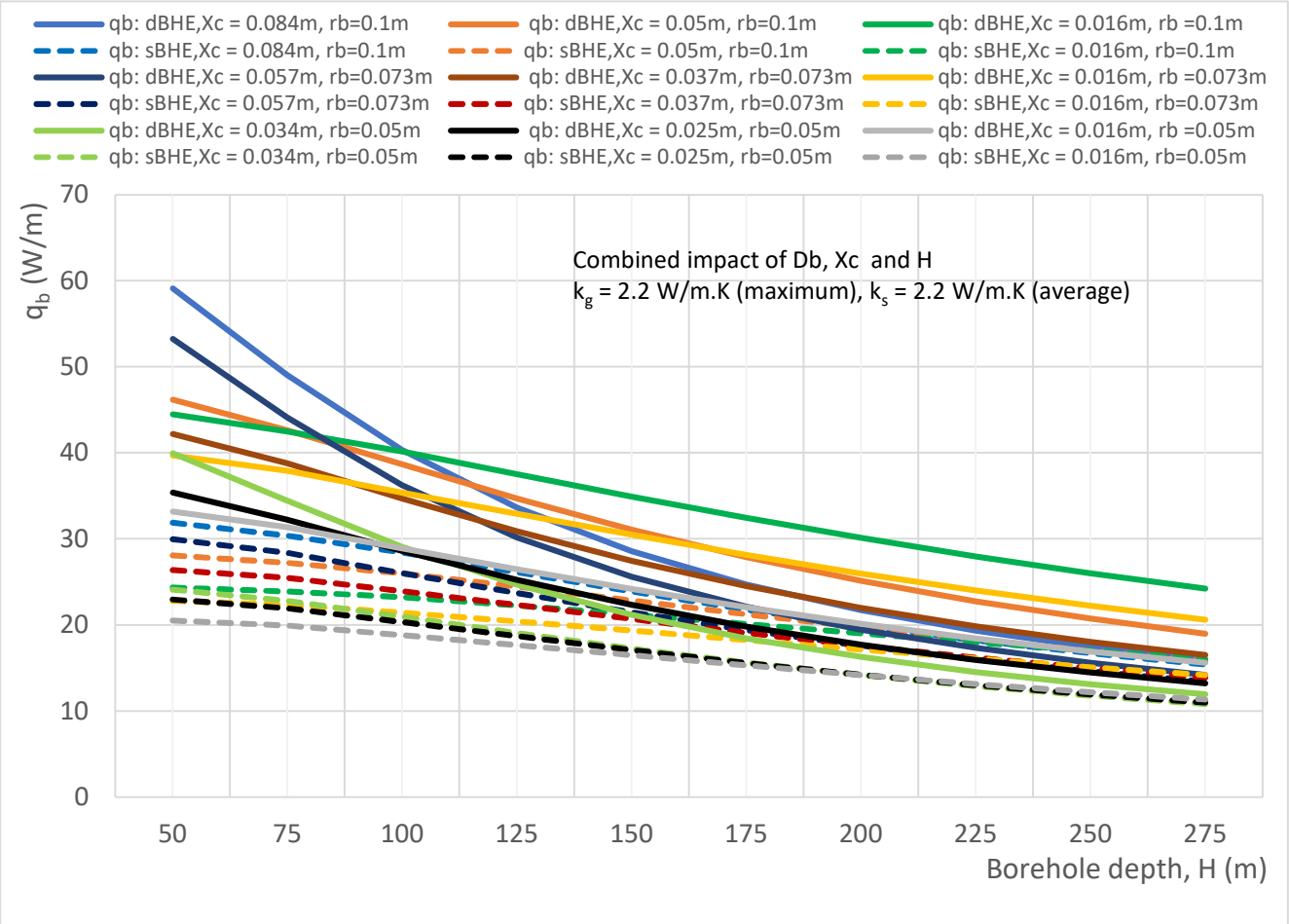

Figure 7. Combined effect of borehole depth, borehole size and shank spacing on heat transfer rate per unit borehole depth in sBHE and dBHE for the case of maximum grout thermal conductivity and average soil thermal conductivity (k_g = 2.2 W/m·K, k_s = 2.2 W/m·K).

 doi:10.20944/preprints202403.0448.v1

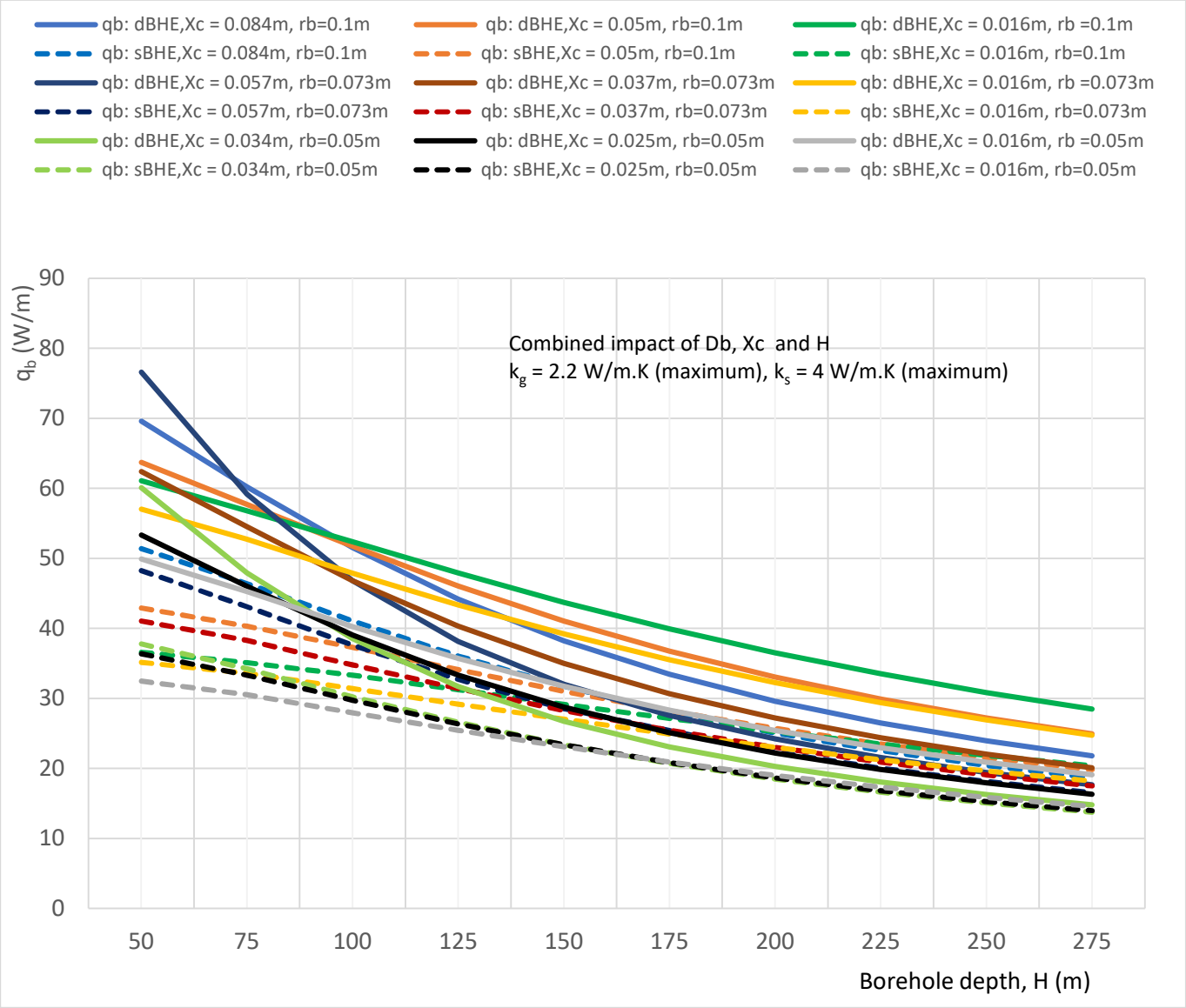

Figure 8. Combined effect of borehole depth, borehole size and shank spacing on heat transfer rate per unit borehole depth in sBHE and dBHE for the case of maximum grout and soil thermal conductivities (k_g = 2.2 W/m·K, k_s = 4.0 W/m·K).

B. Combined Effect of Borehole Depth and Thermal Conductivities of Soil and Grout

In this section, analysis of combined impact of parameters (which includes borehole depth, soil and grout thermal conductivities) on total heat transfer per unit borehole depth with different cases of borehole size (radius) and half shank spacing (half center-to-center distance between U-tube pipe), will be performed. Specifically, the sensitivity analysis was done for minimum (low) soil thermal conductivity (k_s = 0.3 W/m·K), average soil thermal conductivity (k_s = 2.2 W/m·K) and maximum (high) soil thermal conductivity (k_s = 4 W/m·K), where each value of the soil thermal conductivity was combined with minimum (k_g = 0.5 W/m·K), average (k_g = 1.5 W/m·K) and maximum (k_g = 2.2 W/m·K) values of grout thermal conductivity. This is indicated in Table 5-2 under column B. This case of combined effect of borehole depth, soil thermal conductivity and grout thermal conductivity was done for 9 different cases consisting of large borehole size/borehole radius (r_b = 0.1 m), average borehole size (r_b = 0.073 m) and small borehole size (r_b = 0.05 m) each with the corresponding minimum, medium, and maximum half shank spacing values as shown in Table 3 under column B.

This case is important as a quick reference for the design of BHE with a given different cases of borehole size and shank spacing; that is, with the given borehole size and shank spacing, one can

 doi:10.20944/preprints202403.0448.v1

select the BHE case that provides highest heat transfer among the various cases of sBHE and dBHE presented under column B of Table 2. The simulation result of the nine different cases considered in this section, shown under column B of Table 3, is depicted in Figs. 9 through 14. Various important information can be obtained from such results.

Figure 9 to Figure 11 illustrates combined impact of borehole depth, soil and grout thermal conductivities on heat transfer rate per unit borehole depth in both sBHE and dBHE for the case of small borehole size (r_b = 0.05 m) with minimum half shank spacing (X_c = 0.016 m), average half shank spacing (X_c = 0.025 m), maximum half shank spacing (X_c = 0.034 m) respectively. It can be observed that the dBHE with minimum (low) grout thermal conductivity (k_g = 0.5 W/m·K) and high soil thermal conductivity provides more heat transfer than all the three cases shown in Figs. 9 to 11; and similar result is obtained for sBHE. Comparison among Figs. 9 to 11 shows that more heat transfer is achieved by BHE with maximum shank spacing (X_c = 0.034 m) depicted in Figure 9 (see case 3 column B of Table 3). This is because when U-tube legs are widely spaced, the phenomenon of thermal short-circuit between the legs of the U-tube is reduced, and surface area is increased resulting in more heat transfer between working fluid in the BHE and the ground around the BHE. Furthermore, the results depicted in Figs. 9 to 11 show that in some cases sBHE are preferable to transfer more heat than dBHE specially for deep borehole depth. For example, sBHE with minimum grout thermal conductivity (k_g = 0.5 W/m·K) and maximum soil thermal conductivity (k_s = 4 W/m·K) transfer more heat than for most of the cases of the dBHE. The reason for this is associated with the reduced thermal interference between the legs of the sBHE as compared to the dBHE, and low grout thermal conductivity resulting in more heat transfer to the ground. Therefore, low grout thermal conductivity and high soil thermal conductivity case is preferred to transfer more heat to the ground in the BHE. In the longer borehole depth, sBHE is better to transfer more heat than dBHE; while for BHE with shallow borehole depth, dBHE is effective to transfer more heat than sBHE.

 doi:10.20944/preprints202403.0448.v1

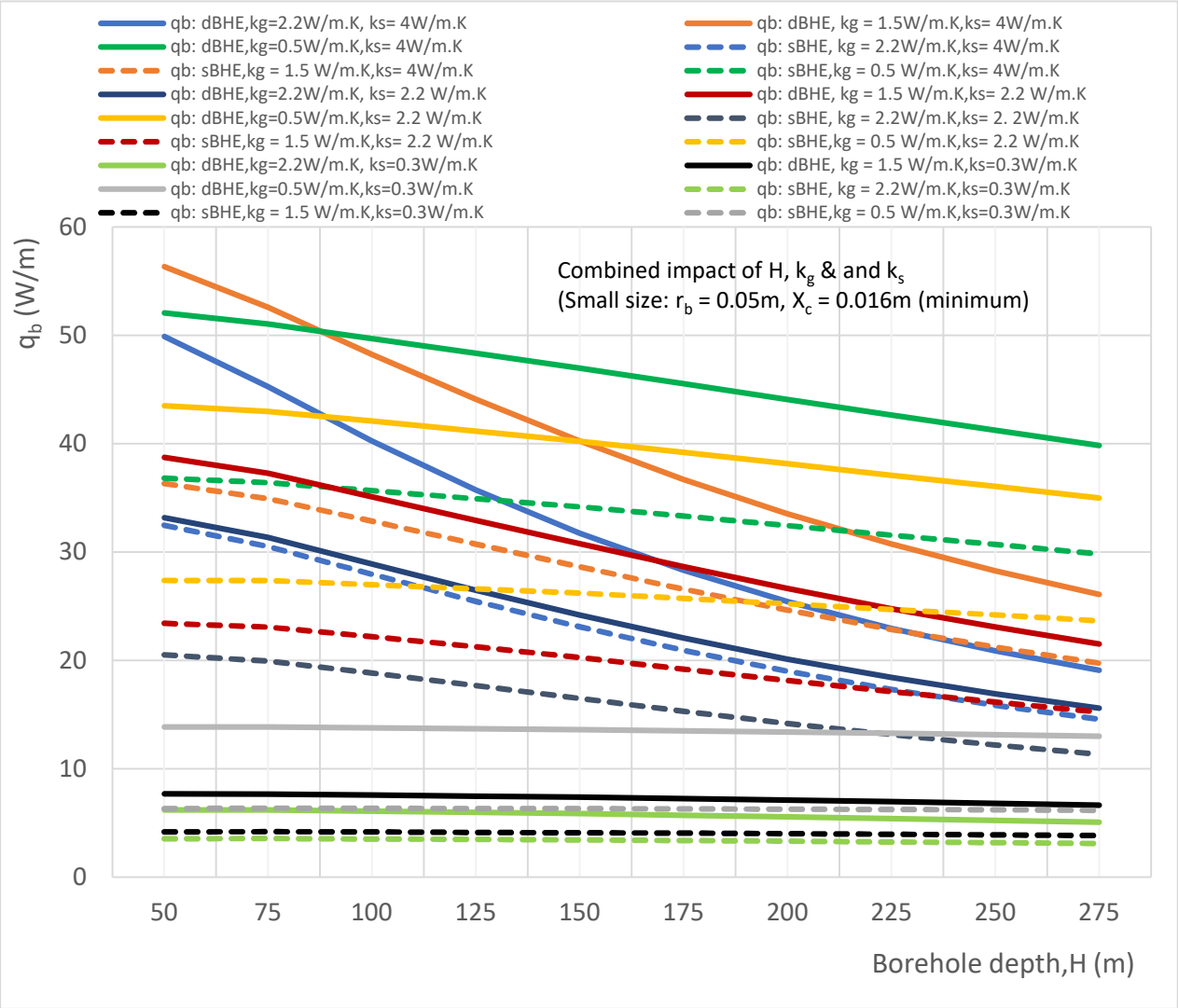

Figure 9. Combined effect of borehole depth, soil and grout thermal conductivities on heat transfer rate per unit borehole depth in sBHE and dBHE for the case of small borehole size (r_b = 0.05 m) with minimum shank spacing (X_c = 0.016 m).

Preprints.org (www.preprints.org) | NOT PEER-REVIEWED | Posted: 7 March 2024 doi:10.20944/preprints202403.0448.v1

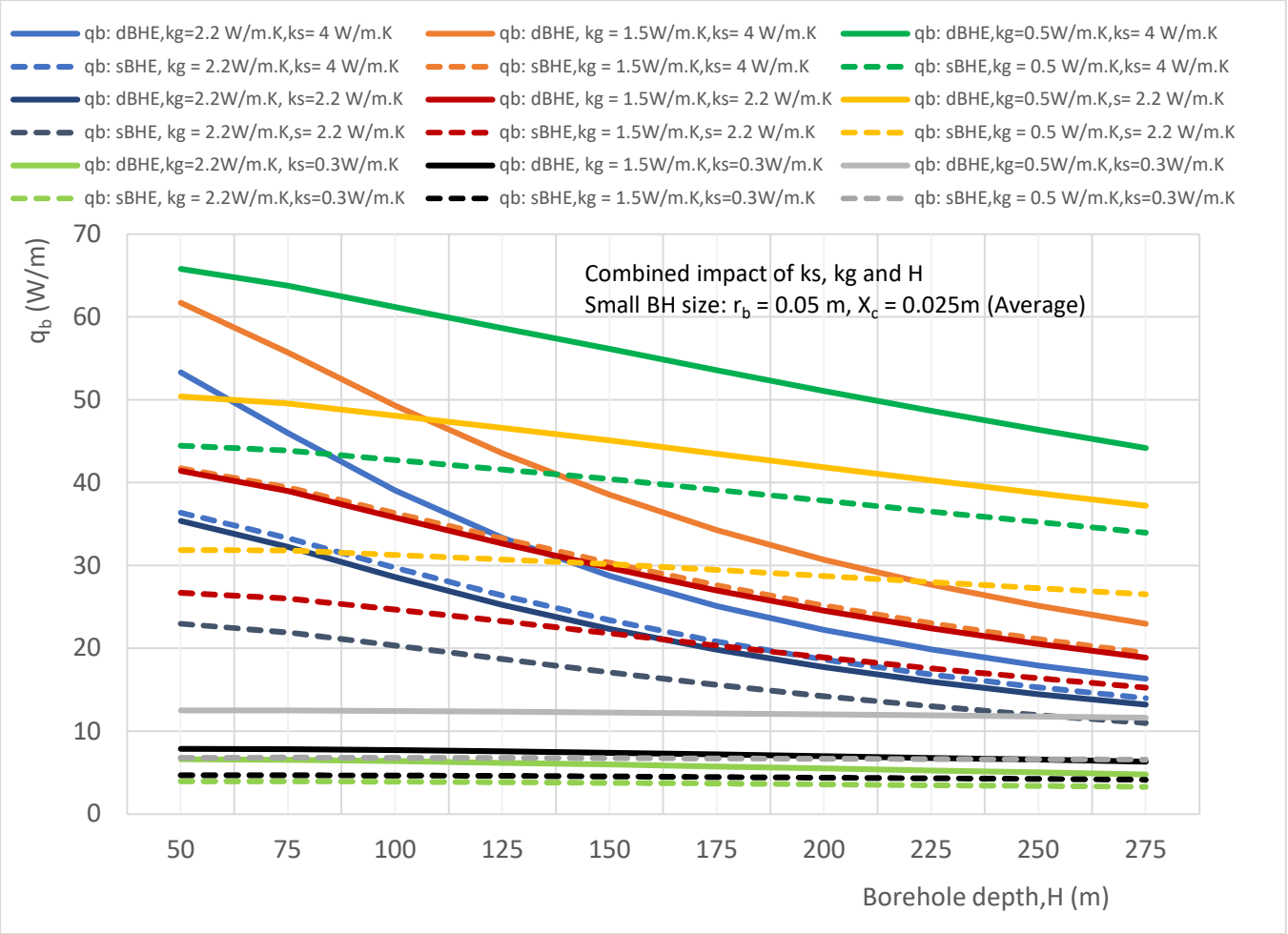

Figure 10. Combined effect of borehole depth, soil and grout thermal conductivities on heat transfer rate per unit borehole depth in sBHE and dBHE for the case of small borehole size (r_b = 0.05m) with average shank spacing (X_c = 0.025m).

 doi:10.20944/preprints202403.0448.v1

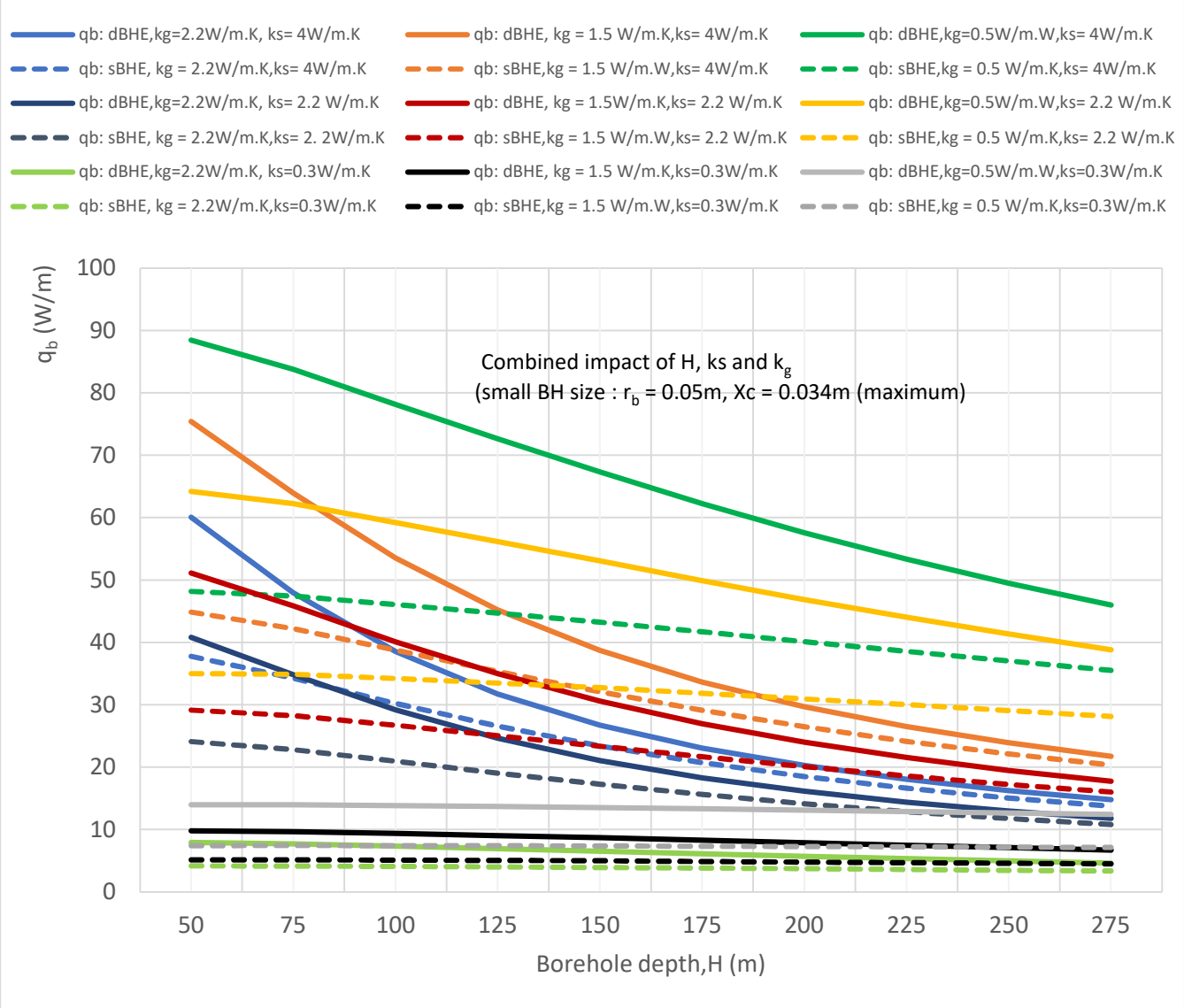

Figure 11. Combined effect of borehole depth, soil and grout thermal conductivities on heat transfer rate per unit borehole depth in sBHE and dBHE for the case of small borehole size (r_b = 0.05m) with maximum shank spacing (X_c = 0.034m).

The results shown in Figs. 12 to 14 illustrate the combined impact of borehole depth, grout, and soil thermal conductivity on heat transfer rate per unit borehole depth in sBHE and dBHE for large borehole size (r_b = 0.1 m) with minimum shank spacing (X_c = 0.016 m), average shank spacing (X_c = 0.05 m) and maximum shank spacing (X_c = 0.084 m) respectively. The result depicted in Figure 12 illustrates the case for large borehole size with minimum shank spacing; it can be seen that dBHE filled with grout with k_g = 1.5 W/m·K and installed at ground with high soil thermal conductivity (k_s = 4 W/m·K) provides the highest heat transfer. However, for the longer borehole depth beyond 275 m, the dBHE with low grout thermal conductivity (k_g = 0.5 W/m·K) and high soil thermal conductivity (k_s = 4 W/m·K) seems to provide more heat transfer than other cases considered in Figure 12. This is more clearly observed in Figure 14 where the dBHE with maximum shank spacing, with k_g = 0.5 W/m·K and k_s = 4 W/m·K provides the highest heat transfer all along the borehole depth.

On the other hand, Figure 13 shows that dBHE with average shank spacing, average grout thermal conductivity and high soil thermal conductivity provides the most heat transfer when used in shorter borehole depth; but dBHE filled with grout with minimum thermal conductivity and high soil thermal conductivity is preferable to transfer more heat into the ground when applied in deeper borehole depth. Similarly, Figure 13 indicates that sBHE with average shank spacing, low (minimum)

 doi:10.20944/preprints202403.0448.v1

grout thermal conductivity and high soil thermal conductivity is preferred to deliver more heat transfer into the ground when applied in deep borehole depth.

Overall, comparison of the results depicted in Figs. 9 to 14 shows that among the 9 cases listed under column B of Table 3, case 9 (depicted in Figure 14) provides the highest heat transfer per unit borehole depth; and of all the cases, dBHE with large borehole size, maximum shank spacing, low grout thermal conductivity and high soil thermal conductivity is the most effective to transfer more heat, especially for borehole with shallow borehole depth, than any other cases, and for borehole with deep borehole depth, sBHE with the same design condition is preferred. Similar important information that can be used as a quick reference for the design of the BHE can be deduced or obtained from the generated results depicted in other Figs.

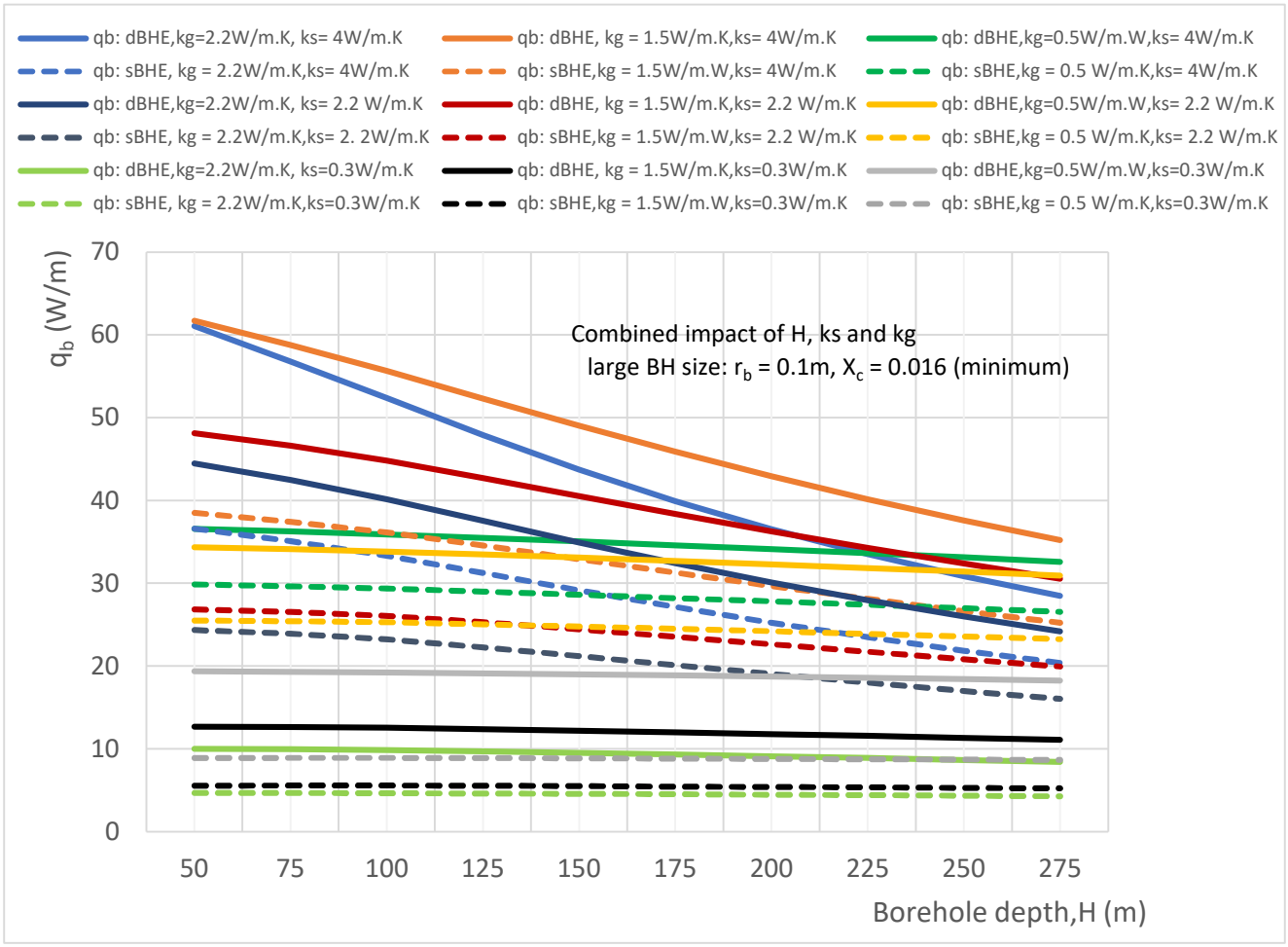

Figure 12. Combined effect of borehole depth, soil and grout thermal conductivities on heat transfer rate per unit borehole depth in sBHE and dBHE for the case of largest borehole size (r_b = 0.1m) with minimum shank spacing (X_c = 0.016m).

 doi:10.20944/preprints202403.0448.v1

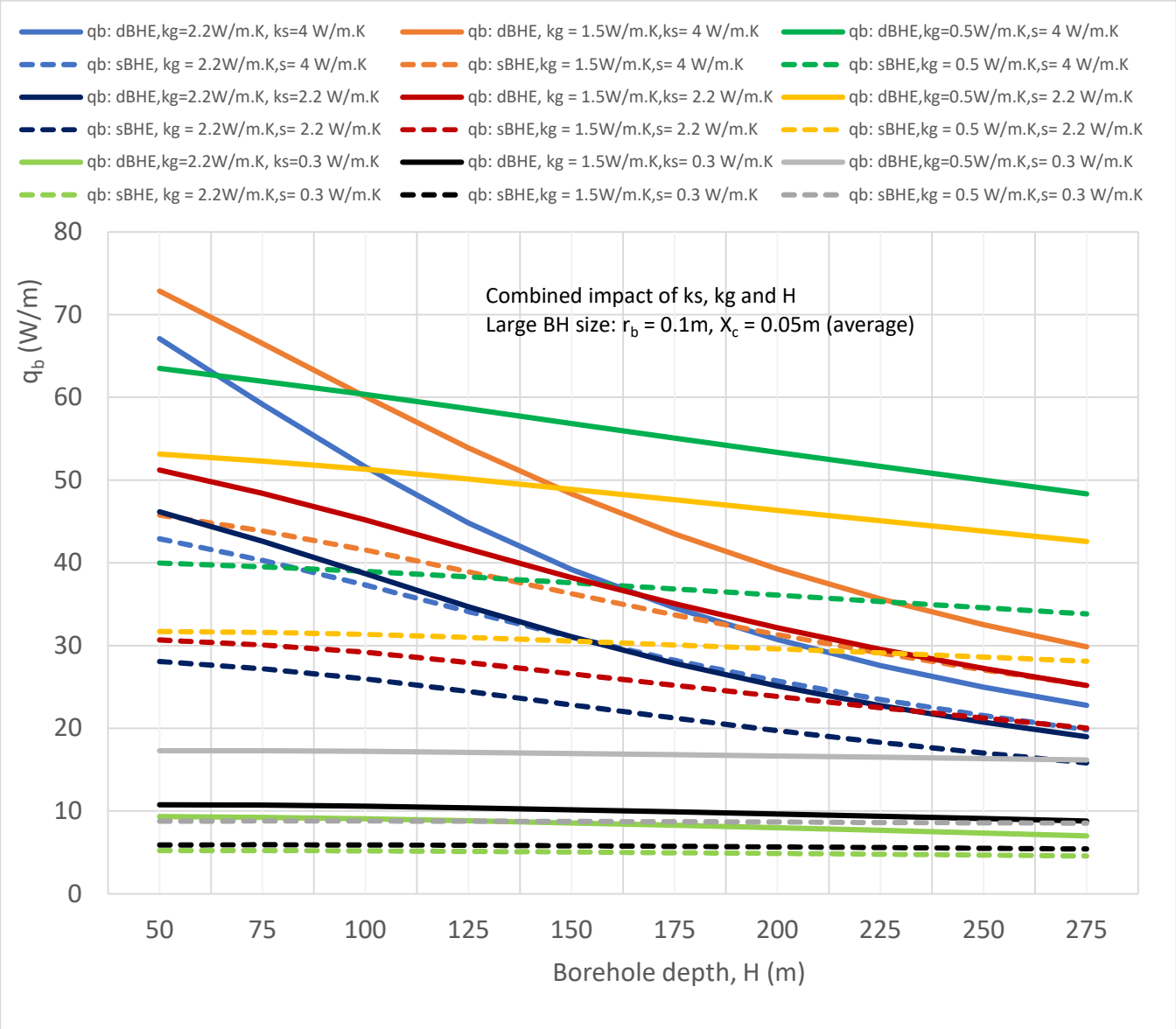

Figure 13. Combined effect of borehole depth, soil and grout thermal conductivities on heat transfer rate per unit borehole depth in sBHE and dBHE for the case of largest borehole size (r_b = 0.1m) with average/medium shank spacing (X_c = 0.05m).

 doi:10.20944/preprints202403.0448.v1

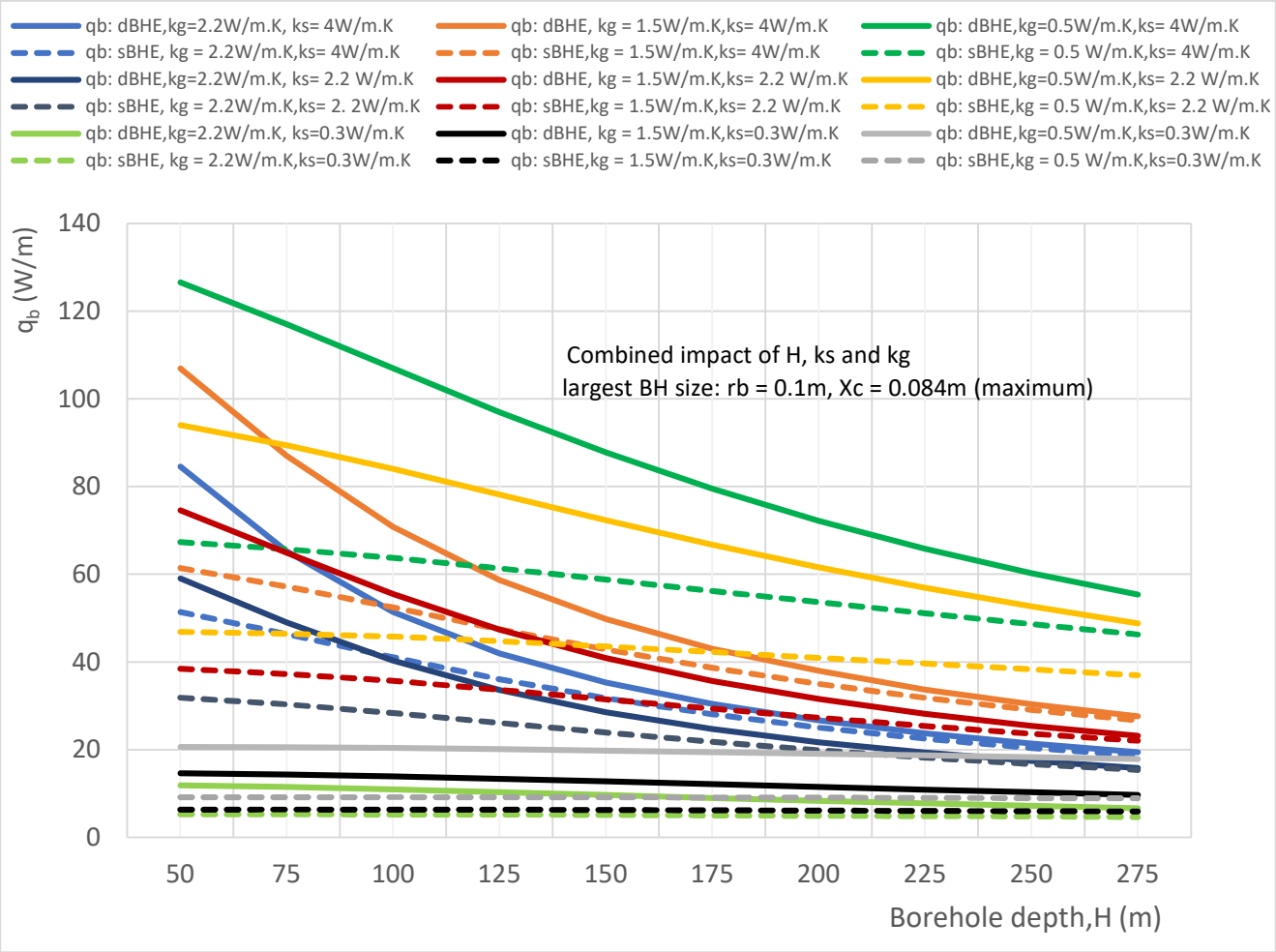

Figure 14. Combined effect of borehole depth, soil, and grout thermal conductivity on heat transfer rate per unit borehole depth in sBHE and dBHE for the case of largest borehole size (r_b = 0.1m) with minimum shank spacing (X_c = 0.084m).

C. Combined Effect of Borehole Size and Thermal Conductivities of Soil and Grout

Thermal conductivity of the ground around the BHE and the back-fill material are among the parameters that affects the heat transfer in the BHE. The higher the soil thermal conductivity, the higher the heat transfer between the ground and the fluid that circulates in the loop between the BHE and the heat pump. This results in increased performance of the ground source heat pump system (GSHP), and hence, leads to the reduced total cost of the power consumed by the GSHP system. Grout thermal conductivity is another thermal parameter that impacts the heat transfer in the BHE. Back-fill material with high thermal conductivity is considered to enhance the heat transfer in the BHE, and hence improves the efficiency of the BHE. However, excessive thermal conductivity of grout may increase thermal short-circuit between U-tube pipes leading to the reduced thermal performance of the BHE. As seen in the previous cases of A and B, high grout thermal conductivity reduces the heat transfer in the BHE particularly for dBHE with deep borehole depth and small shank spacing.

Changing (increasing/reducing) one parameter alone cannot help to improve the thermal performance of the BHE. For example, increasing thermal conductivity of grout or soil alone may not help to improve the heat transfer in the BHE. Hence, sensitivity analysis consisting different combination of borehole parameters and thermal properties must be performed. That is, detailed investigation involving combined effect of parameters (for example, grout thermal conductivity with other parameters such as soil thermal conductivity and other borehole geometrical parameters) should be performed. Presenting such comprehensive sensitivity analysis in graphical/tabular form

 doi:10.20944/preprints202403.0448.v1

conveniently helps the BHE designer to select the case that provides the highest heat transfer. That is, such results can be used as a quick reference for the design and optimization of the BHE.

In this sub-section, combined impact of thermal conductivity of grout and soil as well as borehole size on heat transfer per unit borehole depth of sBHE and dBHE for different cases of borehole depth and shank spacing is discussed. This case is important as a quick reference for the design of the BHE with the given different cases borehole depth and shank spacing, and desired to be installed at the ground with known value of thermal conductivity. Then, one can select the BHE cases that provides highest heat transfer among the various cases of sBHE and dBHE presented under column C of Table 2.

The simulation results of the nine different cases considered in this section, shown under column C of Table 3, are depicted in Figs. 15 through 20. Various important information can be obtained from such results. An essential BHE design information can be obtained from these simulation results. For example, if a BHE (with shallow/deep borehole depth and with a given shank spacing) that can transfer highest heat transfer is required to be installed at a ground with a certain thermal conductivity, then such information can be obtained from the results presented this section.

Nine different cases (listed in Table 3 under column C) consisting of BHE with shallow borehole depth (H = 50 m) and deep borehole depth (H = 300 m) each with small, medium and large borehole sizes (diameters) with corresponding minimum, average and maximum shank spacing are analyzed. The simulation results of the combined impact of thermal conductivities of grout and soil as well as borehole size on heat transfer per unit borehole depth for sBHE and dBHE with different cases of borehole depth and shank spacing are shown in Figs. 15 to 20. More specifically, the results presented in Figs. 15 to 20 provide an important information on how to select the BHE that provides the highest heat transfer among the BHE design options (sBHE and dBHE with small, medium and large borehole sizes, and with minimum, average and maximum thermal conductivities of grout) for a given soil thermal conductivity, borehole depth (H = 50 m, and H = 300 m) and shank spacing. Note that each BHE is with the corresponding minimum, average and maximum shank spacing.

The result depicted in Figs. 15 to 17 illustrates the result of the cases for the shallow borehole depth (H = 50 m) with all borehole sizes with the corresponding minimum shank spacing (r_b = 0.1 m with X_c = 0.016 m; r_b = 0.073 m with X_c = 0.016 m and r_b = 0.05 m with X_c = 0.016 m); all borehole sizes with corresponding average shank spacing (r_b = 0.1 m with X_c = 0.05 m; r_b = 0.073 m with X_c = 0.037 m and r_b = 0.05 m with X_c = 0.025 m); and all borehole sizes with the corresponding maximum shank spacing (r_b = 0.1 m with X_c = 0.084 m; r_b = 0.073 m with X_c = 0.057 m and r_b = 0.05 m with X_c = 0.034 m) respectively. It can be seen from Figure 15 that dBHE with large borehole size (r_b = 0.1 m) and average grout thermal conductivity (k_g = 1.5 W/m·K) provides the highest heat transfer when the soil thermal conductivity is higher than 1 W/m·K. For thermal conductivity lower than about 1 W/m·K, dBHE with large borehole size (r_b = 0.1 m) and low grout thermal conductivity (k_g = 0.5 W/m·K) provides the highest heat transfer while its heat transfer for high soil thermal conductivity becomes lower than other cases (and lower than even some cases of sBHE). This could be attributed to the more thermal short-circuit associated with BHE with minimum shank spacing.

Figure 16 shows the combined effect of soil thermal conductivity, grout thermal conductivity and borehole size on heat transfer rate per unit borehole depth in sBHE and dBHE for the case of shallow borehole depth (50 m) and all borehole sizes with the corresponding average shank spacing (r_b = 0.1 m with X_c = 0.05 m; r_b = 0.073 m with X_c = 0.037 m and r_b = 0.05 m with X_c = 0.025 m). For soil thermal conductivity lower than 2.3 W/m·K, dBHE with large borehole size (r_b = 0.1 m) and low (minimum) grout thermal conductivity (k_g = 0.5 W/m·K) provides the highest heat transfer while for soil thermal conductivity higher than 2.3 W/m·K, dBHE with large borehole size (r_b = 0.1 m) filled with grout with average thermal conductivity (k_g = 1.5 W/m·K) results in highest heat transfer of all cases presented in Figure 16. It is also important to see that dBHE with r_b = 0.05 m and maximum grout thermal conductivity (k_g = 2.2 W/m·K) provides the lowest heat transfer than all the cases of dBHE considered in Figure 16. As depicted in Figure 17, when BHE with corresponding maximum shank spacing is applied in each borehole size, it is observed that dBHE with large borehole size (r_b = 0.1 m) and low (minimum) grout thermal conductivity (k_g = 0.5 W/m·K) provides the highest heat

 doi:10.20944/preprints202403.0448.v1

transfer for the whole range of soil thermal conductivity (0.3 to 4 W/m·K) than other cases of BHE considered under this case. A close look at Figure 17 also shows that dBHE with average borehole size (r_b = 0.073 m) and low grout thermal conductivity (k_g = 0.5 W/m·K) delivers more heat transfer than even dBHE with large borehole size (r_b = 0.1 m) and average (k_g = 1.5 W/m·K) as well as maximum grout thermal conductivity (k_g = 2.2 W/m·K). This could be attributed to the more thermal short-circuit associated with high grout thermal conductivity. This indicates that more impact on heat transfer is observed with reduced grout thermal conductivity combined with increased borehole size than combined increase of borehole size and grout thermal conductivity. Therefore, when BHE with maximum shank spacing is used, more heat transfer can be achieved by combined increase of borehole size and reduced grout thermal conductivity. Finally, comparison among Figs. 15, 16 and 17 shows that more heat transfer is obtained for the case with maximum shank spacing (shown in Figure 17), and in all the cases shown in these figures, dBHE is better to transfer more heat than the corresponding sBHE.

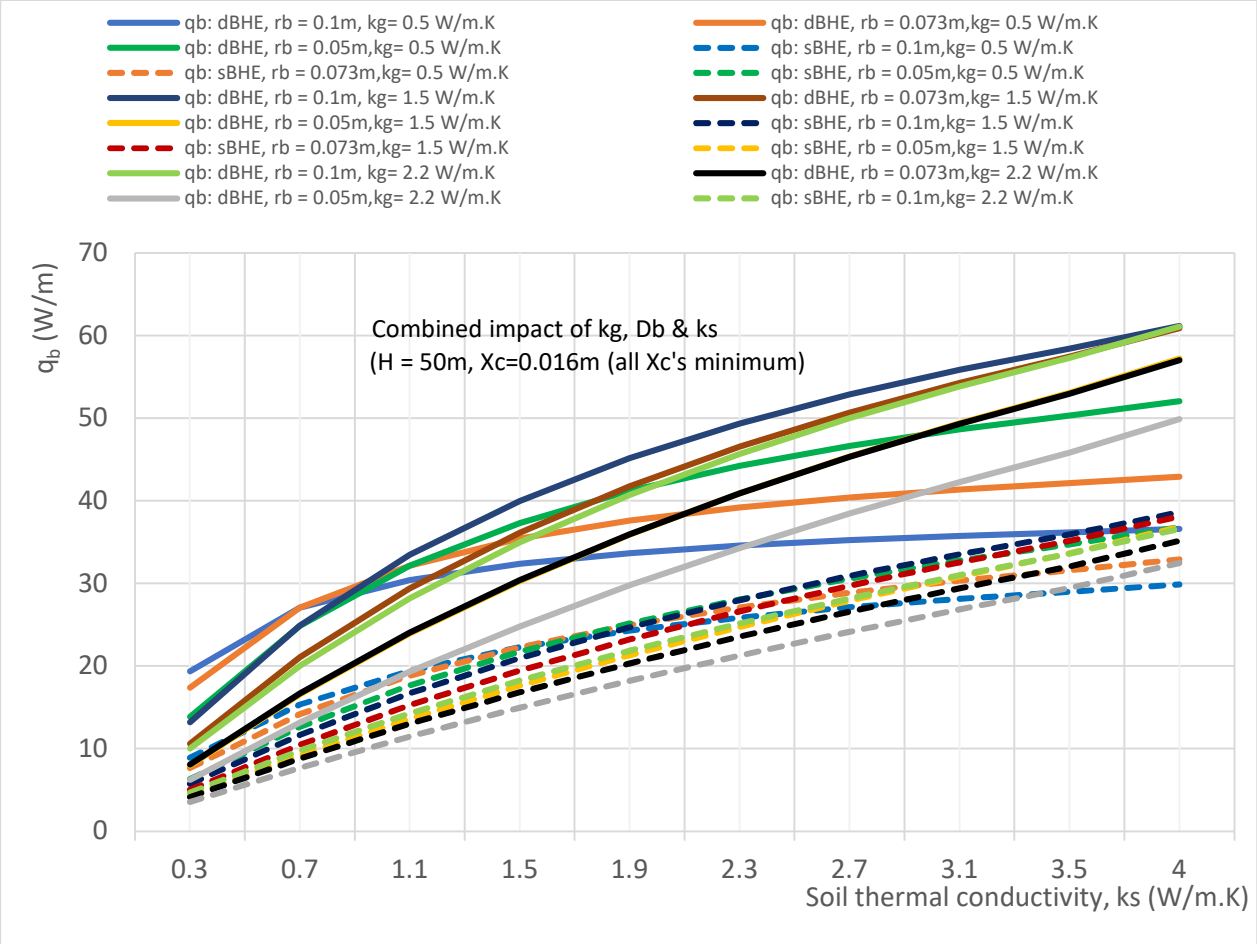

Figure 15. Combined effect of soil thermal conductivity, grout thermal conductivity and borehole size on heat transfer rate per unit borehole depth in sBHE and dBHE for the case of shallow borehole depth (H = 50 m) and all borehole sizes with the corresponding minimum shank spacing (r_b = 0.1 m with X_c = 0.016 m; r_b = 0.073 m with X_c = 0.016 m and r_b = 0.05 m with X_c = 0.016 m).

 doi:10.20944/preprints202403.0448.v1

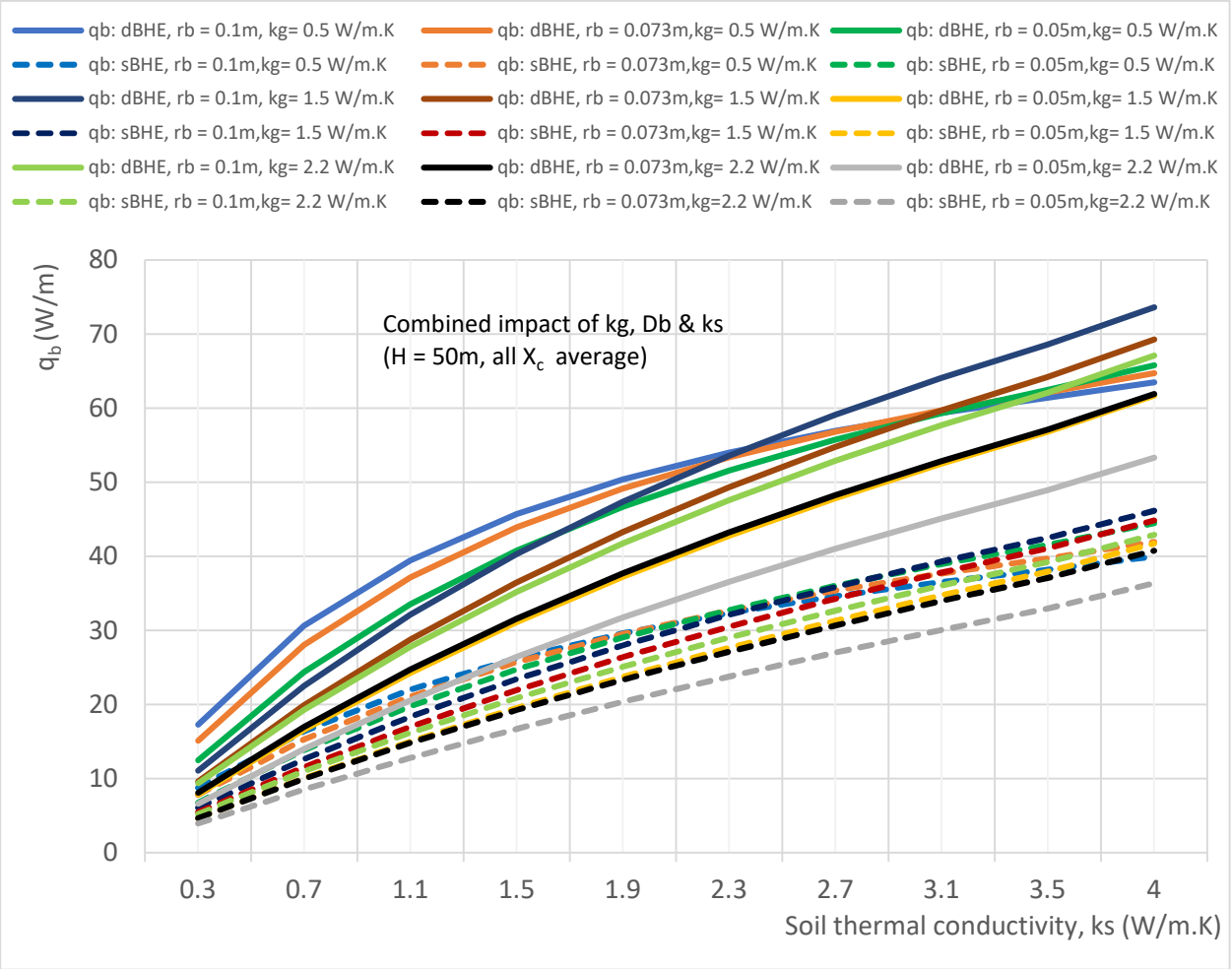

Figure 16. Combined effect of soil thermal conductivity, grout thermal conductivity and borehole size on heat transfer rate per unit borehole depth in sBHE and dBHE for the case of shallow borehole depth (H = 50 m) and all borehole sizes with corresponding average shank spacing (r_b = 0.1 m with X_c = 0.05 m; r_b = 0.073 m with X_c = 0.037 m and r_b = 0.05 m with X_c = 0.025 m).

 doi:10.20944/preprints202403.0448.v1

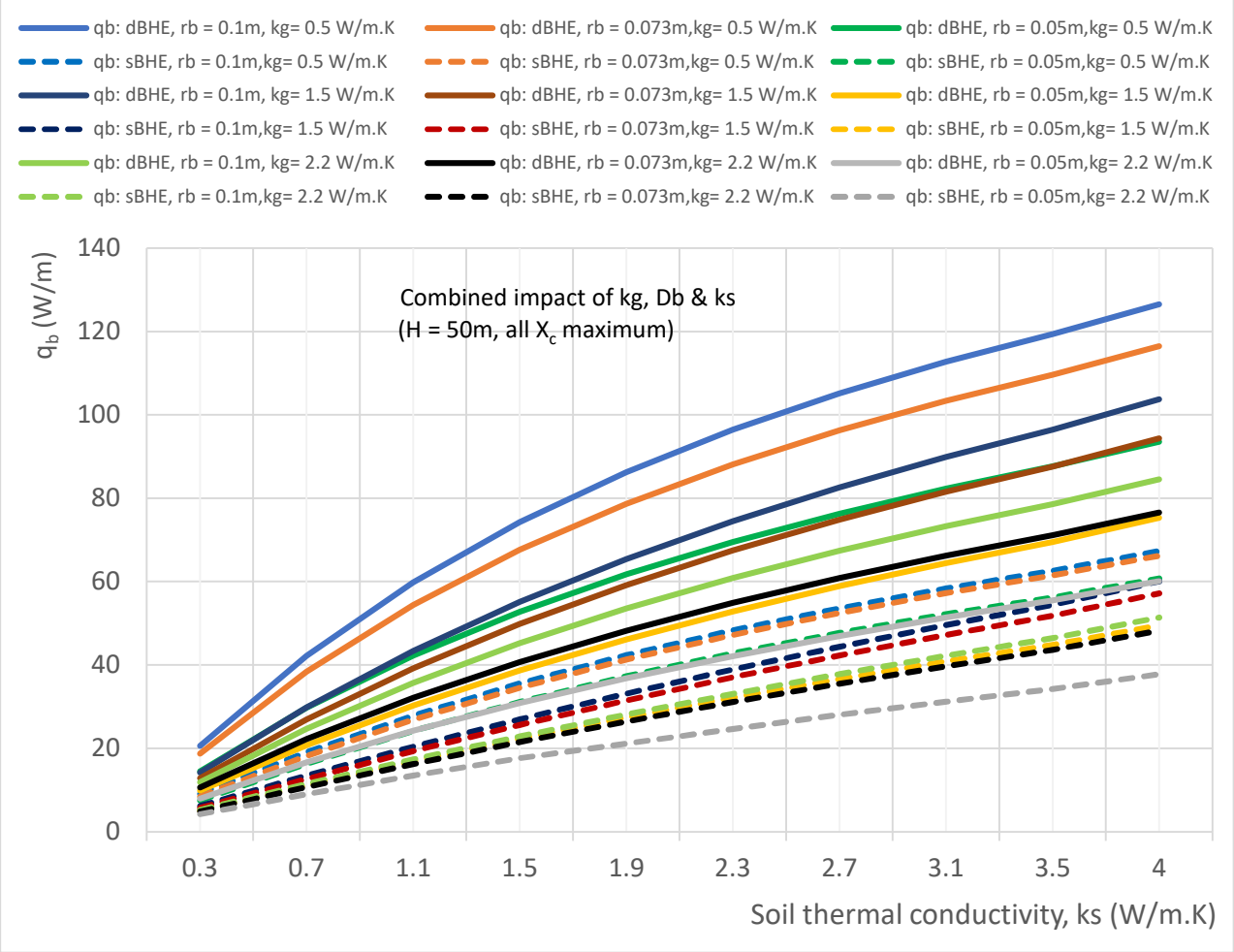

Figure 17. Combined effect of soil thermal conductivity, grout thermal conductivity and borehole size on heat transfer rate per unit borehole depth in sBHE and dBHE for the case of shallow borehole depth (H = 50 m) and all borehole sizes with corresponding maximum shank spacing (r_b = 0.1 m with X_c = 0.084 m; r_b = 0.073 m with X_c = 0.057 m and r_b = 0.05m with X_c = 0.034m).

Further analysis was done for the case considered under column C in Table 3 for the BHE with deep borehole depth (H = 300 m), and the simulation results obtained for this case are presented in Figs. 18 to 20. Figure 18 shows the combined impact of soil and grout thermal conductivities as well as borehole size on heat transfer per unit borehole depth for BHEs with corresponding minimum shank spacing, while Figs. 19 and 20 show the combined effect of parameters on heat transfer for the BHEs with the corresponding average and maximum shank spacing, respectively. It can be seen from Figure 18 that for BHE with deep borehole depth and minimum shank spacing, the heat transferred by the dBHE with small borehole size (r_b = 0.05 m) and minimum grout thermal conductivity is the highest for the soil with thermal conductivity higher than 1.7 W/m·K; and for soil thermal conductivity lower than 0.7 W/m·K, dBHE with large borehole size and low grout thermal conductivity is preferred. This clearly indicates that for the BHE with minimum shank spacing and deep borehole depth, using BHE with large borehole size and with high gout and soil thermal conductivity is not preferred to transfer more heat between the working fluid and the ground around the BHE. This could be due to the augmented phenomenon of thermal short-circuit between the legs of the BHE designed with the minimum shank spacing, large borehole length and filled with grout that has high thermal conductivity. On the other hand, for borehole heat exchangers (BHEs) with corresponding average and maximum shank spacing (shown in Figs. 19 and 20 respectively), dBHE with large borehole size and low grout thermal conductivity provides the highest heat transfer for the whole range of soil thermal conductivity considered in this study (0.3 to 4 W/m·K). This indicates

 doi:10.20944/preprints202403.0448.v1

that if a BHE with deep borehole depth is required to be designed to deliver the highest heat transfer rate per unit borehole depth, then dBHE with large borehole diameter, maximum shank spacing, and low grout thermal conductivity is preferred for all the range of the ground thermal conductivity. A close look at Figure 20 indicates that for BHE designed with maximum shank spacing, deep borehole depth, low grout thermal conductivity, and high soil thermal conductivity, sBHE with large borehole size can provide more heat transfer than dBHE with small borehole size. Finally, comparison of the results presented in Figs. 18 and 20 indicates that for the same borehole depth, borehole size and grout thermal conductivity, the heat transferred by the BHE with high shank spacing is higher than that of the BHE with low shank spacing.

Overall, comparison among the nine cases (listed under column C of Table 3 and depicted in Figs. 15 to 20) shows that the third case (presented in Figure 17) provided the highest heat transfer. Furthermore, the results presented in Figs. 15 to 20 reveals that dBHE provides more heat transfer when used in shallow borehole depth while sBHE is preferred to transfer more heat when applied in deep borehole depth. The reason for this (as stated in the previous section) is due to more thermal interference in dBHE than in sBHE when applied in deep BHE; and to reduce the impact of the thermal loss (due to thermal short-circuit or thermal interference) associated with BHE with deep borehole depth, utilizing large borehole diameter and low grout thermal conductivity could be among the design options that can be considered.

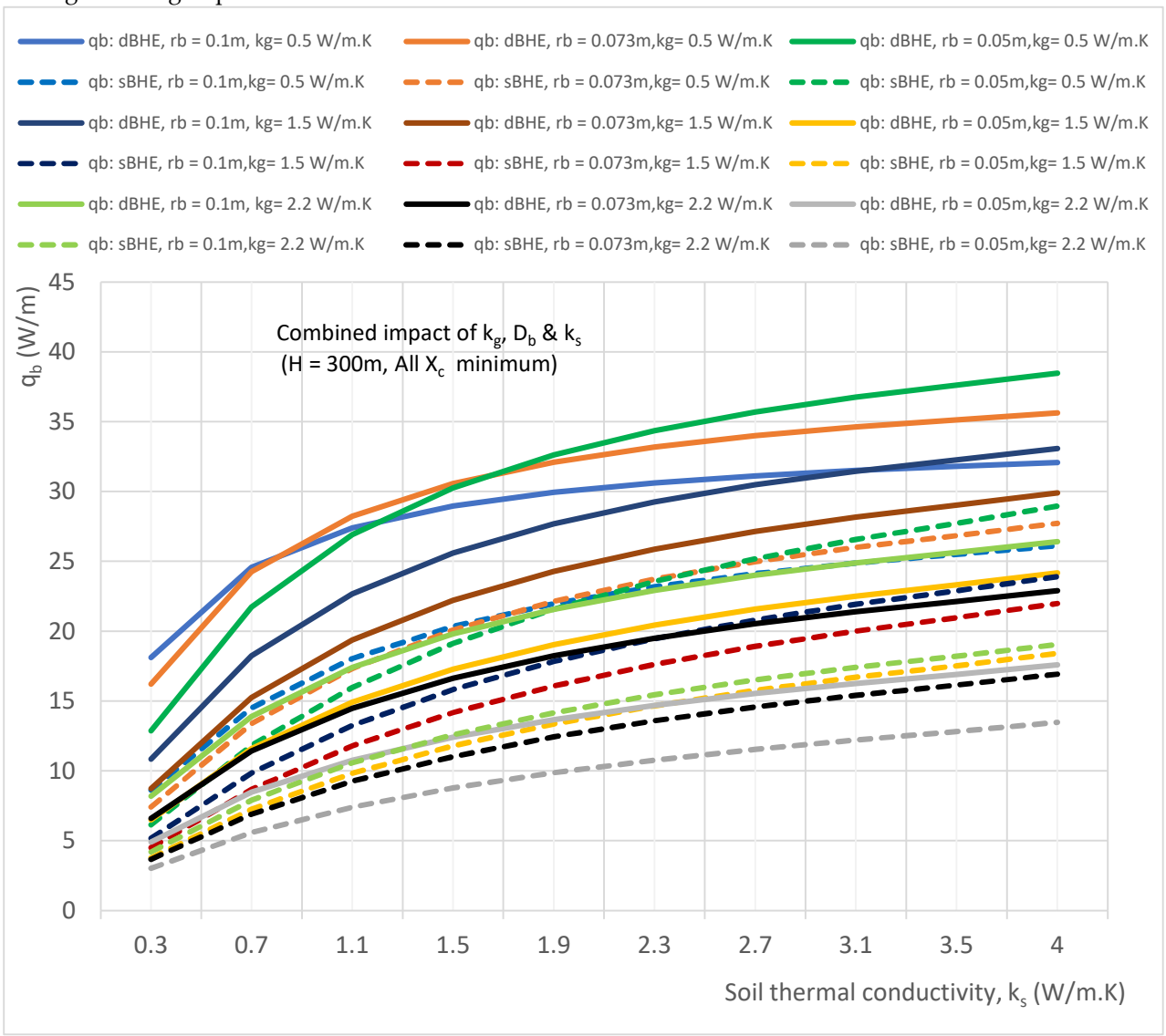

Figure 18. Combined effect of soil thermal conductivity, grout thermal conductivity and borehole size on heat transfer rate per unit borehole depth in sBHE and dBHE for the case of deep borehole depth

 doi:10.20944/preprints202403.0448.v1

(H = 300 m) and all borehole sizes with the corresponding minimum shank spacing (r_b = 0.1 m with X_c = 0.016 m; r_b = 0.073 m with X_c = 0.016 m and r_b = 0.05 m with X_c = 0.016 m).

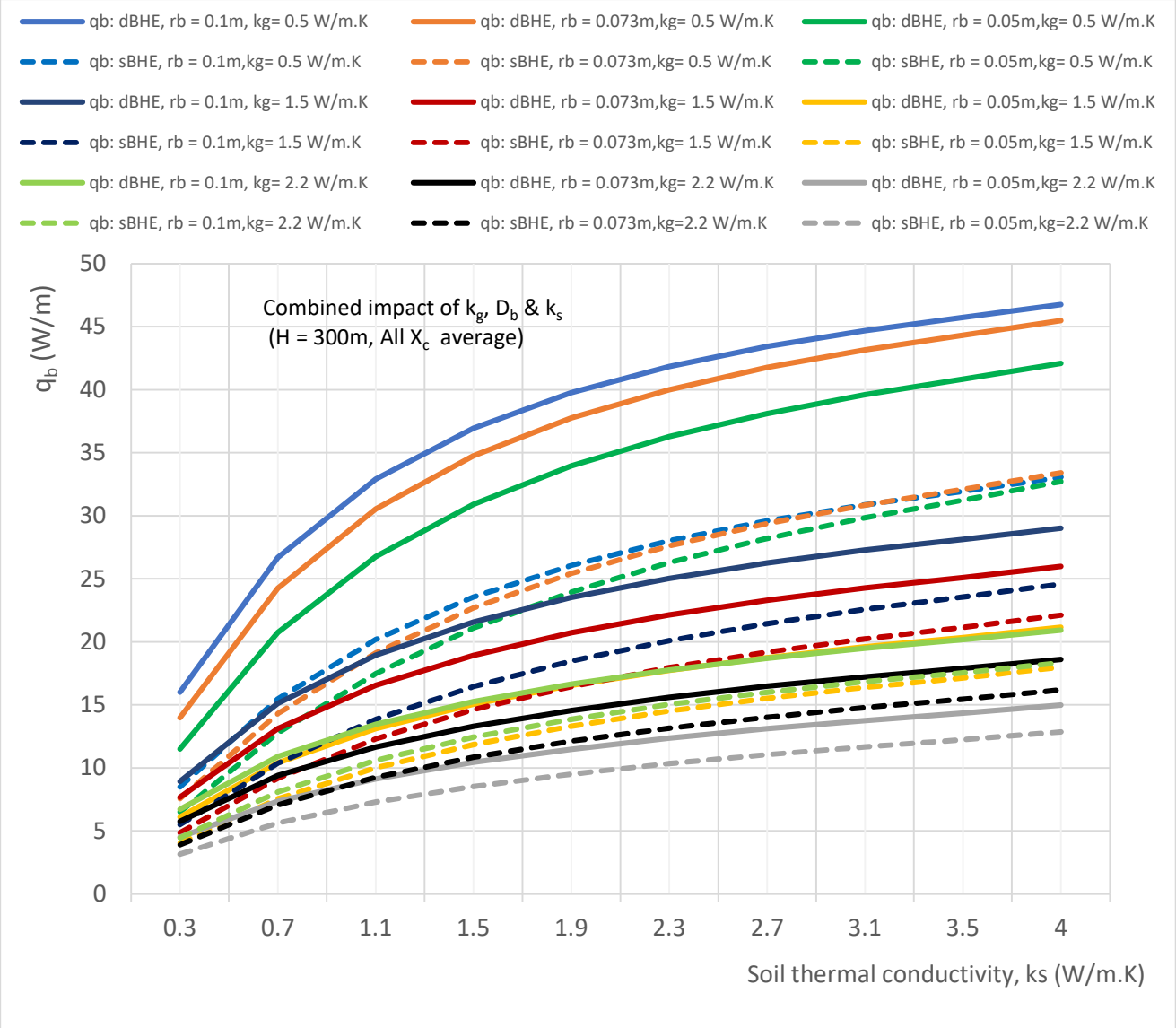

Figure 19. Combined effect of soil thermal conductivity, grout thermal conductivity and borehole size on heat transfer rate per unit borehole depth in sBHE and dBHE for the case of deep borehole depth (H = 300 m) and all borehole sizes with corresponding average shank spacing (r_b = 0.1 m with X_c = 0.05 m; r_b = 0.073 m with X_c = 0.037 m and r_b = 0.05 m with X_c = 0.025 m).

 doi:10.20944/preprints202403.0448.v1

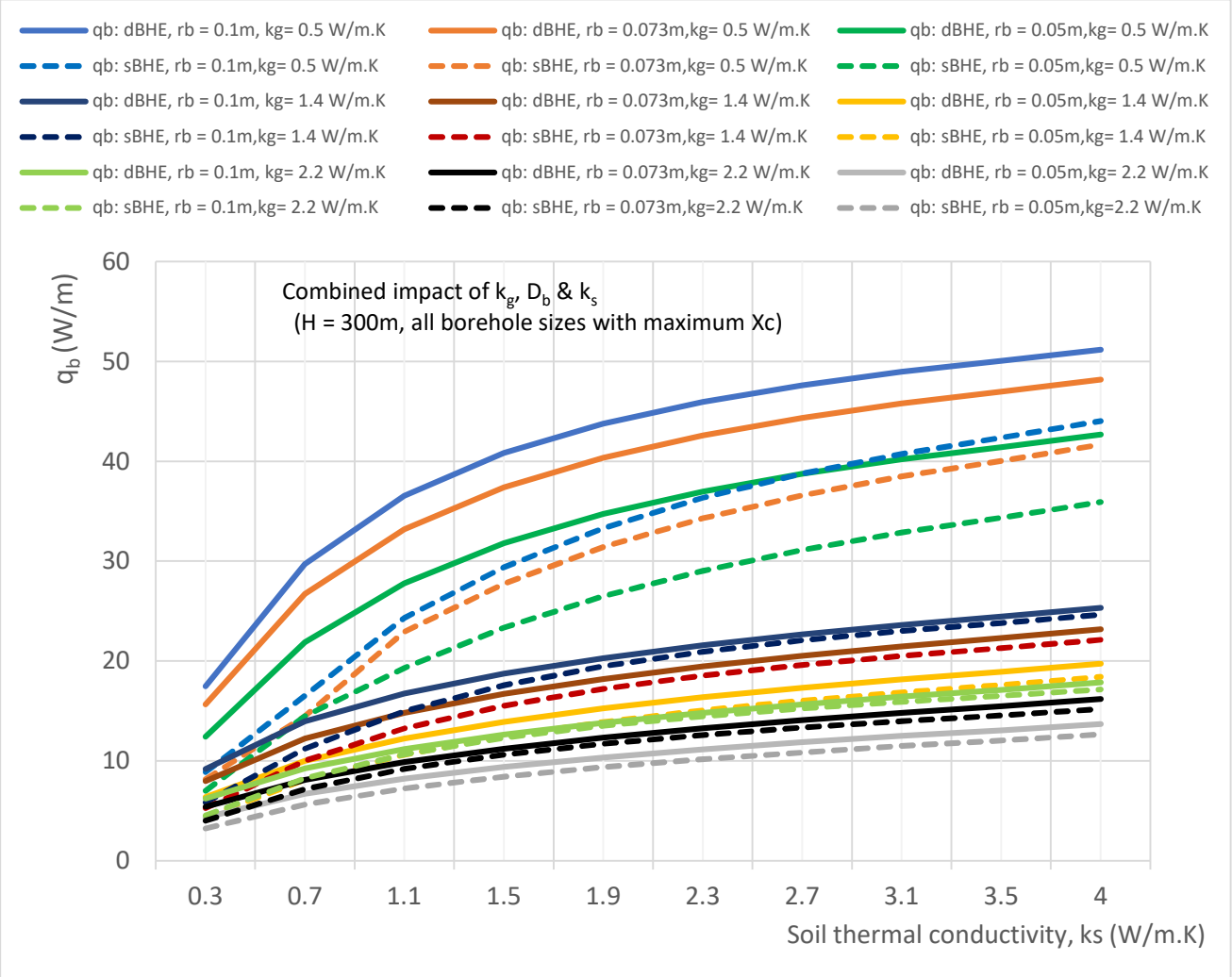

Figure 20. Combined effect of soil thermal conductivity, grout thermal conductivity and borehole size on heat transfer rate per unit borehole depth in sBHE and dBHE for the case of deep borehole depth (H = 300 m) and all borehole sizes with corresponding maximum shank spacing (r_b = 0.1 m with X_c = 0.084 m; r_b = 0.073 m with X_c = 0.057 m and r_b = 0.05 m with X_c = 0.034 m).

D. Combined Effect of Soil Thermal Conductivity, Borehole Size and Shank Spacing

In this subsection, combined impact of soil thermal conductivity, borehole size (diameter) and shank spacing on heat transfer rate per unit borehole depth in sBHE and dBHE for different cases of grout thermal conductivity (minimum, k_g = 0.5 W/m·K; average, k_g = 1.5 W/m·K and maximum, k_g = 2.2 W/m·K) and borehole depth (shallow borehole depth, H = 50 m; average borehole depth, H = 100 m and deep borehole depth, H = 300 m). The simulation result generated under this subsection has different cases (listed in Table 3 under column D) and presented in Figs. 21 to 26). This case is important as a quick reference for the design of the BHE with a given borehole depth and grout thermal conductivity, and desired to be installed at the ground with known (experimentally determined) value of thermal conductivity. Specifically, the results presented in Figs.21 to 26 provide an important information on how to select the BHE that provides the highest heat transfer among the BHE design options (sBHE and dBHE with small, medium and large borehole size and each of them have the corresponding minimum, average and maximum shank spacing) for a given soil thermal conductivity, borehole depth (H = 50 m, H = 100 m and H = 300 m) and grout thermal conductivity (k_g = 0.5 W/m·K (minimum); 1.5 W/m·K (average) and 2.2 W/m·K (maximum)). An important BHE design information can be read/obtained from these simulation results. For example, if a BHE (with shallow/deep borehole depth and with a given grout thermal conductivity) that can transfer highest heat transfer is required to be installed at the ground with a certain thermal conductivity, reference

 doi:10.20944/preprints202403.0448.v1

information suitable for the design of such BHE configuration can be obtained from results presented in Figs. 21 to 26.

The results presented in Figs. 21 to 23 indicate the combined impact of soil thermal conductivity, borehole size and shank spacing on heat transfer rate in both sBHE and dBHE filled by the grout with minimum thermal conductivity (k_g = 0.5 W/m·K) combined with shallow borehole depth (H = 50 m), average borehole depth (H = 100 m) and deep borehole depth (H = 300 m) respectively. Valuable BHE design information can be obtained from these simulation results. For instance, Figs. 21 to 23 show that dBHE with large borehole size (r_b = 0.1 m) and maximum shank spacing (X_c = 0.084 m) provides the highest heat transfer for the whole range of soil of thermal conductivity considered in this study (0.3 to 4 W/m·K). Then, it is followed by the dBHEs with medium and small borehole size each with the corresponding maximum shank spacing. In addition, Figs. 30 and 31 show that in the ground with high soil thermal conductivity (higher than 3.5 W/m·K), sBHE with large borehole size (r_b = 0.1 m) and maximum shank spacing (X_c = 0.084 m) provides more heat transfer than even dBHE with medium size (r_b = 0.073 m) and maximum shank spacing as well as dBHE with small borehole size (r_b = 0.05 m) and maximum shank spacing (X_c = 0.034 m). However, for low ground thermal conductivity (lower than 3.5 W/m·K), dBHE provides more heat transfer than the corresponding sBHE. Furthermore, Figs. 21 to 23 show that increasing shank spacing has more impact on heat transfer of dBHE than the corresponding sBHE, and this impact on heat transfer becomes higher for the ground with high soil thermal conductivity. The results depicted in Figs. 21 to 23 show that the impact of increasing borehole size and shank spacing is less effective for sBHE (as compared to the corresponding dBHE) specially for the case of the BHE with deep borehole depth (H = 300 m) shown in Figure 23. Moreover, comparison among Figs. 21 to 23 shows that case 1 (depicted in Figure 21) provides the highest transfer than the second and third case (presented in Figs. 21 and 23 or listed under column D of Table 3)

 doi:10.20944/preprints202403.0448.v1

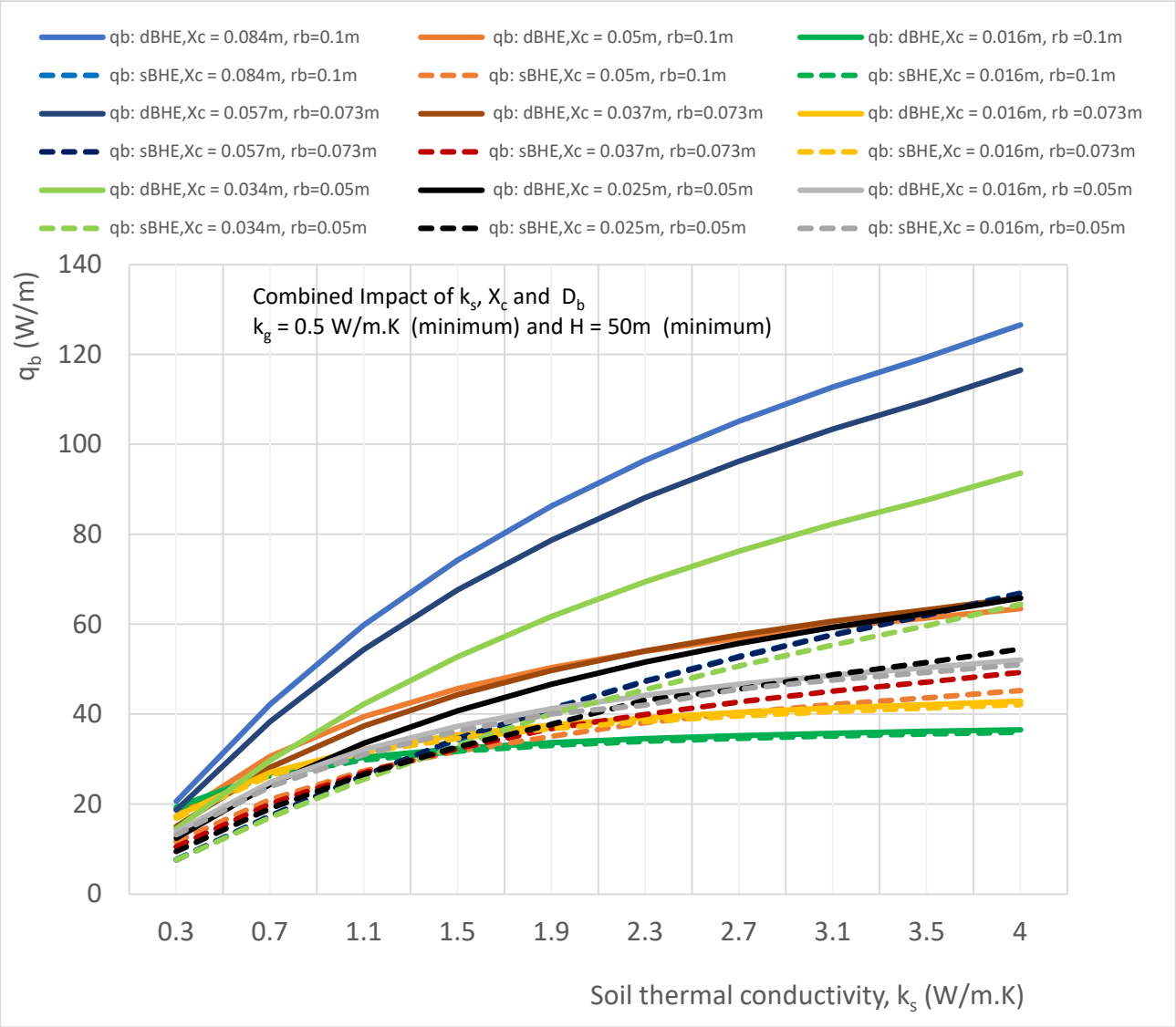

Figure 21. Combined effect of soil thermal conductivity, shank spacing and borehole size on heat transfer rate per unit borehole depth in sBHE and dBHE for the case of minimum grout thermal conductivity (k_g = 0.5 W/m·K) with shallow borehole depth (H = 50 m).

 doi:10.20944/preprints202403.0448.v1

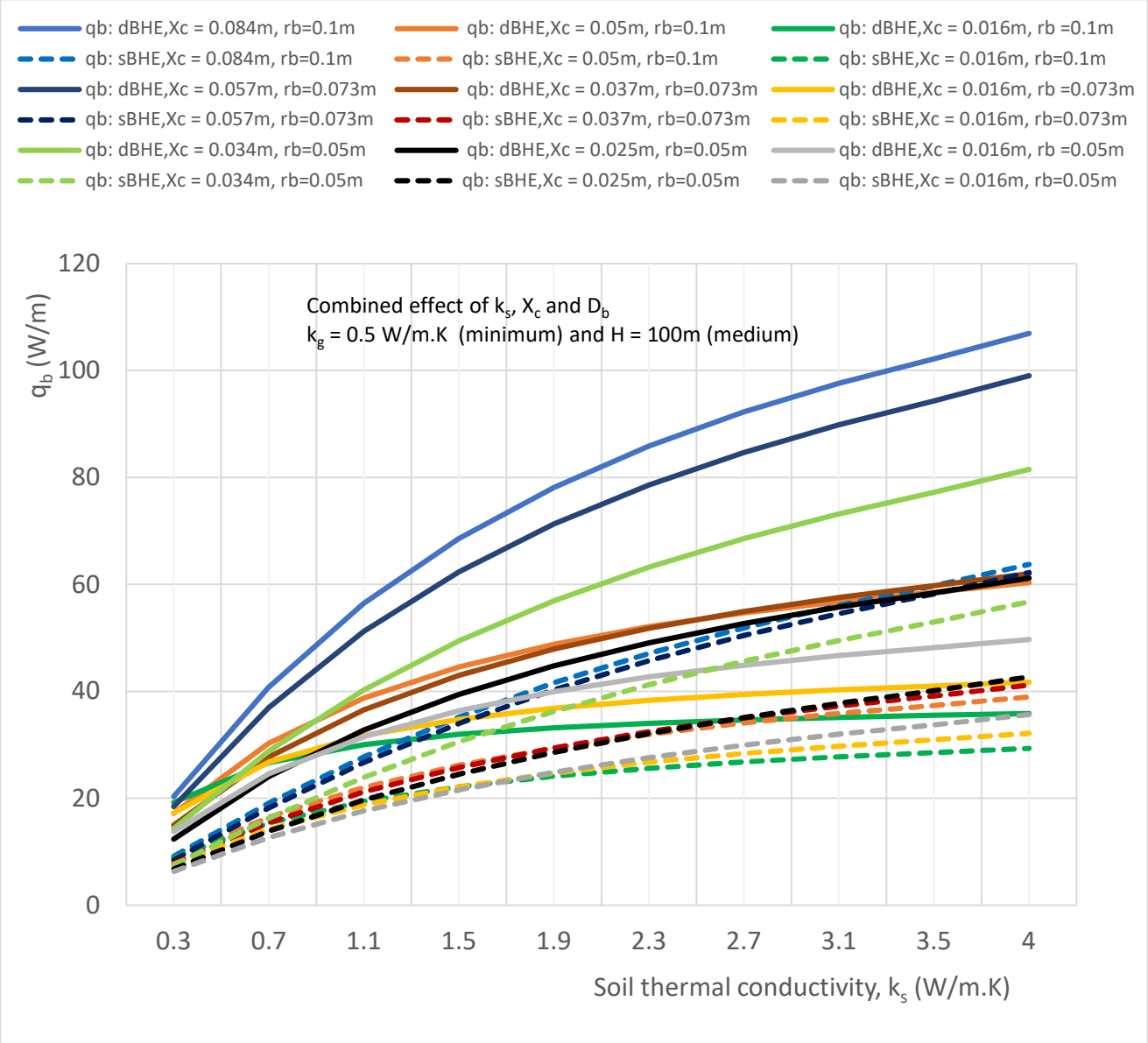

Figure 22. Combined effect of soil thermal conductivity, shank spacing and borehole size on heat transfer rate per unit borehole depth in sBHE and dBHE for the case of minimum grout thermal conductivity (k_g = 0.5 W/m·K) with average borehole depth (H = 100 m).

 doi:10.20944/preprints202403.0448.v1

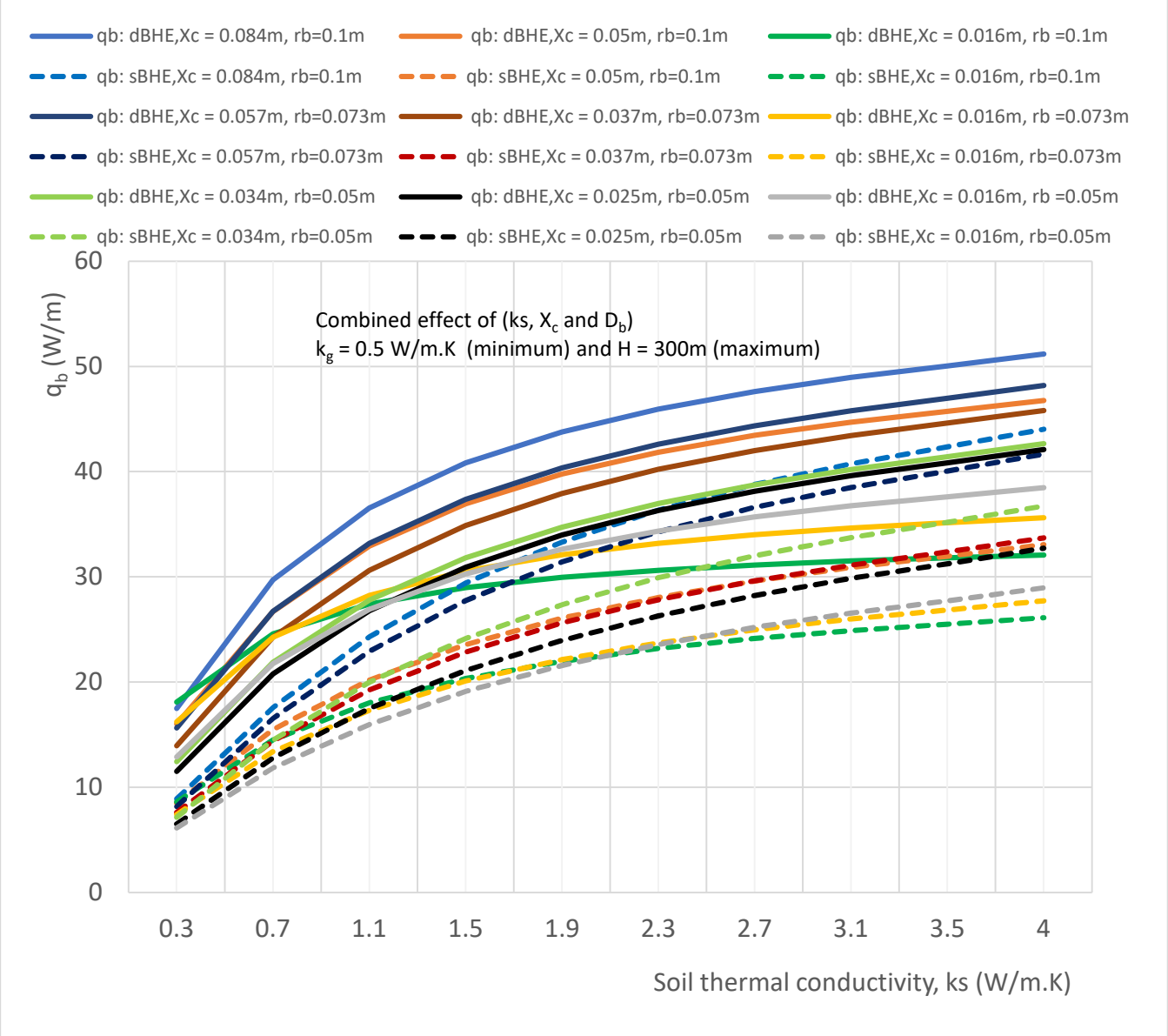

Figure 23. Combined effect of soil thermal conductivity, shank spacing and borehole size on heat transfer rate per unit borehole depth in sBHE and dBHE for the case of minimum grout thermal conductivity (k_g = 0.5 W/m·K) with high borehole depth (H = 300 m).

The results presented in Figs. 24 to 26 illustrates the combined impact of soil thermal conductivity, borehole size and shank spacing on heat transfer rate per unit borehole depth in sBHE and dBHE for the case of grout with maximum thermal conductivity (k_g = 2.2 W/m·K) borehole with shallow borehole depth (H = 50 m), average borehole depth (H = 100 m) and deep borehole depth (H = 300 m) respectively. The simulation results reveal that the heat transfer per unit borehole depth for these cases (with maximum grout thermal conductivity) indicated in Figs. 24 to 26 are the lowest as compared to the corresponding heat transfer values obtained for the remaining cases considered Table 3 under column D. The reduction in heat transfer of the BHE of these cases could be due to the thermal short-circuit associated with grout with high/maximum thermal conductivity. The impact of this thermal interference between the legs of the BHE becomes more amplified in BHE with deep borehole depth as presented in Figure 26, and hence, the heat transfer per unit borehole depth is further reduced and become the lowest as compared to all other cases considered under column D of Table 3 (Figs. 24 to 26).

 doi:10.20944/preprints202403.0448.v1

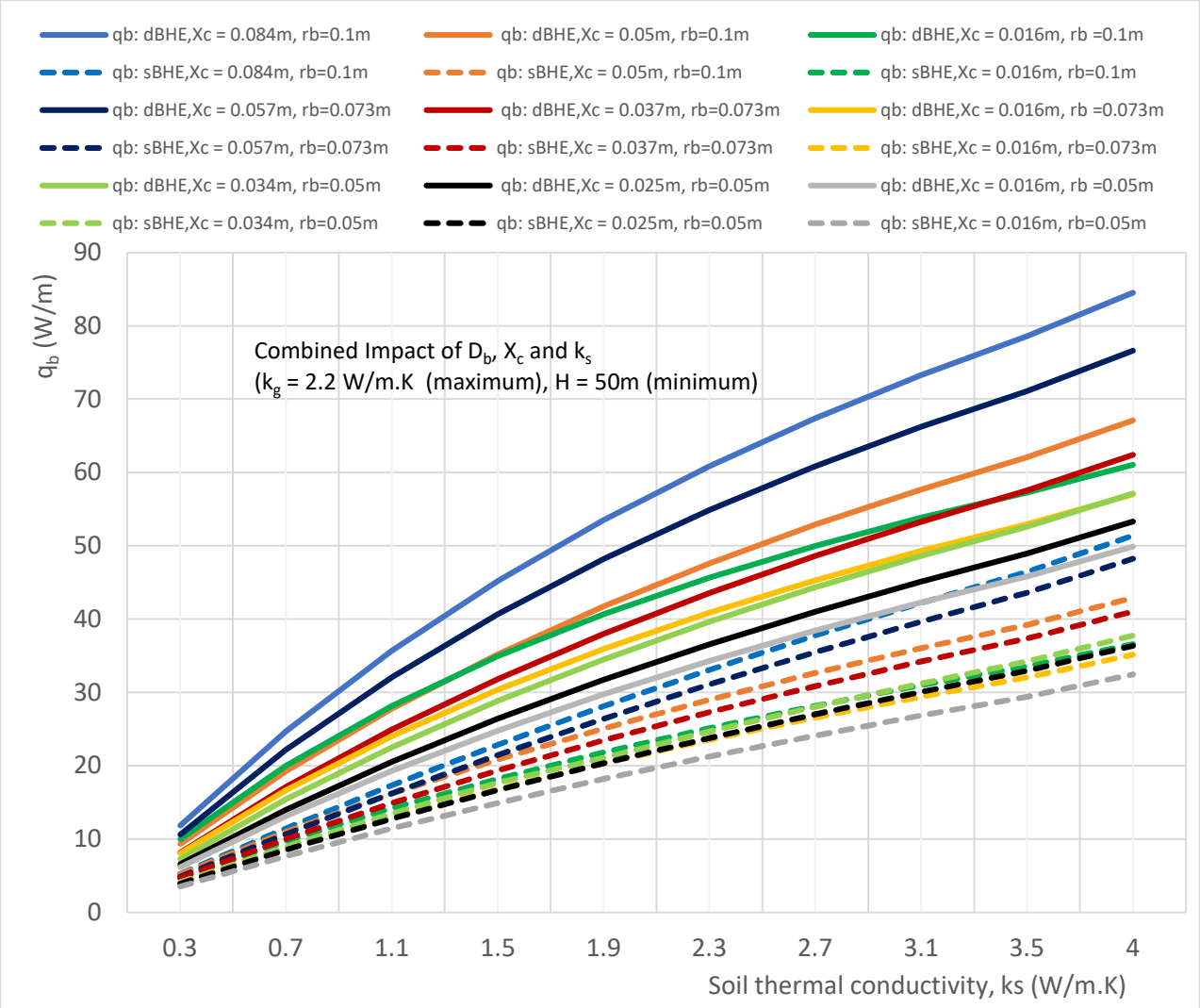

Figure 24. Combined effect of soil thermal conductivity, shank spacing and borehole size on heat transfer rate per unit borehole depth in sBHE and dBHE for the case of maximum grout thermal conductivity (k_g = 2.2 W/m·K) with shallow borehole depth (H = 50 m).

 doi:10.20944/preprints202403.0448.v1

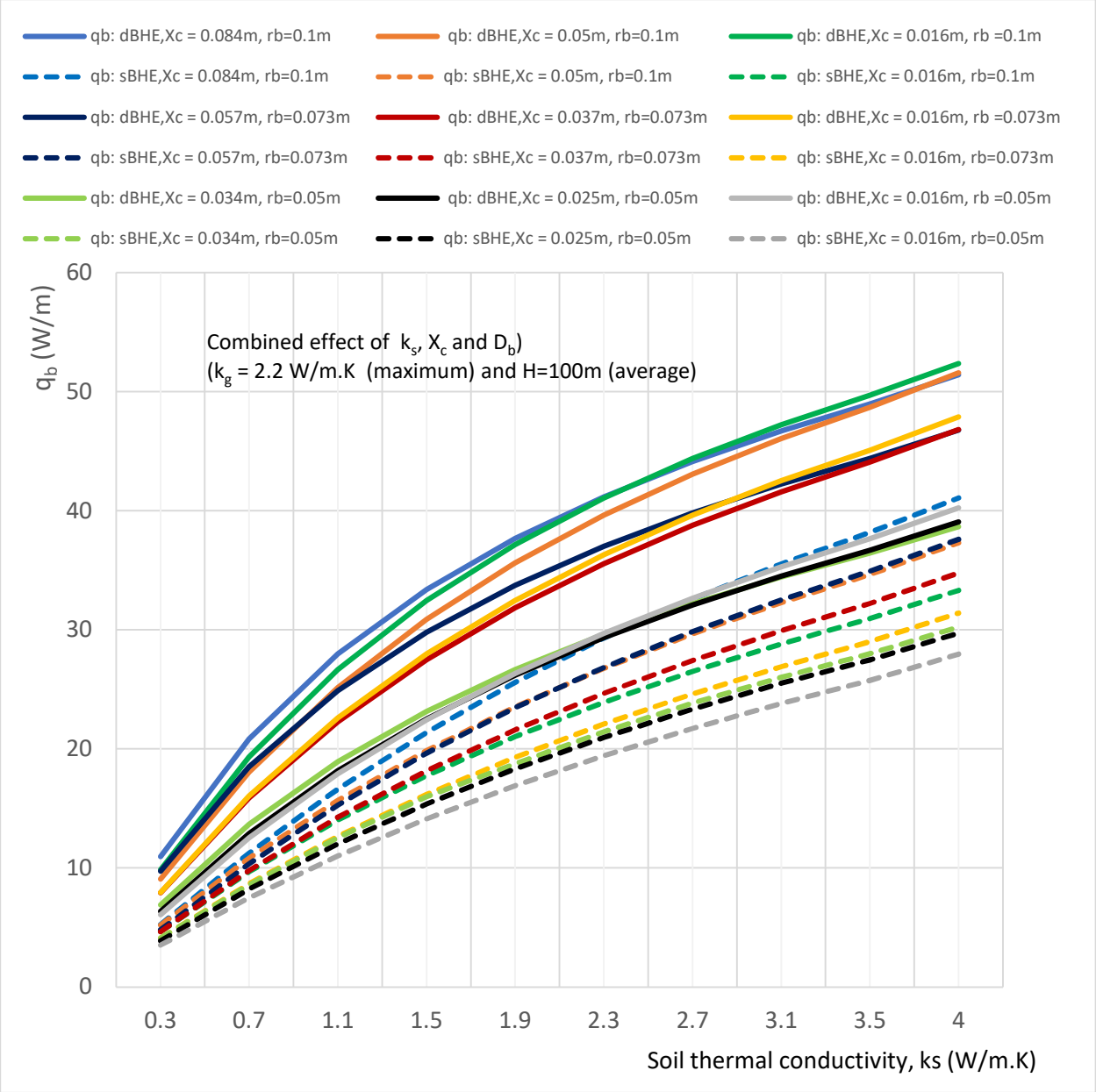

Figure 25. Combined effect of soil thermal conductivity, shank spacing and borehole size on heat transfer rate per unit borehole depth in sBHE and dBHE for the case of maximum grout thermal conductivity (k_g = 2.2 W/m·K) with medium borehole depth (H = 100 m).

 doi:10.20944/preprints202403.0448.v1

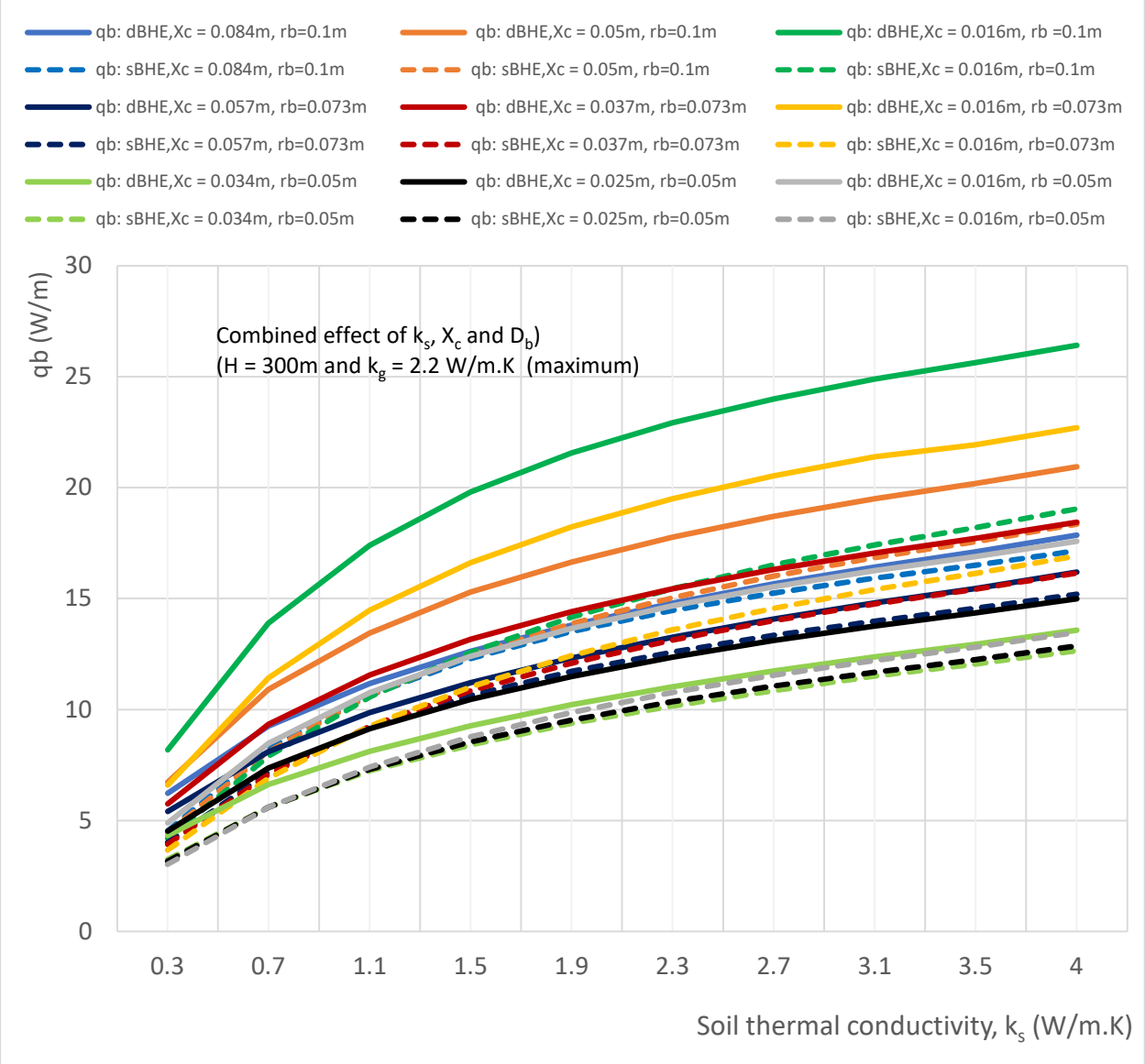

Figure 26. Combined effect of soil thermal conductivity, shank spacing and borehole size on heat transfer rate per unit borehole depth in sBHE and dBHE for the case of maximum grout thermal conductivity (k_g = 2.2 W/m·K) with deep borehole depth (H = 300 m).

3.2. Impact of Convection Heat Transfer Coefficient and Flow Regime on Heat Transfer in the BHE

The total heat transfer between the working fluid in the BHE and the soil/ground predominantly consists of convection and conduction heat transfer. The convection heat transfer, which occurs between the fluid and U-tube pipe wall, is a strong function of the parameter, convection heat transfer coefficient (h_f) which in turn depends on several factors such as velocity, surface area, type of geometry, friction factor, flow regime, etc.

In this section, the impact of convection heat transfer coefficient (h_f) and flow regime on the total heat transfer from working fluid to the ground around the BHE is discussed. In order to investigate the impact of increasing convection heat transfer coefficient on total heat transfer, the double U-tube BHE (dBHE) with different borehole sizes (small, medium and large borehole sizes) which are indicated in Table 4a, 4b and 4c) were considered respectively. The U-tube pipe used in all the three borehole sizes is HDPE (with pipe thermal conductivity of 0.4 W/m·K, outside diameter of 32 mm and inside diameter of 28 mm). To study the impact, the convection heat transfer coefficient of each flow regime (laminar and turbulent) was artificially increased by multiplying the calculated corresponding heat transfer coefficient by a factor of 2 as shown in Table 4a, 4b and 4c. For example,

 doi:10.20944/preprints202403.0448.v1

for laminar flow and turbulent flow of small size BHE (Table 4a), the calculated h_f values were 77.7 and 916.2 W/m²·K respectively.

The simulation results reveal that increasing the convection heat transfer coefficient by 100%, with mass flowrate kept constant, has insignificant impact on total heat transfer per unit borehole depth in both laminar and turbulent flows. For the smaller borehole size (shown in Table 4a), the average improvements in heat transfer per borehole depth (due to increased h_f by 100%) for laminar and turbulent flows are only 0.44 W/m (5.4%) and 0.07 W/m (0.61%), respectively. For the larger borehole size (r_b = 0.1 m, Table 4c), the corresponding average improvements in heat transfer in the laminar and turbulent flow are 0.33 W/m (8.9%) and 0.2 W/m (0.59%), respectively. Thus, when the mass flow rate is kept fixed and convective heat transfer coefficient is artificially increased even by two orders of magnitude, the increase in heat transfer is negligible particularly when the flow is turbulent. Based on this result, there is no benefit of increasing internal convective heat transfer coefficient on the improvement of the overall heat transfer in the BHE. Furthermore, the results presented in Table 4a, 4b and 4c show that the heat transfer rate is highest in the turbulent flow regime. This increase of the total heat transfer for turbulent flow could be due to the convective heat transfer coefficient of the convective heat transfer between the fluid and the pipe surface.

Table 4. a. The impact of convection heat transfer coefficient (h_f) on the total heat transfer rate of dBHE with small borehole size (r_b = 0.05 m, X_c = 0.025 m, k_g = 0.5 W/m·K, H = 25 m, $T_{f,in}$ = 15 °C).

Soil thermal conductivity k_s (W/m·K)	**q_b (W/m)**			
	Laminar flow Re = 1021 ($\dot{m}$ = 0.02 kg/s)		**Turbulent flow** Re = 5617 ($\dot{m}$ = 0.11 kg/s)	
	@ $h_{f,1}$ = 77.7 W/m²·K	@ $h_{f,2}$ = 2 × $h_{f,1}$	@ $h_{f,1}$ = 916.2 W/m²·K	@ $h_{f,2}$ = 2 × $h_{f,1}$
0.3	2.68	2.8	3.07	3.08
0.7	4.92	5.15	5.95	5.98
1.1	6.49	6.82	8.19	8.23
1.5	7.66	8.06	9.98	10.04
1.9	8.57	9.03	11.47	11.53
2.3	9.3	9.81	12.72	12.8
2.7	9.9	10.44	13.79	13.88
3.1	10.4	10.98	14.73	14.82
3.5	10.83	11.44	15.54	15.64
4.0	11.28	11.92	16.42	16.54

Table 4. b. The impact of convection heat transfer coefficient on the total heat transfer rate of dBHE with medium borehole size (r_b = 0.07 m, X_c = 0.035 m, k_g = 1.3 W/m·K, H = 125 m, $T_{f,in}$ = 27 °C).

Soil thermal conductivity k_s (W/m·K)	**q_b (W/m)**			
	Laminar flow Re = 1021 ($\dot{m}$ = 0.02 kg/s)		**Turbulent flow** Re = 7660 ($\dot{m}$ = 0.15 kg/s)	
	@ $h_{f,1}$ = 77.7 W/m²·K	@ $h_{f,2}$ = 2 × $h_{f,1}$	@ $h_{f,1}$ = 1244.5 W/m²·K	@ $h_{f,2}$ = 2 × $h_{f,1}$
0.3	3.39	3.54	6.81	7.47
0.7	4.81	5.01	13.58	14.89

Preprints.org (www.preprints.org) | NOT PEER-REVIEWED | Posted: 7 March 2024 doi:10.20944/preprints202403.0448.v1

1.1	5.62	5.85	18.91	20.72
1.5	6.18	6.44	23.2	25.39
1.9	6.6	6.89	26.72	29.23
2.3	6.93	7.25	29.68	32.46
2.7	7.2	7.54	32.19	35.20
3.1	7.42	7.78	34.36	37.56
3.5	7.62	7.99	36.26	39.62
4.0	7.82	8.22	38.32	41.86

Table 4. c. The impact of convection heat transfer coefficient (h_f) on the total heat transfer rate of dBHE with large borehole size (r_b = 0.1 m, X_c = 0.05 m, k_g = 2.5 W/m·K, H = 250 m, $T_{f,in}$ = 42 °C).

Soil thermal conductivity k_s (W/m·K)	**qb (W/m)**			
	Laminar flow Re =1021 ($\dot{m}$ = 0.02 kg/s)		**Turbulent flow** Re = 10213 ($\dot{m}$ = 0.2 kg/s)	
	@ $h_{f,1}$ = 77.7 W/m^2·K	@ $h_{f,2}$ = 2 × $h_{f,1}$	@ $h_{f,1}$ = 1631.6 W/m^2·K	@ $h_{f,2}$ = 2 × $h_{f,1}$
0.3	1.97	2.11	12.01	12.12
0.7	2.74	2.95	21.35	21.50
1.1	3.22	3.49	27.61	27.79
1.5	3.58	3.88	32.17	32.36
1.9	3.84	4.19	35.69	35.90
2.3	4.08	4.44	38.55	38.77
2.7	4.26	4.65	40.93	41.15
3.1	4.42	4.83	42.95	43.19
3.5	4.56	4.99	44.72	44.96
4.0	4.71	5.16	46.63	46.88

Analysis has also been made to investigate the impact of flow regimes on total heat transfer in the BHE. To generate the heat transfer profiles in different flow regime (shown in Figs. 27 and 28), the input values of the fixed parameters to the model are specified as: borehole radius, r_b = 0.1 m, half shank spacing, X_c = 0.05 m; grout thermal conductivity, k_g = 1.5 W/m·K, borehole depth, H = 100 m, $T_{f,in}$ = 40 °C, undisturbed ground temperature, T_o = 10 °C, pipe thermal conductivity, k_p = 0.4 W/m·K; outer pipe diameter, 32 mm; inner pipe diameter, 28 mm. The input values of the other fixed parameters of the thermal properties of fluid (water), back-fill material and soil are listed in Table 1. Figure 27 illustrates the variation of total heat transfer in the laminar, transitional and turbulent flow in the dBHE at different values of soil thermal conductivity. The profile of the total heat transfer in different flow regime of sBHE is presented in Figure 28. Looking at Figs. 27 and 28, there is a significant difference in heat transfer profile in between laminar and turbulent flow. The heat transfer in the laminar flow is lower and increases linearly with mass flow rate while it gets higher and increases nonlinearly in the turbulent flow. When the mass flow rate is too high, the fluid temperature will change slowly along the U-tube, and hence, keeping the larger temperature difference between the fluid and the ground for a longer period and resulting in higher heat transfer in the turbulent flow. The reverse is true for laminar flow with lower mass flow rate, resulting in lower heat transfer. It is also interesting to notice from Figs. 27 and 28 that with further increase in mass flowrate, the heat transfer profile in the turbulent flow tends to reach a plateau (i.e., the increase in heat transfer is

 doi:10.20944/preprints202403.0448.v1

insignificant). Moreover, the improvement in heat transfer from laminar to turbulent flow regime is greatest when the soil thermal conductivity is highest (in this case, at k_s = 4 W/m·K).

Finally, if one wants to have laminar flow for reducing pumping power, it may be beneficial to use a nanofluid to enhance heat transfer provided that the nanofluid does not have a high viscosity. However, if the flow is already turbulent, using a nanofluid is a waste of money. In addition, in the turbulent flow when mass flowrate is too high, the associated operational energy consumption gets higher without improvement in total heat transfer since the increased pressure loss causes an increased in flow resistance resulting in reduced overall heat exchange performance.

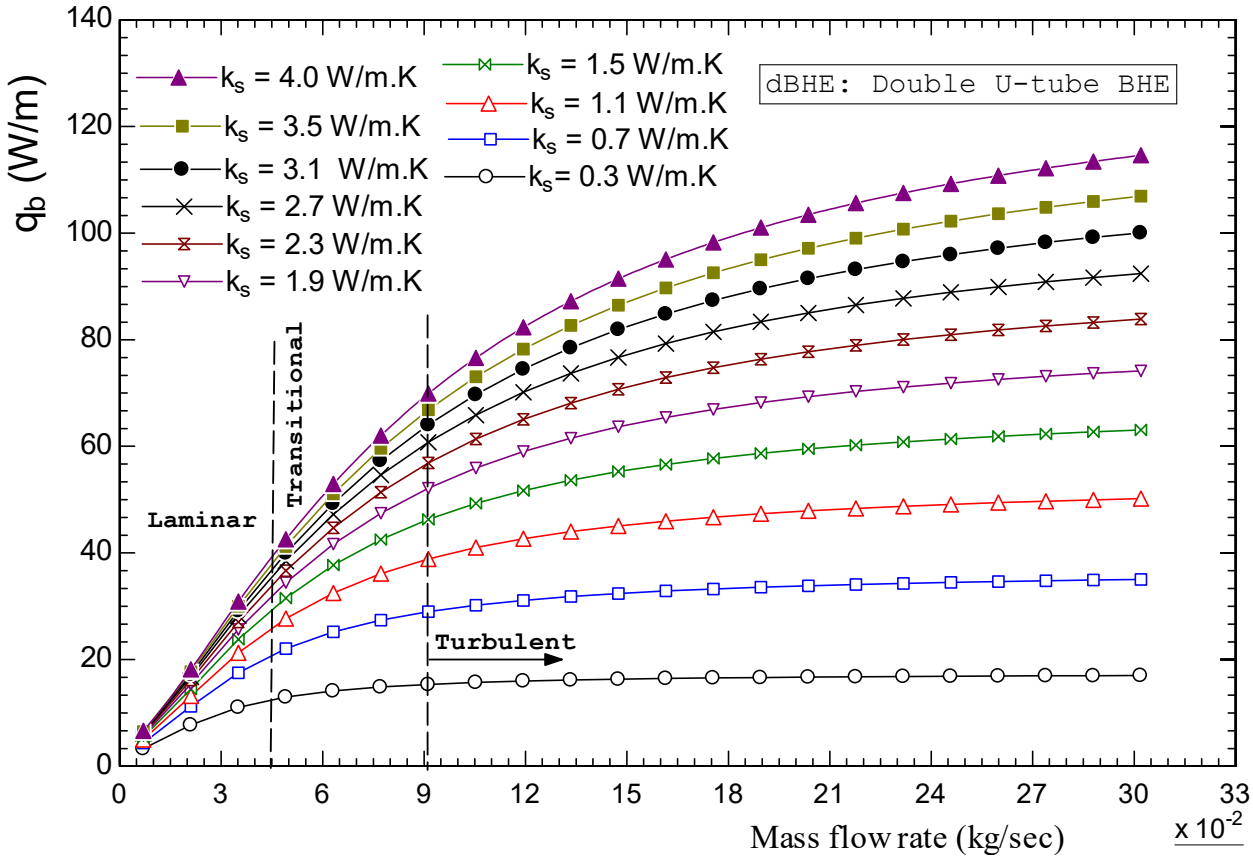

Figure 27. Profile of the total heat transfer rate per unit bore hole depth in different flow regimes in the double U-tube BHE.

 doi:10.20944/preprints202403.0448.v1

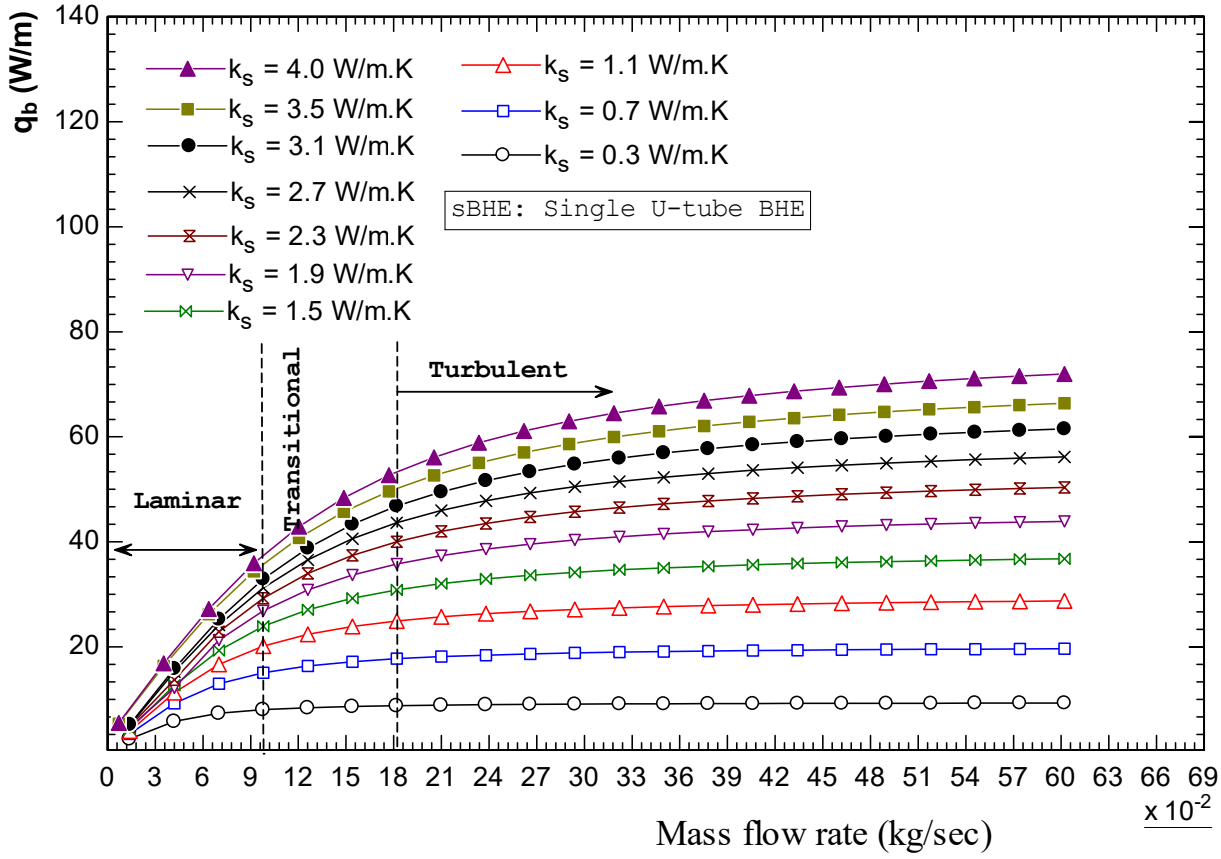

Figure 28. Profile of the total heat transfer per unit bore hole depth in different flow regimes in the single U-tube BHE.

3.3. Pumping Power and Pressure Loss in the BHE

Another crucial feature that is required in the design of a BHE is the pumping power which is required to circulate the working fluid in the closed loop of the BHE. Particularly, in the BHE with deep borehole, there is high pressure loss and head loss incurred resulting in high pumping energy consumption to circulate the working fluid. The pumping energy consumption is directly related to the total cost of the ground source heat pump system that delivers space heating and cooling. As a result, including analysis of pumping power and pressure loss or head loss in the performance analysis of BHE is important.

In this paper, analysis and comparison of pumping power and pressure loss as well as the head loss in between sBHE and dBHE is performed. The variation of pressure drop and head loss with total mass flowrate of the working fluid (0.22 to 0.4 kg/s) for sBHE and dBHE with borehole depth of 100 m and U-tube pipe (made of HDPE with k_p of 0.4 W/m·K, 32 mm outside diameter and 28 mm inner diameter) is illustrated in Figure 29. The comparison result indicates that the total pressure drops and head loss in the sBHE is higher than that of dBHE leading to higher pump power consumption. Accordingly, as evidenced in Figure 30, for the same operating condition, the corresponding circulating pump power is more when sBHE is utilized than that of the dBHE. At the flow rate of 0.22 kg/s, the pumping power for sBHE is 1.21 W more than that of the dBHE. Furthermore, the difference in pumping power between sBHE and dBHE reaches about 6.36 W when the fluid flow rate is increased to 0.4 kg/s. Therefore, based on this analysis, to reduce the pressure drop to a reasonable range (and hence reduce the required pumping energy consumption), it is better to utilize the dBHE. But still, further analysis that compares the total cost between the two BHEs needs be performed to select the configuration that consumes lower power with reasonable total cost along with improved thermal performance.

Furthermore, for the detail understanding of the pumping power consumption of a BHE, the pressure loss as a function of borehole depth is analyzed. As indicated in Figure 31, the total pressure

 doi:10.20944/preprints202403.0448.v1

loss gets higher as the borehole depth increases. This in turn leads to higher pumping power consumption for the longer borehole depth as depicted in Figure 32. Hence, both the pressure loss and pumping power increase parabolically with the borehole depth; when the borehole length is raised from 100 m to 250 m, pumping rate increases by 5.7 and 5.6 times for sBHE and dBHE, respectively. The corresponding pressure loss is raised up by 3.7 and 3.6 times for sBHE and dBHE, respectively. This shows that BHE with shallow borehole depth and lower mass flowrate within reasonable range of velocity is preferable since BHE with large depth and mass flowrate results in high pressure loss and increased pumping power consumption.

Moreover, as can be inferred from Figs. 29 to 32, at all the borehole depth, both pressure loss and pumping power of the sBHE is higher than that of the dBHE. Further comparative analysis also indicates that the difference in pressure drop and pumping power between the two BHEs becomes higher and higher with further increase of mass flow rate and borehole depth. For the borehole depth (H) of 25 m, the decrease in both pressure loss and pumping power when the dBHE is utilized is 39.7%; whereas for the deep borehole depth of 250 m, if the dBHE configuration is used, then the pressure loss and pumping power are reduced by 40.5% and 38.6%, respectively.

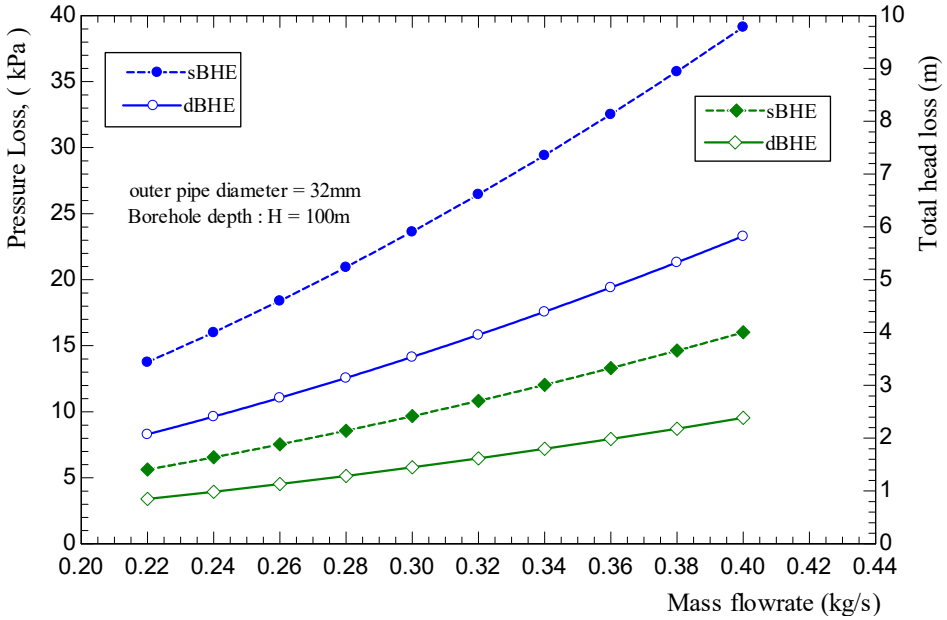

Figure 29. Pressure and head losses in the single and double U-tube BHEs with borehole depth of 100 m and outside pipe diameter of 32 mm.

Preprints.org (www.preprints.org) | NOT PEER-REVIEWED | Posted: 7 March 2024 doi:10.20944/preprints202403.0448.v1

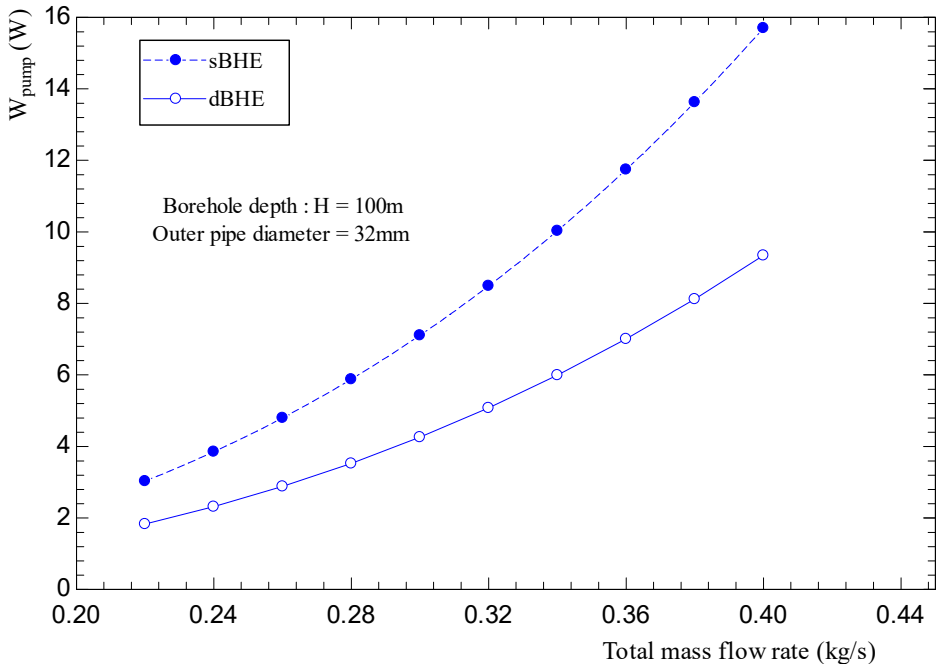

Figure 30. Theoretical pumping power to circulate working fluid in the single and double U-tube BHEs with borehole depth of 100 m and outside pipe diameter of 32 mm.

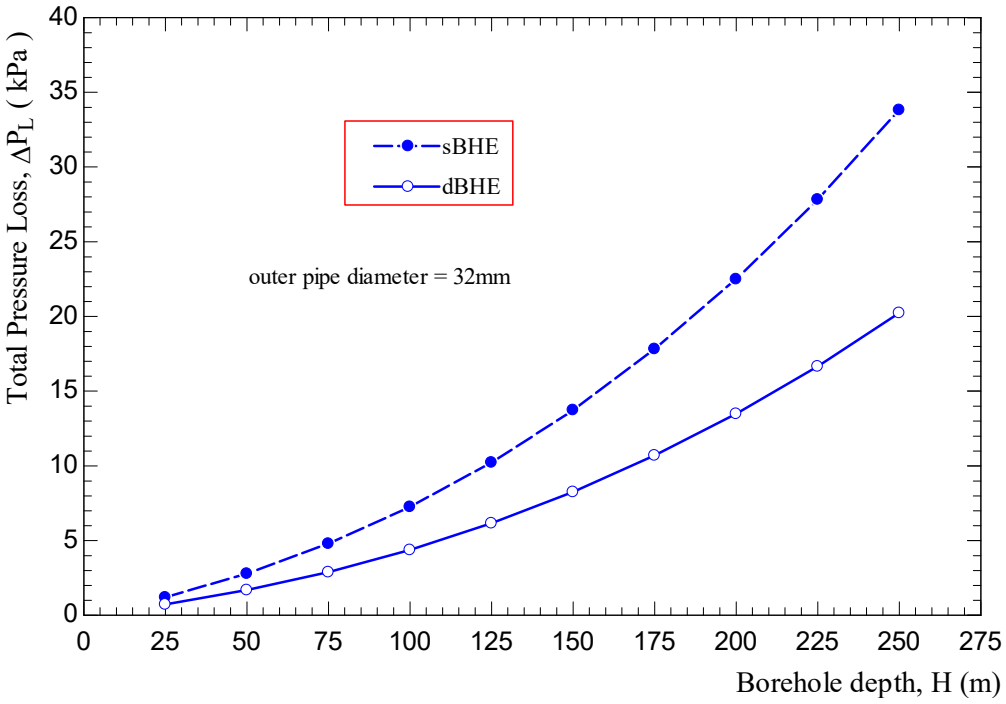

Figure 31. Pressure drop variation with borehole depth for single and double U-tube BHEs with HDPE pipe outer diameter of 32 mm.

 doi:10.20944/preprints202403.0448.v1

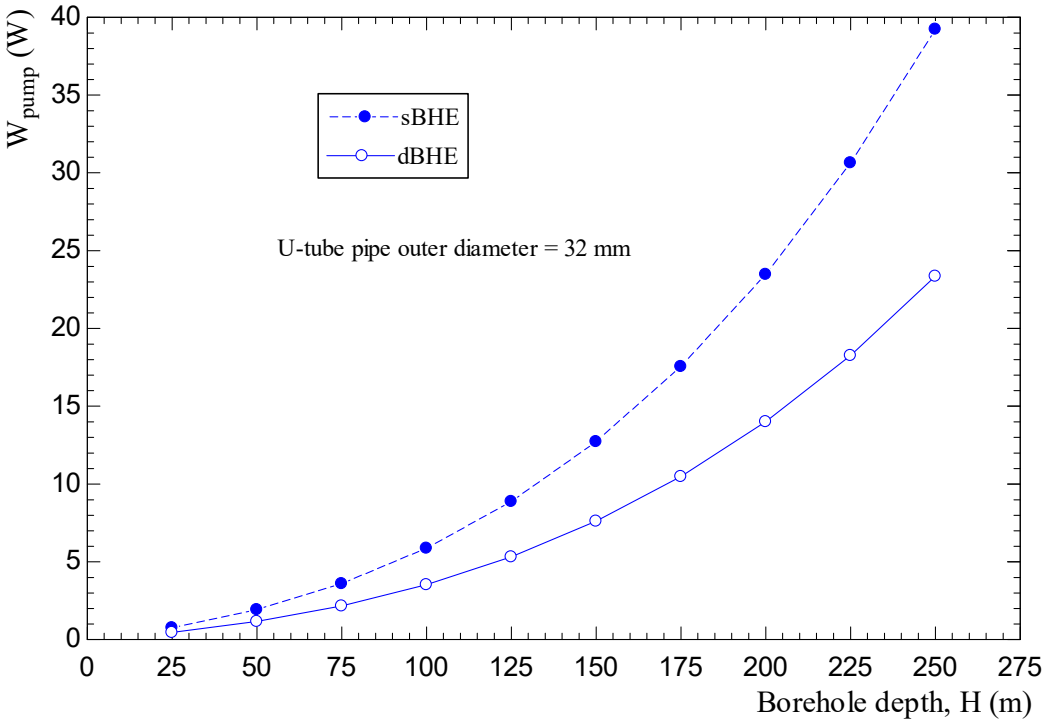

Figure 32. Pumping power variation with borehole depth for single and double U-tubes made of HDPE pipe (outer diameter of 32mm).

4. Conclusion

In this paper, combined effect of major influencing parameters that affect the performance of both single U-tube BHE (sBHE) and double U-tube BHE (dBHE) was numerically studied. Geometrical parameters, such as shank spacing (with maximum, average and minimum values) and borehole size/diameters (large, medium and small borehole sizes) and borehole depth (shallow, average and deep borehole depths) were considered. Thermal conductivities of soil and grout which ranges from minimum to high values were also taken into consideration. The combined impact of different parameters was included under four major cases: (A) combined effect of borehole depth, borehole size and shank spacing, (B) combined effect of borehole depth, and soil and grout thermal conductivities, (C) combined effect of soil and grout thermal conductivities and borehole size, and (D) combined effect of soil thermal conductivity, borehole size and shank spacing. Each of these major cases has nine different design options of sBHE and dBHE. Using the previously developed numerical heat transfer model, series of heat transfer data in graphical form that helps to investigate the combined impact of various parameters on heat transfer per unit borehole depth were generated for some of the considered cases. With the given parameters, one can select the BHE case that provides highest heat transfer among the various cases of sBHE and dBHE.

Finally, the impact of convection heat transfer coefficient and flow regime on heat transfer per unit borehole depth of sBHE and dBHE was studied. Evaluation of total pressure loss in the BHE as well as pumping power required to circulate the fluid in the BHE was made; and the two BHEs were also compared in terms of total pressure loss/head loss as well as pumping power.

The key findings are recapped as in the following:

- Among the cases considered under Case A, dBHE with large borehole size, maximum shank spacing, minimum grout thermal conductivity and maximum soil thermal conductivity provides the highest heat transfer per unit borehole depth while the lowest heat transfer is obtained for case 7 (column A) with maximum grout thermal conductivity and low soil thermal conductivity.

 doi:10.20944/preprints202403.0448.v1

- For deep borehole depth and with high grout thermal conductivity, dBHE with large borehole size and minimum shank spacing provides the highest heat transfer; while for shallow borehole depth, dBHE with large borehole size and maximum shank spacing is the most effective.
- When grout conductivity is low and soil thermal conductivity is at average or high value, using BHE with maximum shank spacing is effective in large borehole size, while minimum shank spacing is more effective in BHE with small borehole size.
- Among the cases considered under case B, case 9 (see Table 3) provides the highest heat transfer per unit borehole depth; and of all the cases, dBHE with large borehole size, maximum shank spacing, low grout thermal conductivity and high soil thermal conductivity is the most effective to transfer heat (especially for borehole with shallow borehole depth) than any other cases; and for borehole with deep borehole depth, sBHE with the same design conditions is preferred. This confirms the results obtained under case A.
- Comparison among the cases (listed under column C of Table 3) shows that the third case with shallow borehole depth (H = 50 m) and all BHEs with maximum shank spacing provided the highest heat transfer per unit borehole depth; while the lowest heat transfer was obtained for the BHE with deep borehole depth and all BHEs with minimum shank spacing.
- dBHE is effective for shallow borehole depth while sBHE is preferred for deep borehole depth due to thermal interference; and to reduce the impact of the thermal loss due to thermal short-circuit associated with BHE with deep borehole depth, increasing the shank spacing, utilizing large borehole diameter and low grout thermal conductivity could be among the design options that can be considered.

- Reduced grout thermal conductivity combined with increased borehole size has more impact on heat transfer than combined increase of borehole size and grout thermal conductivity. High grout thermal conductivity reduces heat transfer, particularly for dBHE with deep borehole depth and low shank spacing.
- For BHE with minimum shank spacing and deep borehole depth, using BHE with large borehole size is not preferred to transfer more heat. This could be due to the augmented phenomenon of thermal short-circuit between the legs of the BHE with the minimum shank spacing and deep borehole depth.
- If a BHE with deep borehole depth is required to be designed to deliver the highest heat transfer rate per unit borehole depth, then dBHE with large borehole diameter, large shank spacing, low grout thermal conductivity and high soil thermal conductivity is preferred.
- Increasing internal convective heat transfer coefficient has negligible impact on the improvement of the overall heat transfer in the BHE particularly when the flow is turbulent; and if one wants to have laminar flow for reducing pumping power, it may be beneficial to use a nanofluid to enhance heat transfer provided that the nanofluid does not have a high viscosity.
- The total pressure loss and pumping power required to circulate fluid in the sBHE is higher than that of dBHE; and the total pressure loss and fluid pumping power increases parabolically with the borehole depth.

Overall, the obtained result can be used as a quick reference in the design and optimization of single and double U-tube BHEs that can be integrated with ground source heat pump system.

Acknowledgements: The authors would like to acknowledge the Natural Sciences and Engineering Research Council (NSERC) of Canada Discovery Grant for their financial support of this research.

 doi:10.20944/preprints202403.0448.v1

Nomenclature

C	specific heat capacity (J/kgK)
X_c	half of the shank spacing of U-tube (m)
H	borehole depth (m)
h	heat transfer coefficient (W/m^2K)
k_f	fluid thermal conductivity (W/mK)
k_g	grout thermal conductivity(W/mK)
k_s	ground (soil) thermal conductivity (W/mK)
$\dot{m}_f$	fluid mass flowrate (kg/s)
M_f	mass of the fluid node (kg)
M_g	mass of the grout node (kg)
M_s	mass of the soil node (kg)
$\dot{Q}$	heat transfer rate (W)
q_b	total heat transfer rate into/out of the borehole (W/m)
r_b	radius of the borehole (m)
r_{po}	pipe outer radius (m)
r_{pi}	pipe inner radius (m)
R	thermal resistance per unit length (mK/W)
Re	Reynolds number
T	temperature (°C)
T_f	fluid temperature (°C)
$T_{f1,0}$	inlet temperature of the working fluid in U-tube 1-3 (°C)
$T_{f2,0}$	inlet temperature of the fluid U-tube 2-4 (°C)
T_{f1}	fluid temperature of down flow in U-tube 1-3 (°C)
T_{f3}	fluid temperature of upward flow in U-tube 1-3 (°C)
T_{f2}	fluid temperature of down flow in U-tube 2-4 (°C)
T_{f4}	fluid temperature of upward flow in U-tube 2-4 (°C)
T_g	temperature fill material (grout) (°C)
T_b	wall temperature of the borehole (°C)
T_s	temperature of ground (soil) (°C)
T_o	undisturbed ground temperature (°C)
Greek Symbols	
Δz	vertical distance between adjacent nodes (m)
Δt	duration of time step (s)
ρ	density (kg/m^3)
α	Thermal diffusivity (m^2/s)
μ	dynamic viscosity (kg/ms)
ϵ	thermal effectiveness
Subscripts	
b	borehole
g	grout (fill-material)

 doi:10.20944/preprints202403.0448.v1

f	fluid
s	ground (soil)

References

- Adamovsky D., Neuberger P., Adamovsky R. Results of operational verification of vertical ground heat exchangers. Energy and Buildings 152 (2017) 185-193.
- Bauer D., Heidemann W., Muller-Steinhagen H., Diersch H.J. Thermal resistance and capacity models for borehole heat exchangers. International Journal of Energy Research 35 (2011) 312-320.
- Beier R.A., Acuna J., Mogensen P., Palm B. Transient heat transfer in a coaxial borehole heat exchanger. Geothermics 51 (2014) 470-482.
- Biglarian, H., Abbaspour, M., Saidi, M.H. A numerical model for transient simulation of borehole heat exchangers. Renew. Energy 104 (2017) 224–237.
- Cao S., Kong X., Deng Y., Zhang W., Yang L, Ye Z. Investigation on thermal performance of steel heat exchanger for ground source heat pump systems using full-scale experiments and numerical simulations. Applied Thermal Engineering 115 (2017) 91-98.
- Casasso A., Sethi R. Efficiency of closed loop geothermal heat pumps: A sensitivity analysis. Renewable Energy 62 (2014) 737-746.
- Chen S., Mao J., Han X. Heat transfer analysis of a vertical ground heat exchanger using numerical simulation and multiple regression model. Energy Build 129 (2016) 81-91.
- Choi W., Kikumoto H., Ooka R. Probabilistic uncertainty quantification of borehole thermal resistance in real-world scenarios, Energy 254(2022)124400.
- Conti P., Testi D., Grassi W. Revised heat transfer modeling of double-U vertical ground-couple heat exchangers. Applied Thermal Engineering. 106 (2016)1257-1267.
- Erbay Z., Hepbasli A. Exergoeconomic evaluation of a ground-source heat pump food dryer at varying dead state temperatures, J. Clean. Prod. 142 (2017a) 1425–1435.
- Erbay Z., Hepbasli A. Assessment of cost sources and improvement potentials of a ground-source heat pump food drying system through advanced exergoeconomic analysis method, Energy 127 (2017b) 502–515.
- Fang L., Diao N., Fang Z., Ke Zhu K., Zhang W. Study on the efficiency of single and double U-tube heat exchangers. Procedia Engineering 205 (2017) 4045-4051.
- Florides G.A., Christodoulides P., Pouloupatis P. Single and double U-tube ground heat exchangers in multiple-layer substrates. Appl Energy 102 (2013) 364 -373.
- Florides G., Kalogirou S. Ground heat exchangers: a review of systems, models and applications. Renew Energy 32(2007) 2461-78.
- Fox R.W., McDonald A.T., Pritchard P.J., Mitchell J.W. Fox and McDonald's Introduction to Fluid Mechanics. 8th ed., John Wiley & Sons, 2011, chapter 8.
- Gao J., Zhang X., Liu J., Li K.S., Yang J. Thermal performance and ground temperature of vertical pile-foundation heat exchangers: A case study. Applied Thermal Engineering 28 (2008) 2295-2304.
- Han C., Yu X. (Bill). Sensitivity analysis of a vertical geothermal heat pump system, Appl. Energy 170 (2016) 148-160.
- Hu P., Yub Z., Zhua N., Leia F, Yuan X. Performance study of a ground heat exchanger based on the multipole theory heat transfer model. Energy and Buildings 65 (2013) 231-241.
- Jalaluddin M.A, Tsubaki K., Inoue S., Yoshida K., Experimental study of several types of ground heat exchanger using a steel pile foundation, Renew. Energy 36 (2011) 764-771.
- Javed S. and Spitler J. Calculation of borehole thermal resistance. In: S. Rees, ed., Advances in Ground-Source Heat Pump Systems, 1st ed. Cambridge: Woodhead Publishing (2016)71-89.
- Jun L., Xu Z., Jun G., Jie Y. Evaluation of heat exchange rate of GHE in geothermal heat pump systems. Renewable Energy 34 (2009) 2898-2904.
- Jung C.C, Lee S.R, Lee D.S. Numerical simulation of vertical ground heat exchangers: Intermittent operation in unsaturated soil conditions, Computer. Geotech. 38(2011) 949-958.
- Kerme E.D., Fung A.S. Heat transfer simulation, analysis and performance study of single U-tube borehole heat exchanger. Renewable Energy 145 (2020a) 1430 -1448.
- Kerme E.D., Fung A.S. Transient heat transfer simulation, analysis and thermal performance study of double U-tube borehole heat exchanger based on numerical heat transfer model. Applied thermal Engineering 173 (2020b)115189.
- Nellis G., Klien S. Heat Transfer, Cambridge University Press, 2009.
- Li X, Chen Y, Chen Z, Zhao J. Thermal performances of different types of underground heat exchangers. Energy Build 38 (2006) 543-7.
- Li Y., Mao J., Geng S., Han X., Zhang H. Evaluation of thermal short-circuiting and influence on thermal response test for borehole heat exchanger. Geothermics 50 (2014) 136-47.

 doi:10.20944/preprints202403.0448.v1

- Luo J., Rohn J., Bayer M., Priess A. Performance and economic evaluation of double U-tube borehole heat exchanger with three different borehole diameters. Energy and Buildings 67(2013)217-224.
- Makasis N., Narsilio G.A., Bidarmaghz A., Johnston I.W. Ground-source heat pump systems: the effect of variable pipe separation in ground heat exchangers. Comput Geotech 100 (2018) 97-109.
- Marcotte B., Bernier M. Experimental validation of a TRC model for a double U-tube borehole with two independent circuits. Applied Thermal Engineering 162 (2019) 114229.
- Minaei, A., Maerefat, M. Thermal resistance capacity model for short-term borehole heat exchanger simulation with non-stiff ordinary differential equations. Geothermics 70 (2017a) 260-270.
- Minaei A., Maerefat M. A new analytical model for short-term borehole heat exchanger based on thermal resistance capacity model, Energy Build. 146(2017b), 233-242.
- Molina-Giraldo N, Blum P., Zhu K., Bayer P., Fang Z. A moving finite line source model to simulate borehole heat exchangers with groundwater advection. Int J. Therm. Sci 2011; 50:2506-13.
- Pu L., Qi D., Li K., Tan H., Li Y. Simulation study on the thermal performance of vertical U-tube heat exchangers for ground source heat pump system. Applied Thermal Engineering 79 (2015) 202-213.
- Qi D., Pu L., Ma Z., Xia L., Li Y. Effects of ground heat exchangers with different connection configurations on the heating performance of GSHP systems. Geothermics 80 (2019) 20-30.
- Rosen MA, Koohi-Fayegh S. Geothermal energy: sustainable heating and cooling using the ground. John Wiley & Sons; 2017.
- Sandler S., Zajaczkowski B., Bialko B., Malecha Z.M. Evaluation of the impact of the thermal shunt effect on the U-pipe ground borehole heat exchanger performance. Geothermics 65(2017) 244-54.
- Sivasakthivel T., Philippe M., Murugesan K., Vikas Verma V., Hu P. Experimental thermal performance analysis of ground heat exchangers for space heating and cooling applications. Renewable Energy 113(2017)1168-1181.
- Shah R.K., Sekulic, D.P. Fundamentals of Heat Exchanger Design, Chap. 7. John Wiley, New Jersey, 2003.
- Tang F., Nowamooz H. Factors influencing the performance of shallow Borehole Heat Exchanger. Energy Conversion and Management 181 (2019) 571-583.
- Xu Z., Lu J., Xing S., "Thermal performance of greenhouse heating with loop heat pipe solar collector and ground source heat pump," *Results*, Engineering 15 (2022), 100626.
- Yang X., Sun D., Li J., Yu C., Deng Y., Yu B., Demonstration study on ground source heat pump heating system with solar thermal energy storage for greenhouse heating, J. Storage Mater. 54 (2022), 105298.
- Yang W., Zhang S, Chen Y. A dynamic simulation method of ground coupled heat pump system based on borehole heat exchange effectiveness. Energy and Buildings 77 (2014) 17-27.
- Zanchini E., Jahanbin A. Effects of the temperature distribution on the thermal resistance of double u-tube borehole heat exchangers. Geothermics 71 (2018) 46-54.
- Zeng H., Diao N., Fang Z. Heat transfer analysis of boreholes in vertical ground heat exchangers. International Journal of Heat and Mass Transfer 46 (2003a) 4467-4481.
- Zeng H., Diao N., Fang Z. Efficiency of vertical geothermal heat exchangers in the ground source heat pump system. J. Therm. Sci. 12 (2003b) 77-81.
- Zhai X.Q., Cheng X.W., Wang R.Z. Heating and cooling performance of a mini type ground source heat pump system. Appl Thermal Engineering 111 (2017)1366-70.
- Zhang C., Chen P., Liu Y., Sun S., Peng D. An improved evaluation method for thermal performance of borehole heat exchanger. Renewable Energy 77 (2015) 142-151.
- Zhang C., Wang X., Sun P., Kong X., Sun S. Effect of depth and fluid flow rate on estimate for borehole thermal resistance of single U-pipe borehole heat exchanger. Renewable Energy 147 (2020) 2399-2408.
- Zhang W., Yang H., Lu L., Fang Z., Investigation on influential factors of engineering design of geothermal heat exchangers, Appl. Therm. Eng. 84 (2015) 310-319.
- Zhu N., Hu P., Xu L, Jiang Z., Lei F. Recent research and applications of ground source heat pump integrated with thermal energy storage systems: A review. Applied Thermal Engineering 71 (2014) 142-151.
- Zhou H., Lv J., Li T. Applicability of the pipe structure and flow velocity of vertical ground heat exchanger for ground source heat pump. Energy and Buildings 117 (2016) 109-119.
- Zhu L., Chen S., Yang Y., Sun Y. Transient heat transfer performance of a vertical double U-tube borehole heat exchanger under different operation conditions. Renewable Energy 131 (2019) 494-505.